# An investigation into the $SiO_2$ impregnation of spruce wood under vacuum conditions for engineering applications

By

Mathieu Lemaire-Paul

Under the supervision of

Dr. Reza Foruzanmehr

Thesis submitted to the University of Ottawa in partial fulfillment of the requirements of the degree of

**Master of Applied Science in Civil Engineering**

uOttawa

Department of Civil Engineering

Faculty of Engineering

University of Ottawa

## Abstract

Wood is a widely used construction material that has many advantageous properties, and some drawbacks. These drawbacks are mainly associated with the porous vascular structure of wood that makes it a high water-absorbent material. In addition, wood's properties alter substantially with respect to the moisture content. Amongst the treatment techniques that limit the water uptake capacity of wood, vacuum-aided impregnation has exhibited promising results. However, little research has explored the effect of key parameters (such as the vacuum pressure) on the effectiveness of the impregnation. This study aims to optimize the performance of $SiO_2$ impregnation of spruce wood under vacuum pressures. The main objective of this research is to overcome wood's weakness by reducing its water uptake capacity through a vacuum-aided impregnation technique and study its effect on the physico-mechanical properties of wood under dry and saturated conditions. The study was conducted in two parts. In the first part, wood samples underwent impregnation under atmospheric and three vacuum pressures. Density measurements, water uptake tests, microscopy examination, thermogravimetric analysis, and dynamic mechanical analysis were conducted on non-treated and $SiO_2$-treated samples. Quantitative and qualitative analyses demonstrated that $SiO_2$ impregnation performed under -90 kPa was able to effectively enhance the wood's properties compared to the other conditions. The $SiO_2$ impregnation under high vacuum pressure demonstrated an effective increase in the density of the wood and achieved a significant reduction in the water uptake capacity. The analysis of the wood's viscoelastic properties revealed that $SiO_2$ impregnation under atmospheric and vacuum conditions triggered two different reinforcing mechanisms: a solid film, causing stick-slip oscillation, and particle diffusion, causing particle-particle and particle-lumen wall friction, respectively. For the second part, characterization methods such as Impact test, DMA, SEM, EDS, Porosity, and SAXS tests were conducted on non-treated and -90 kPa treated spruce wood samples in dry, saturated, and submerged states in order to reveal the synergistic effect of the $SiO_2$ impregnation pressure and water uptake on the wood's properties. The results showed that high vacuum impregnation pressure has a significant positive reinforcing effect on the wood's properties. It increased the impact resistance of wood in dry and saturated conditions. A high vacuum impregnation was able to overcome the softening effect of water and caused a significant increase in the Storage modulus by strengthening the wood's vascular structure, which accordingly increased the wood's capacity to absorb energy. High vacuum impregnation was also able to counteract the plasticizing effect of water and significantly increased the Loss modulus by increasing the internal friction in the wood with the diffusion of the nanoparticles in the wood's cell walls and vascular structure. This phenomenon increased the wood's capacity to absorb and dissipate energy under dry and submerged conditions.

**Keywords:** Spruce Wood; $SiO_2$ Nanoparticles; Vacuum-Aided Impregnation; Dynamic Mechanical Analysis; Water Uptake; Sustainability; Wood Fibers; Synergistic Effect; Submerged Viscoelastic Properties; Impact Properties; SEM.

**Acknowledgments**

I would like to express my most sincere gratitude and appreciation to my research supervisor, Dr. Reza Foruzanmehr, who believed in me and gave me the opportunity to conduct this research and complete this thesis. Without him, none of this would have been possible. I would like to thank him for the support and the excellent knowledge input that he provided me throughout the process. Thanks for believing in me and showing me the way through this research with your great insight and dedication.

I would also like to thank the National Research Council of Canada for the partnership we had the opportunity to share. Their help and input were much appreciated and beneficial to this research's completion.

Last but not least, I would like to thank my family and friends for the love and support that they provided me throughout the journey. Thanks for believing in me and helping me get through. I will forever be grateful.

Altogether, we managed to get through the Covid-19 pandemic, conduct a successful research, and contribute valuable findings to the research knowledge in sustainable material development.

## Table of Contents

## List of Figures

## List of Tables

# CHAPTER 1

**Introduction**

# CHAPTER 1

## 1.0 Introduction

## 1.1 Background

Because of its numerous advantages, wood is a popular construction material in the industry [1,2]. Nevertheless, wood also has some disadvantages that limit its use and reduce its durability.

Wood is a naturally occurring composite that consists of a matrix of lignin and hemicellulose reinforced by cellulose fibrils. Cellulose is a hydrophilic polymer with weak glycosidic bonds susceptible to hydrolysis [3,4]. Cellulose is also prone to dimensional instability due to its viscoelastic nature [5,6]. Accordingly, wood's properties are strongly dependent on its moisture content [7,8,9]. Most mechanical properties vary with a change in its moisture content below the fiber saturation point (FSP) [7,8,9]. In general, increasing the moisture content leads to a lower Storage modulus, higher Loss modulus, and higher ductility [7,8,9].

Water can enter the wood's structure due to capillary action through its vascular system that consists of pores and lumens (small tubular openings inside the wood fibers) [10]. Once inside, water can permeate into cell walls and act as a plasticizing agent, which reduces the friction between the long molecular chains of cellulose, allowing them to move more freely and induce swelling [9].

Wood's durability is strongly dependent on its moisture content and environmental factors [8]. Wood is susceptible to attacks by biological agencies such as fungus and insects [8,11]. The possibility and the rate of deterioration of biological attacks strongly depend on the moisture content in the wood's structure [8].

The well-known solutions that can control the high water uptake level in wood and increase its durability include the externally-applied coatings of water repellents and physico-chemical treatments. These treatments are usually toxic due to the chemicals involved [12] and are not truly efficient in preventing the water uptake capacity of wood due to the incompatibility of the products with the wood. These treatments leave a gap between the inner wall of the lumen and the chemical product into which water can permeate [13]. Over time, coated wood will swell the same as non-coated wood [10]. Also, the performance and lifespan of these coatings depend on the environmental conditions exposed to wood [10,14]. These coatings may deteriorate or be washed away over time [10,14], and thus they require reapplication over the years for optimal performance [14].

One prospect method to decrease the water absorption capacity of wood and mitigate the mentioned shortcomings involves the impregnation of wood with dense materials like ceramics to homogenously coat and obstruct its vascular system [15]. Ceramic nanoparticles in an aqueous colloid like Silicon dioxide ($SiO_2$) can be used to fill the porous vascular system structure through an impregnation process [16]. The process consists of infusing the colloid into the vascular system of wood, where the nanoparticles

fill the lumens, agglomerate, and obstruct the vascular structure as the solvent evaporates. Previous studies showed positive outcomes on the physical and mechanical properties of the $SiO_2$ impregnated wood under vacuum conditions [17,18,19,20]. However, the research is still limited and has yet to investigate and discover the effect of key parameters on the $SiO_2$ impregnation of wood, especially under vacuum conditions. For example, past research did not investigate the efficiency of vacuum impregnation and the influence of different impregnation pressures on the diffusion of $SiO_2$ nanoparticles within the wood's vascular system and their effect on the wood's properties. Previous research also did not study the effect of moisture on the mechanical and viscoelastic properties of the $SiO_2$ impregnated wood. Most of the time, the researchers would only apply a vacuum during impregnation and test the samples in a dry state. In other words, the research has yet to reveal the effect of vacuum pressure on the effectiveness of $SiO_2$ impregnation, as well as the synergistic effect of the moisture content and $SiO_2$ impregnation on the mechanical and viscoelastic properties of wood.

## 1.2 Research significance and objectives

To date, the research on $SiO_2$ impregnation of wood has shown a great potential for improving wood's properties, especially under vacuum conditions. However, little research has investigated the vacuum impregnation parameters.

This study was conducted to bring additional valuable knowledge to the research on $SiO_2$ impregnation of wood. Accordingly, this research studied the effect of vacuum pressures on the impregnation effectiveness of white spruce wood. This effectiveness was probed by measuring the physical and viscoelastic properties of wood before and after the treatments. Additional mechanical tests under dry and submerged conditions were performed to fill the gap of knowledge.

## 1.3 Research Methodology

The research was conducted in two sections.

The first section involved evaluating the effect of vacuum pressure on the $SiO_2$ impregnation of wood and finding the optimal impregnation condition. This was done by measuring density, water uptake capacity, and dynamic mechanical analysis before and after the impregnation treatment under atmospheric and three vacuum pressures. The electron microscopy was also used to verify the diffusion of the $SiO_2$ in the vascular system of the wood with respect to the impregnation pressure.

The second section involved an investigation into the synergistic effect of the optimal impregnation pressure and water content at saturation on the wood's mechanical and viscoelastic properties. This was done by conducting impact tests and dynamic mechanical analysis under dry and saturated conditions before and after impregnation.

## 1.4 Thesis Outline

The thesis is written in an article-based format and consists of 5 chapters. The description and contents of each chapter are presented below:

- Chapter 1 consists of the introduction of the thesis, which provides adequate information to describe the content, such as the research background, the objectives, and the outline.
- Chapter 2 consists of the literature review, which presents the rationale and the essential concepts related to the study.
- Chapter 3 consists of the first article, which relies on evaluating the effect of vacuum pressure on the $SiO_2$ impregnation and finding the optimal impregnation condition.
- Chapter 4 consists of the second article, which relies on implementing the optimal $SiO_2$ impregnation pressure and studying the synergistic effect on the wood properties under dry and saturated states.
- Chapter 5 consists of the conclusions of the thesis, which highlights the key findings of the research and presents recommendations.

## 1.5 References


1. Brunner M. (2000). On The Plastic Design Of Timber Beams With A Complex Cross-Section. Paper presented at the World Conference on Timber Engineering, British Columbia, Canada, July 31–August 3 2000.

2. Atlantic WoodWORKS!. (2017). WOOD FOR MID-RISE CONSTRUCTION. doi: https://wood-works.ca/wp-content/uploads/160601-Wood-4-Mid-Rise-Report-FINAL-2017-03-28-sm.pdf

3. Di Blasi C, Galgano A, Branca C. (2009). Influences of the chemical state of alkaline compounds and the nature of alkali metal on wood pyrolysis. *Industrial & Engineering Chemistry Research, 48*, 3359–3369. doi: 10.1021/ie801468y

4. Ioelovich, M. (2021). Adjustment of Hydrophobic Properties of Cellulose Materials. *Polymers*, 13, 1241. doi: https://doi.org/10.3390/ polym13081241

5. Olsson A-M, Salmén L. (1997). The effect of lignin composition on the viscoelastic properties of wood. *Nordic Pulp & Paper Research Journal, 12*, 140–144. doi: 10.3183/npprj-1997-12-03-p140-144

6. Thoemen H, Irle M, Sernek M. (2010). *Wood-Based Panels – An Introduction for Specialists.* London, England: Brunel University Press

7. University of Cambridge. (2020). Water's effect on the mechanical behaviour of wood. In: Dissemination of IT for the Promotion of Materials Science (DoITPoMS). doi: https://www.doitpoms.ac.uk/tlplib/wood/water_effect.php.

8. David W. Green, Jerrold E. Winandy, and David E. Kretschmann. (1999). Chapter 4 - Mechanical Properties of Wood. In Forest Product Laboratory. *Wood Handbook - Wood as an Engineering Material* (463). Madison, WI: U.S. Department of Agriculture, Forest Service. doi: https://www.fpl.fs.fed.us/documnts/fplgtr/fplgtr113/fplgtr113.pdf

9. Wagner et al. (2015). Effect of Water on the Mechanical Properties of Wood Cell Walls – Results of a Nanoindentation Study. *BioResources, 10*(3), 4011-4025. doi: 10.15376/biores.10.3.4011-4025

10. Rowell RM, Banks WB. (1985). Water repellency and dimensional stability of wood. *Forest Products Laboratory*. doi: 10.2737/fpl-gtr-50

11. Illston J.M, Domone P. (2001). *Construction Materials – Their Nature and Behavior* (3rd ed.). London, England: CRC Press.

12. Williams RS, Feist WC. (1999). Water repellents and water-repellent preservatives for Wood. *Forest Products Laboratory*. doi: 10.2737/fpl-gtr-109

13. Denes AR, Tshabalala MA, Rowell R, et al. (1999). Hexamethyldisiloxane-plasma coating of wood surfaces for creating water repellent characteristics. *Holzforschung*, *53(3)*, 318–326. doi: 10.1515/hf.1999.052

14. Beaulieu D, Biermeier D. (2020). How to Seal a Deck With Thompson's WaterSeal. In: The Spruce. doi: https://www.thespruce.com/seal-a-deck-with-thompsons-water-seal-2131998.

15. Grosse C, Noël M, Thévenom M.F, Rautkari L, Gérardin P. (2018). Influence of Water and Humidity on Wood Modification with Lactic Acid. *Journal of Renewable Materials, 6*(3), 259-269. doi:10.7569/JRM.2017.634176

16. Boulos L, Foruzanmehr MR, Tagnit-Hamou A, et al. (2017). Wetting analysis and surface characterization of flax fibers modified with zirconia by sol-gel method. *Surface and Coatings Technology, 313*, 407–416. doi: 10.1016/j.surfcoat.2017.02.008

17. Enguang Xu, Yanjuan Zhang, Lanying Lin. (2020). Improvement of Mechanical, Hydrophobicity and Thermal Properties of Chinese Fir Wood by Impregnation of

Nano Silica Sol. *Polymers 2020, 12*(8), 1632. doi: https://doi.org/10.3390/polym12081632

18. Zhang, N., Xu, M. & Cai, L. (2019). Improvement of mechanical, humidity resistance and thermal properties of heat-treated rubber wood by impregnation of $SiO_2$ precursor. *Scientific Reports, 9*, 982. doi: https://doi.org/10.1038/s41598-018-37363-3

19. Przystupa K, Pieniak D, Samociuk W, Walczak A, Bartnik G, Kamocka-Bronisz R, Sutuła M. (2020). Mechanical Properties and Strength Reliability of Impregnated Wood after High Temperature Conditions. *Materials, 13*(23), 5521. doi: https://doi.org/10.3390/ma13235521

20. Lin, Lan Ying, and Feng Fu. (2012). The Composite Wood Impregnated with Silicon Sol Solution. *Advanced Materials Research*, 466–467, 121–126. doi: https://doi.org/10.4028/www.scientific.net/amr.466-467.121

# CHAPTER 2

**Literature Review**

# CHAPTER 2

## 2.0 Literature Review

### 2.1 Environmental impact and construction needs

Construction and its use of synthetic materials have played a crucial role in the development of the modern human society [1]. However, it has also had several negative impacts on land pollution, waste generation, and $CO_2$ emission [1]. With an always-growing population, the demand for housing and the construction of new infrastructure is always on the rise, resulting in higher demand for building materials [1]. Exploiting these non-renewable resources to meet the forever-increasing demand is leading toward a material shortage and significant price increases, and ultimately, a crucial environmental crisis [1]. One method to offset this crisis would be to opt for more sustainable and renewable building materials to ensure that the supplies could always meet the demand, all while reducing the environmental footprint. Wood is a good example of such material: it is renewable and affordable and also produces 85% and 88% less carbon to harvest, process, and transport compared to steel and concrete, respectively [2].

There are several different construction materials available on the market to be exploited. The general conventional construction materials that are extensively used are steel, concrete, and wood. When selecting a construction material, the following criteria have to be taken into consideration:

- Cost
- Environmental Footprint
- Strength
- Durability
- Aesthetic
- Weight

Some criteria may have a greater importance than others depending on the needs and scope of work of the project. There is not yet a perfect material that can always achieve all the aforementioned criteria. In other words, each material has its advantages and disadvantages.

Wood is one of the most sustainable materials available if harvested and replanted appropriately. Wood is abundant in North America. Canada has approximately 38% of its total landmass that is covered by forest, which equals about 347 million hectares, making it readily available [2]. Figure 2.1 shows the forest regions of Canada and their principal tree species.

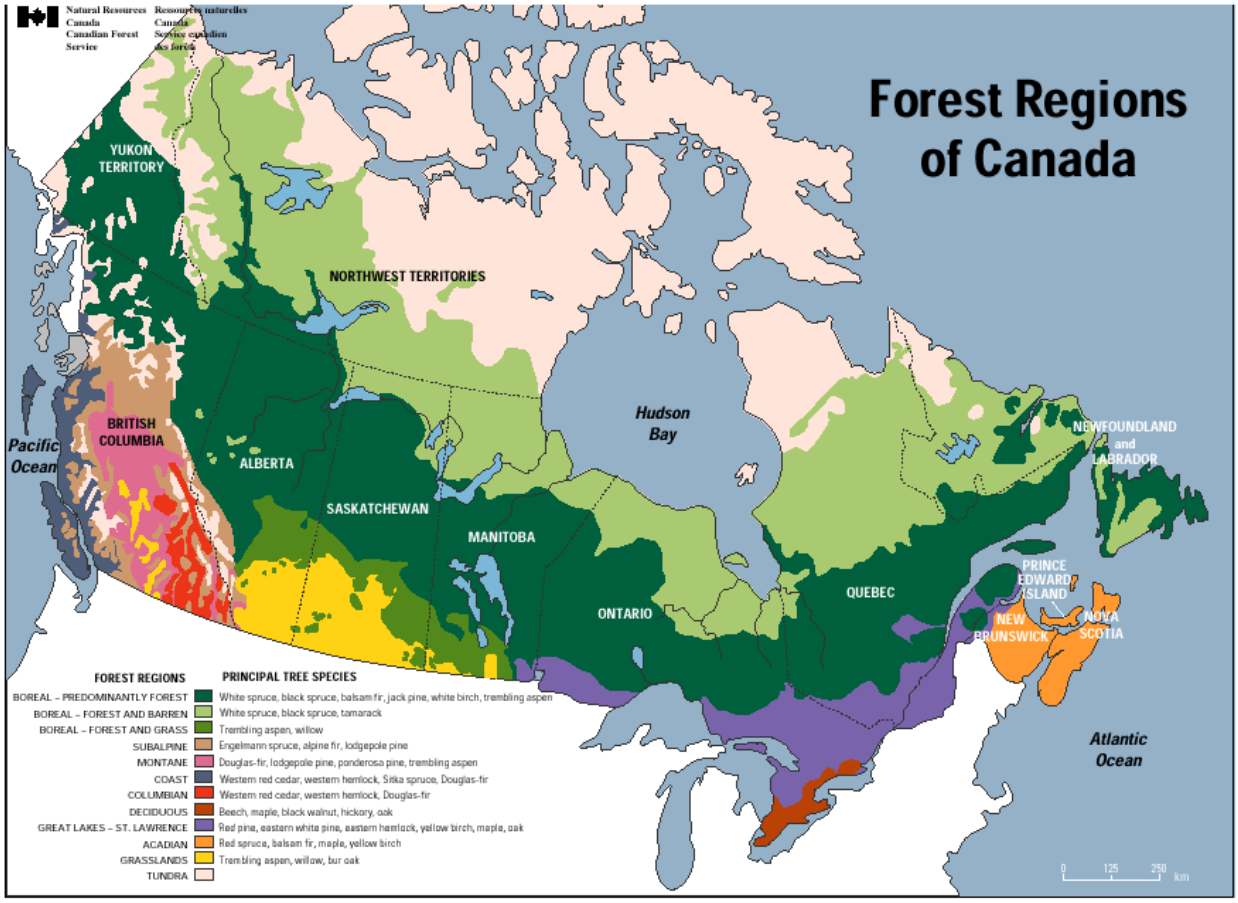


*Figure 2.1: Forest regions of Canada* [3]

Although wood is an ancient material and has a long history as a building material, it is complex and its properties have not been thoroughly investigated [4]. Researchers and industries are still exploring new techniques to unleash its full potential in various applications [4]. There is a lack of understanding in the chemistry and material properties of wood that restrains its effective utilization [4].

Wood has good mechanical properties, shows significant advantages over other building materials, and is attractive to the construction industry [2,5]. However, wood has some drawbacks, which limit its use and reduce its durability. The advantages and drawbacks of wood will be further discussed in detail in the following sections.

## 2.2 Wood Background

### 2.2.1 Advantages

Wood has long been exploited in construction in Europe and North America [2]. This lies in the fact that wood is a naturally occurring material and thus is renewable in comparison with other synthetic construction materials such as steel and concrete. In addition to renewability and its abundance, wood is strong, lightweight, and has fairly good acoustic

and thermal properties [5,6,7]. All these aspects make wood an attractive material for the construction industry.

### 2.2.2 Disadvantages

Wood's hydrophilic nature and its porous structure make it a water-absorbent material due to the high capillary action capacity of its lumens. Furthermore, as a result of its cellulose content, a viscoelastic polymer, wood has low dimensional stability, and its mechanical properties are dependent on its moisture content. Wood is also an orthotropic material due to its internal structural composition of mainly longitudinal fibers, and thus its mechanical properties also depend on the loading direction [9].

Wood also suffers from low durability in alkaline environments because the glycosidic links of the cellulosic chains can irreversibly undergo degradation by hydrolysis in the presence of hydroxyl groups [8,9]. These degradations reduce the mechanical properties of wood and are permanent and non-reversible [9].

Wood's mechanical properties are also negatively impacted by an increase in the water content up to the Fiber Saturation Point (FSP), where a plateau is reached; loss of strength and an increase in mass, volume, and ductility are experienced accordingly [10,11,12]. Additionally, variation in the moisture content below the FSP (approximately 30 wt%) directly leads to swelling and shrinkage, which can result in mechanical stresses, inducing cracks and deformation [13].

Furthermore, the biodegradation and optimal performance of wood is strongly influenced by its moisture content. Due to the presence of moisture, wood can rot and decay, which negatively affects its mechanical properties and can significantly shorten its life span [6,9].

Therefore the wood's water uptake needs to be limited through physico-chemical modifications to stabilize the performance of wood in its engineering applications. These modifications depend on many factors such as morphology, chemical composition, and the type of wood.

### 2.2.3 Type of wood: Hardwood vs Softwood

Generally speaking, there are three categories of wood that exist and are available on the market: hardwood, softwood, and engineered wood [14]. Hardwood comes from deciduous trees, also known as Angiosperms (i.e., oak, maple, cherry, mahogany, and walnut), and softwood comes from coniferous trees, also known as Gymnosperms (i.e., pine, cedar, fir, spruce, and redwood). Softwood and hardwood are both naturally occurring in the environment and are abundant in Canada, hence one of the reasons why they are highly exploited. On the other hand, engineered wood is not a naturally occurring product, but rather is manufactured from manipulated and modified wood to achieve

certain properties and dimensions that naturally occurring wood cannot achieve [14]. Commonly available engineered wood products are plywood, oriented strand board, fiberboard, and composite board.

### 2.3 Morphology & Chemical Composition of Wood

The wood used for the construction industry and engineering applications usually consists of cut sections from the trunk. The trunk is the main structural element of a tree and ensures the water and nutrient transport from the roots to the branches. The trunk can be subdivided into 3 main layers of wood such as heartwood, sapwood, and bark [15] (see Figure 2.2). The bark consists of the outermost layer of the tree and is made of dead tissues, and its role is said to protect the tree against the environment. The second outermost layer consists of the sapwood, which is made of active living cells. Additionally, this is the zone in which the growth of the tree occurs [15]. Each year, new wood cells are added between the bark and sapwood resulting in additional growth rings [15]. The innermost layer, to say the central zone of the tree, consists of the heartwood which is made of dead wood cells. Over the years, as new wood cells are formed (sapwood), older wood cells die and are converted into heartwood [15]. Sapwood and heartwood can usually be distinguished by their color, heartwood usually being darker. Sapwood and heartwood can also be referred to together as the xylem of the trunk.

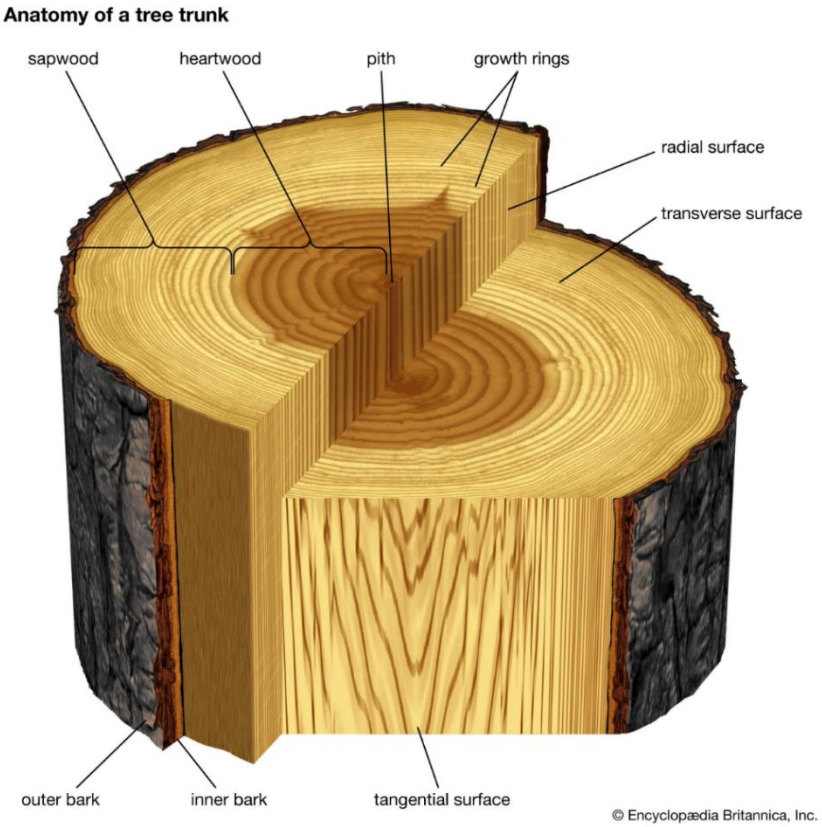


*Figure 2.2: Wood trunk transversal slice* [16]

### 2.3.1 Vascular system of wood

Both hardwood and softwood have similarities, but ultimately they have their own different composition and anatomy, hardwood being more complex [4,15]. One of the main differences between the two is the presence of wood vessel cells which are only present in hardwood. Figure 2.3 shows the different hardwood and softwood cells.

The following sections will be dedicated to softwood.

Wood is a porous material. Its pores can be subcategorized into 4 classes based on their size distribution as follows: macropores (radius (58–2) μm and (2–0.5) μm), mesopores ((500–80) nm), and micropores ((80–1.8) nm) [17].

Softwoods, like spruce wood, are made of two main types of cells: tracheid and parenchyma. The tracheids are responsible for the wood's structural integrity and govern the physical and chemical properties of the wood [15]. These cells are oriented parallel to the length of the wood / tree (in the longitudinal direction), forming about 90% of the total volume [15]. Visually, tracheids are small thin elongated cylindrical openings. They vary in size but generally speaking, for softwood, they range from 3 to 5 mm in length and 20μm to 80μm in width [15]. Due to their nature, shape, and size, tracheids are the designated way for water to penetrate and distribute itself through the tree / wood [15].

On the other hand, parenchymas are the cells that store the nutrients of the growing trees [15]. They can be located near the resin canals as a strand, as epithelial cells in the wood's longitudinal axis, or as part of the wood rays perpendicular to the longitudinal axis of the tree [18]. They represent about 10% of the total wood volume [15].

Softwood, like spruce wood, also has some pits, commonly known as boarded pits. These pits are located along the tracheid and allow for water transport between the wood cells [18].

Wood is a natural organic material that grows all year-round. Its macroscopic structure is influenced by the growing seasons, therefore it results in two different types of wood such as earlywood and latewood [15]. The main difference between the two types of wood is the porosity of the tracheid. Latewood is denser, has a thicker cell wall resulting in smaller cross-sectional-area lumens, and usually is of a darker color [15]. On the other hand, earlywood is less dense and has a thinner cell wall, thus the lumens have larger cross-sectional areas with a lighter color [15]. Accordingly, latewood has a better structural capacity to support the tree, and earlywood is better suited to conduct water and nutrients [15]. Figure 2.4 demonstrates a general conception of the softwood vascular system.

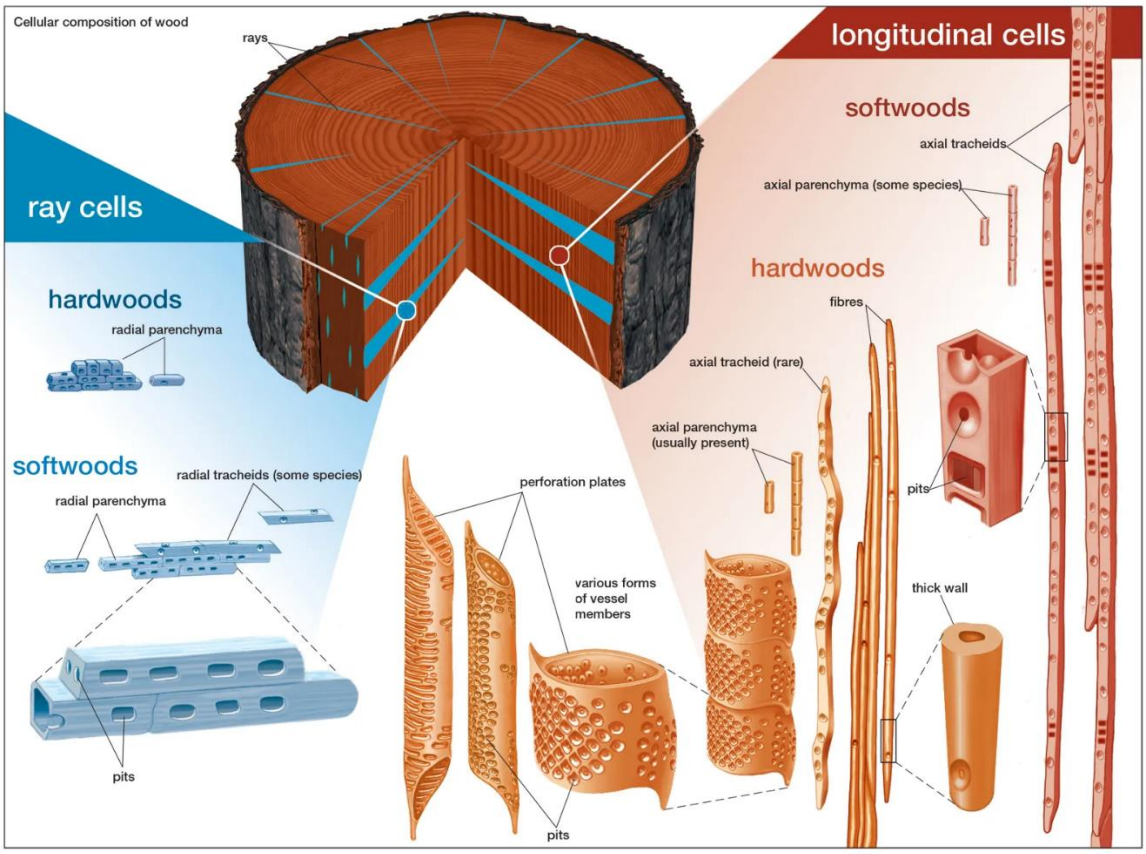


*Figure 2.3: Hardwood and Softwood types of cells* [16]

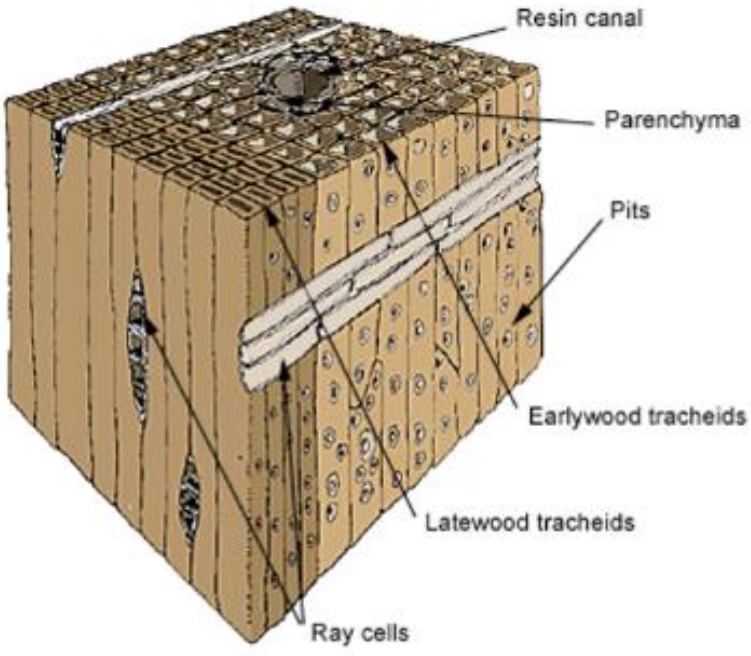


*Figure 2.4: Softwood anatomy* [19]

### 2.3.2 Wood cells compositions

Wood cell walls are considered chemically heterogeneous. They primarily consist of 95-98% cellulose, hemicellulose, and lignin; all polymeric molecules [15]. The remaining 2-5% is a mix of extractive compounds. These components will be further discussed in detail in the following sections.

Softwood such as spruce wood generally consists of 42% ± 2% cellulose, 27% ± 2% hemicellulose, 28% ± 3% lignin and 3% ± 2% extractives [15].

Wood cell walls can be subdivided into 3 layers denoted by S1, S2, and S3 (see Figure 2.5). Each cell wall layer consists of a different density and orientation of microfibrils [15]. Microfibrils are small elongated thread-like components (see Figure 2.6). Their width varies from 100 to 300 angstroms, their thickness is usually half their width, and their lengths are not well defined [15].

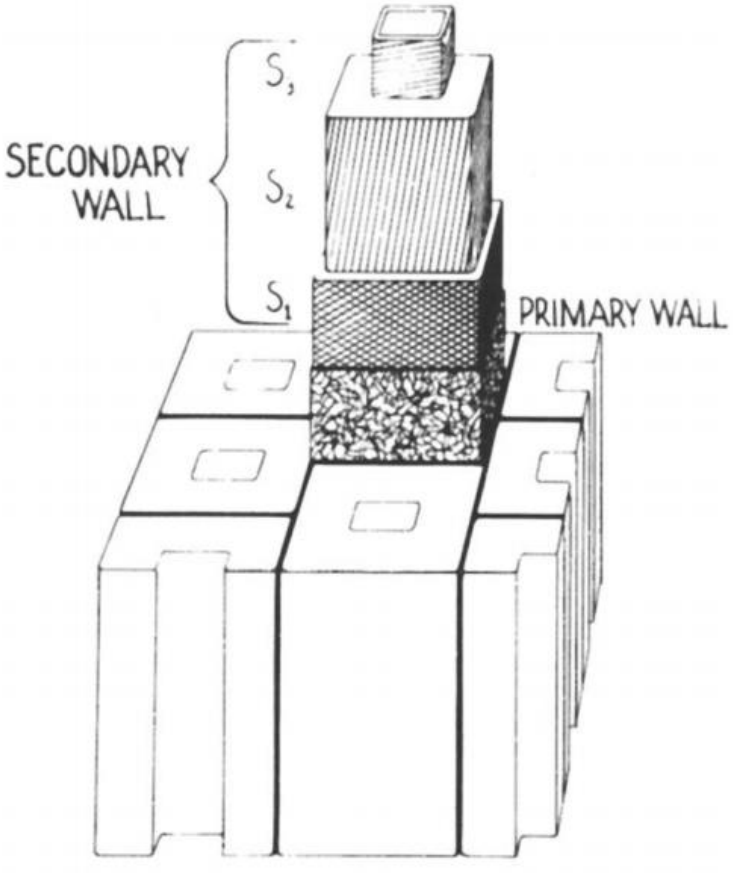


*Figure 2.5: Idealized wood cell wall layering* [15]

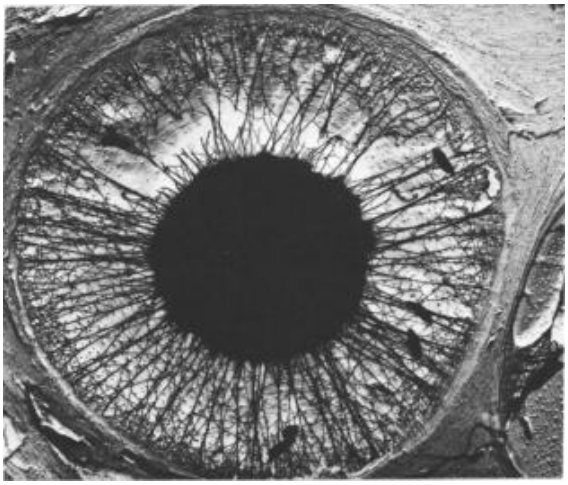

*Figure 2.6: Wood cell view close-up, bordered pit membrane with microfibrils* [15]

### 2.3.3 Cellulose

Cellulose is a linear polymer made of individual anhydro-D-glucopyranose molecules joined by glycosidic and hydrogen bonds. More precisely, the polymer chain groups are linked lengthwise by glycosidic bonds and laterally by strong hydrogen bonds. Additionally, the molecular chains yield an excellent crystalline structure due to their excellent alignment [15]. Figure 2.7 presents the cellulose molecule, which is repeated along its polymer chain.

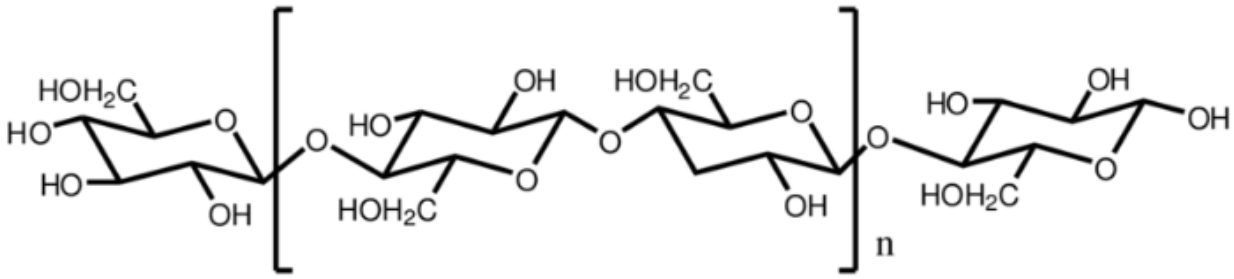


*Figure 2.7: Cellulose mollecules & polymer chain* [20]

### 2.3.4 Hemicellulose

Hemicellulose is similar to cellulose; it is also a polymer of anhydrosugar units. This being said, hemicellulose molecules may be consisted of different sugar units, which is not the case for cellulose, and the polymer chains are usually shorter. The sugar units of hemicellulose usually found in wood consist of D-glucose, D-galactose, D-xylose, D-mannose, L-arabinose and 4-0-methyl-D-glucuronic acid. Naturally, hemicellulose can be located surrounding the cellulose crystalline structure along with lignin [15]. Similar to

cellulose, hemicellulose is sensitive to alkaline solutions and is soluble in these solutions. Figure 2.8 shows the interaction of hemicellulose and its constitution in wood along with the cellulose and lignin.

### 2.3.5 Lignin

Lignin is the most abundant non-carbohydrate component of wood. It is a very complex 3-dimensional polymer consisting of phenolic units [15]. The polymer chains vary significantly, from a few to several hundred units. It is generally made up of C-O-C and C-C linkages [4]. Comparatively to cellulose and hemicellulose, it does not have one repeating unit [4]. Lignin is a hydrophobic polymer in nature due to the aromatic nature of the phenolic units. Lignin gives structural integrity to wood. Lignin's rigidity and resistance to compression mainly come from the arrangement of its 3-dimensional structure [15]. The lignin in softwood is different compared to hardwood. Ultimately, softwood lignin has more cross-linking and thus has a greater molecular weight and is more durable [15]. Lignin acts as a bonding agent to the cell wall's component and provides additional stiffness. Figure 2.8 shows the interaction of the lignin and its constitution in wood along with the cellulose and hemicellulose.

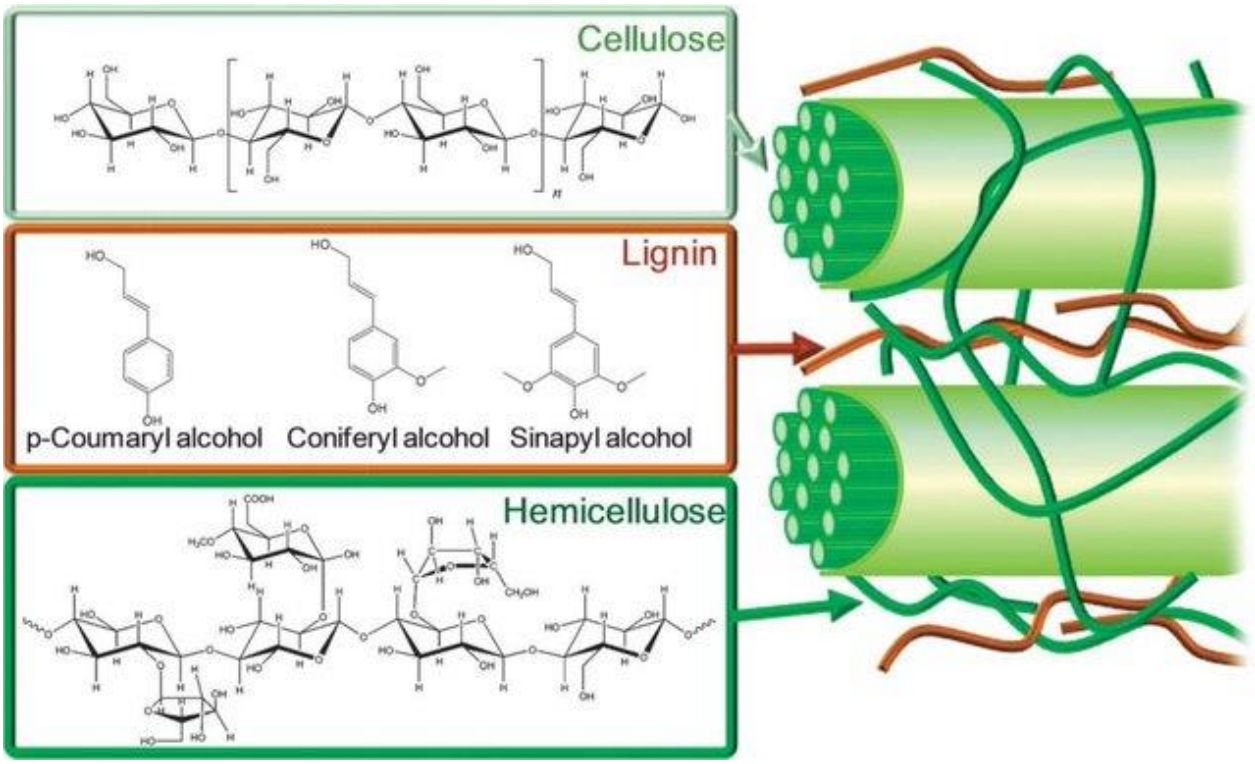


*Figure 2.8: Structure of lignocellulosic biomass with cellulose, hemicellulose, and lignin represented* [21]

### 2.3.6 Extractive Compounds

Extractive compounds are non-structural related, but they can still influence wood's properties. They are usually produced and present to make wood resistant against natural environmental conditions such as biological attacks [22]. They are usually concentrated in the heartwood but can also be found in the sapwood [22]. They can also provide some esthetic value due to their given colors, and some useful products due to their nature. These extractive chemicals and compounds can be for the majority: Terpenes and related compounds, Fatty acids, Aromatic compounds, and Volatile oils. In the end, they vary and differ largely in quantity and distribution from different wood species [15].

## 2.4 Mechanical Properties

### 2.4.1 Natural discontinuities and defects influence

As a naturally occurring material, wood has natural discontinuities or defects such as: knots, different fiber orientations and sizes, and pitch pockets (internal cavity) [9]. The existence of these discontinuities significantly alters wood's mechanical properties. Accordingly, wood's properties vary from different wood sources, locations within the same tree, down to a few cm apart on the same board and plane [9].

### 2.4.2 Orthotropic material

Wood is classified as an orthotropic material which means that wood's mechanical properties are different depending on the loading direction (Longitudinal, Radial, and Tangential) [9]. This phenomenon is mainly due to the internal structural composition of wood and its fiber directions which are mainly parallel to its longitudinal axis. Accordingly, when it comes to axial load, wood is strongest when the load is acting parallel to its fibers, which is in the longitudinal direction. Wood is weakest if axially loaded in tension perpendicular to its fibers (radial or tangential), as the strength will be limited by the lignin bond between the fibers. Studies found that wood's flexural resistance (bending) and its relation to the loading axis differ depending on the wood species [23]. For spruce wood, it was found to be similar in both axes, and the difference was found to be negligible [23]. Figure 2.9 shows a wood plank and its corresponding axes respective to the wood fibers.

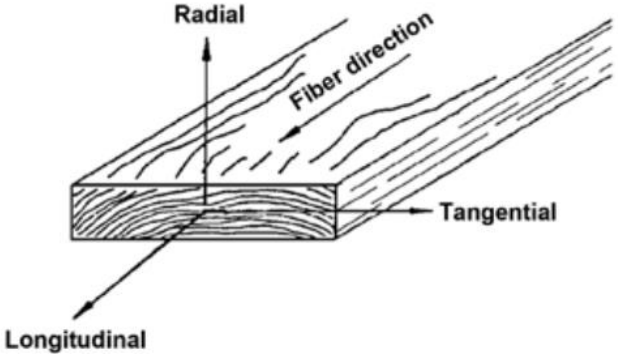


*Figure 2.9: Wood principle loading axis [9]*

### 2.4.3 Viscoelastic Properties

A viscoelastic material is a material that has the ability to behave elastically and viscously, meaning that it has the ability to absorb and dissipate energy [24]. Viscoelastic materials have a stress-strain dependency with respect to time, meaning that if a stress is applied to a viscoelastic material, its strain response might not be instantaneous and can be delayed. Figure 2.10 presents an idealization of the phenomenon.

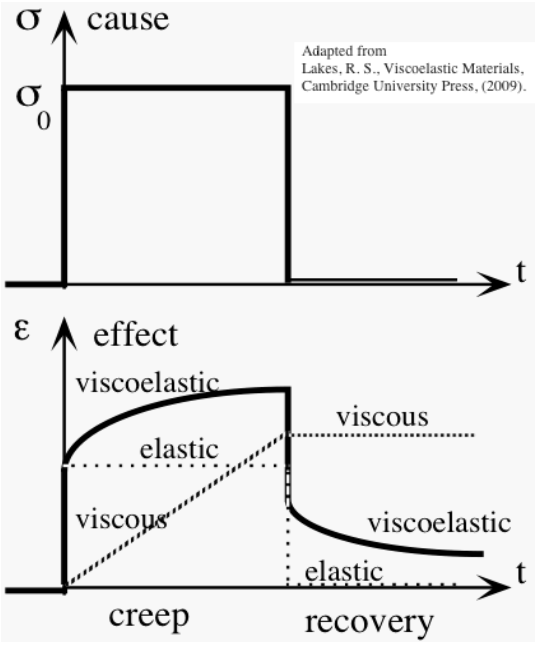


*Figure 2.10: Viscoelastic behavior response* [25]

This delay is represented by a phase angle (δ). A perfectly elastic material has no time dependency, meaning that the stress and deformation are simultaneous, and thus the phase angle is 0°. For a perfectly viscous material, there is an offset in the response which is represented by a 90° phase angle. Accordingly, a viscoelastic material is somewhere in between sharing both properties and having a phase angle greater than 0° but smaller than 90°. Figure 2.11 presents the 3 scenarios with a sinusoidal cyclic loading.

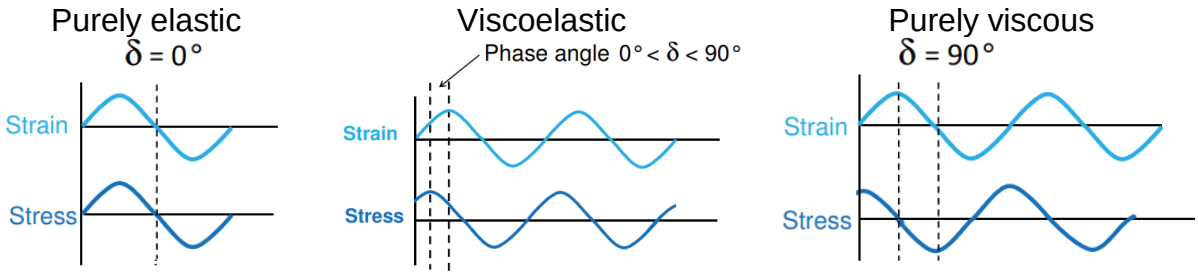


*Figure 2.11: Stress strain response with phase angle* [26]

Viscoelastic properties are measured and represented by the Storage modulus (E'), Loss modulus (E''), and Tan δ [24]. All together, they identify the viscous and elastic response of materials when they undergo oscillating loads or deformations [24].

The Storage modulus is the measure of the capacity of a material to store (absorb) energy. It is a measure of the elastic stress over the elastic strain under cyclic load and deformation. It is similar to Young's modulus, for a perfectly elastic material. It is representative of the stiffness: the higher the Storage modulus, the higher the stiffness.

The Loss modulus is a measure of the dissipation of energy. A higher Loss modulus means that there is higher dissipation of energy. Dissipation of energy occurs through internal friction and heat during deformation. Accordingly, Loss modulus is a measure and is representative of the internal friction of the material.

The Tan δ is the ratio of Loss modulus over the Storage modulus. Accordingly, a higher Tan δ means the material is more elastic, and a lower Tan δ means the material is more viscous. Ultimately, it represents the damping capacity of a material. Higher Tan δ means higher damping capacity.

Wood is a viscoelastic material. As mentioned before, wood is composed of three main natural polymers (cellulose, hemicellulose, and lining). The viscoelastic behavior of wood is a complex mechanism that is derived from the interactions of each of these three polymers and their responses to water [27]. When wood undergoes deformation, energy is dissipated through heat with respect to its internal friction and long polymeric chains [11]. The dissipation mechanism is dependent on the temperature and moisture content of the wood [11]. Water is a plasticizing agent to wood. Water interaction with wood leads to a lower rigidity and an increase in ductility because of its capability to mediate the hydrogen bonding of the organic polymers with water-carbohydrates links, which reduces the strength of the polymer network and enhances their movement capability and ultimately induces softening [10,27]. There is an optimal moisture content that varies with temperature, below the Fiber Saturation Point (FSP), at which the internal friction is minimal [11]. When the moisture content drops below the optimal point, it increases static friction, which enhances energy absorption (i.e., Storage modulus). On the other hand, when the moisture content increases toward FSP, the kinetic friction increases, which expands energy dissipation (i.e., Loss modulus). Additionally, the increase in moisture content beyond the FSP reduces the internal friction, and as a result both the Storage and Loss modulus, due to the wood softening and plasticizing effect of water molecules [11]. It goes to say that the viscoelastic properties of wood are dependent on its moisture content.

Table 2.1 presents some studies conducted on different wood species related to their viscoelastic properties.

*Table 2.1: Wood viscoelastic properties studies*

| Type of Wood | Test Conditions | | Tested Properties | Outcome | Ref |
|---|---|---|---|---|---|
| | Temperature (°C) | Water content | | | |
| Oak, Beech, Spruce, Fir | 10-80 | Saturated | Storage modulus | Decrease at a constant temperature of 80°C. | [28] |
| Oak, Beech, Poplar, Spruce | 0-95 | Saturated | Storage modulus | Decrease in radial and tangential direction. Different behavior in both directions. | [29] |
| Clear Green Poplar | Ambient | Different moisture content (50-130%) | Storage modulus<br>Loss modulus | Decrease of Storage modulus and increase of Loss modulus with an increase in moisture content. | [30] |
| Chinese Fir | -125 to 25 | Different moisture content (0.6-25.2%) | Storage modulus | Decrease with an increase in temperature. The results showed an anisotropy at all moisture content. | [31] |
| Chinese Fir | 20 to 180 | Different moisture content (0.6-25.2%) | Storage modulus | Influenced simultaneously by temperature and moisture content. Less water results in more stiffness, higher temperature results in lower stiffness. | [32] |

### 2.4.4 Impact strength

The impact strength of a material depends on its ability to absorb and dissipate energy at deformation [33]. Wood's mechanical properties under impact loading differ from the static loading conditions [34,35]. This being said, to this day, there are still relatively few studies on the impact properties of wood, and the old studies are questionable as their data seems to contradict the newer results [36]. From what is known, the impact strength of wood increases with density, and unlike other mechanical properties, also increases with an increase in the moisture content [33]. It is also dependent on the loading orientation. Higher impact strength is achieved in the radial direction [33]. A study shows that the difference between radial and tangential impact strength varies with the wood species [23]. It was revealed that spruce wood had 50% more strength in the radial direction compared to tangential [23]. Better understanding and improvement of the impact resistance of wood could be an asset to designing more efficient infrastructures with improved safety.

Nevertheless, there is a need to further research the impact properties of wood to better assess and understand the fracture mechanism under dynamic loads. This will help better design the structures and apparatuses that may undergo impact loads such as guardrails [33].

Table 2.2 presents some studies conducted on different wood species related to their impact properties.

*Table 2.2: Wood impact properties studies*

| Type of Wood | Test Conditions | | Tested Properties | Outcome | Ref |
|---|---|---|---|---|---|
| | Temperature (°C) | Water content | | | |
| Spruce | 20 | 65% humidity | Impact strength<br><br>Modulus of Elasticity | Good correlation between the modulus of elasticity and the impact strength. Impact resistance shows to be higher in the radial plane but is more consistent in the tangential plane as showing less variability. | [37] |
| Norway Spruce | Ambient | 10% Moisture content | Impact strength | Higher density lead to higher impact resistance. Wider growth rings lead to lower impact resistance. | [38] |
| Sitka Spruce | Heat treated at 160 Conditioned at 20 | 65% humidity | Impact Strength | Heat treatment reduced impact strength and increased brittleness. | [39] |
| European Oak, Norway Spruce | Different heat treatment (160-210) Conditioned at 20 | 65% Humidity 12% Moisture content | Impact Strength | Resistance is affected by heat treatment. At 160°C, the impact strength was increased. Over 160°C, the impact strength decreased, with 210°C having the lowest resistance of all. | [40] |
| Cedro, Cambará Rosa, Cedrorana, Catanudo, Cupiúba, Angelim Saia, Tatajuba, Guaiçara, Cumaru, Angelim Vermelho | Ambient | 12% Moisture content | Impact Strength<br><br>Modulus of Elasticity<br><br>Compression parallel to grain | No correlation could be derived from the impact resistance to the modulus of elasticity and the strength in compression parallel to the grain. | [41] |

### 2.4.5 Moisture dependent properties

Wood's mechanical properties are dependent on the moisture content up to the fiber saturation point [9]. With the exception of impact strength, mechanical properties of wood are reduced with the presence of water, alcohol or other organic liquids.

Wood's significant amount of hydroxyl groups (OH) makes it very reactive with water and other organic liquids that are capable of forming hydrogen bonds with the cell walls once inside its vascular system.

To specify, these mentioned fluids do not decay or degrade the wood; they cause wood to soften, swell and decrease the friction within its internal structure acting as plasticizers, which leads to a reduction of the mechanical properties [9]. However, these reductions in the mechanical properties are reversible; when the liquids are removed, wood re-densifies and regains its internal friction and thus recovers its strength accordingly.

Figure 2.12 presents a graph that represents the general correlation of moisture content with the mechanical properties of wood.

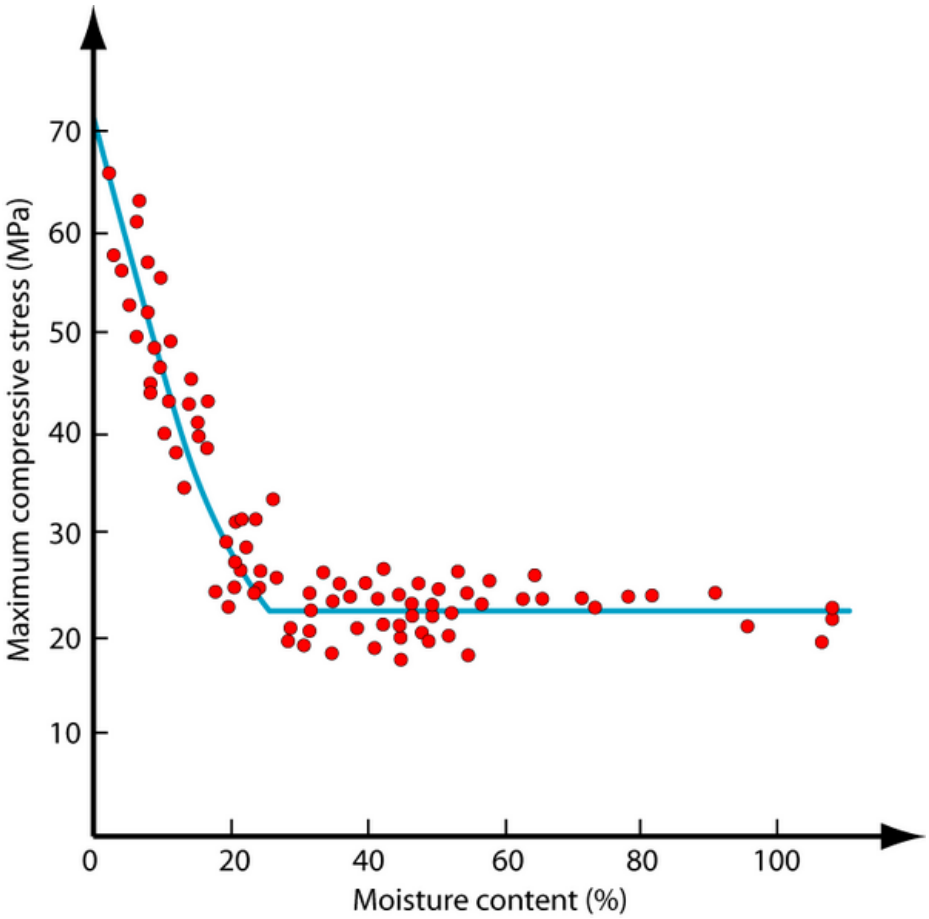


*Figure 2.12: Compressive stress vs water content* [10]

## 2.5 Wood treatment method to limit water absorption and enhance durability

Several methods have been suggested and tested to modify the hydrophilic nature of wood to remedy its inconveniences. However, none of these solutions have been able to significantly decrease the water uptake capacity of wood.

Currently, the available treatments to reduce wood's water absorption and extend its durability are: chemical, thermo-chemical, and impregnation modifications [6].

Some of the most relevant methods discovered and investigated to reduce wood's hydrophilic nature and limit its water uptake capacity will be discussed in the following sections.

### 2.5.1 Physical wood surface modification

#### 2.5.1.1 Coating

Superficial coatings are usually applied to help wood counteract harsh conditions and extend its lifespan. Coating of wood is amongst the most common routes that are taken to help prevent a high water uptake level in wood and to increase its durability. There is a vast selection of coating products that can be bought from hardware stores and applied to wood externally. Some of the conventional chemicals that are being used on the market are inorganic copper-based and organic creosote or pentachlorophenol preservatives which are hazardous to the environment and are receiving more and more restrictions on their use across the world [6].

These surface modifications create a hydrophobic surface that reduces the rate of water uptake, but they are unable to reduce the level of water absorption at saturation because a rise of the liquid through the fiber lumen can still occur [42]. The coatings are not truly effective due to an incompatibility of the products with wood. These treatments leave a gap between the inner wall of the wood's lumens and the product which allows water to penetrate [42]. As a result, over time, coated wood will swell the same as non-coated wood [43]. Additionally, the lifespan of the product is strongly dependent on the exposure of the wood to the environment. The product can also decay and wash away [43,44]. Therefore, for the best performance, the products need to be reapplied over time [44]. Additionally, the coating agents are usually toxic due to the chemicals involved [45].

### 2.5.2 Chemical wood surface modification

The chemical modification method of wood relies on the reactivity of the hydroxyl groups of the wood's compositions [6]. Accordingly, these hydroxyls can be subjected to many chemical reactions such as etherification, esterification, or furfurylation. For hydrophobization purposes, these hydroxyl groups are targeted and converted into hydrophobic groups (for example, acetate), which helps limit wood's interaction with

moisture and improves dimensional stabilization and durability [46]. However, chemical treatment processes usually have adverse effects on the mechanical properties [6].

### 2.5.2.1 Acetylation

Acetylation is a prominent process that relies on the chemical modification (full or partial) of the wood cell wall [46]. The process has been around since 1928, when it was first introduced in Germany by Fuchs using acetic anhydride chemical agents and sulphuric acid as a catalyst. The process was then investigated over the years and carried out in a variety of different ways with different types of wood [46]. The research brought the technique to a scalable level bringing the initial high cost down and was brought to the market on the industrial level. The process can be done with or without catalysts. Nowadays, most acetylation reactions are carried out without the use of catalysts [4]. The process consists of the reaction of acetic anhydride with the accessible hydroxyl groups of the wood polymers (i.e., lignin and hemicellulose), resulting in their esterification. This process also results in the formation of acetic acid as a by-product [47] (see Figure 2.13).

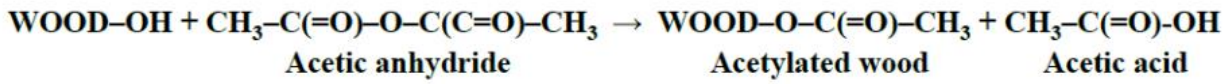


*Figure 2.13: Acetylation reaction of wood with acetic anhydride* [47]

The by-product of acetic acid has a strong smell and is unpleasant. Accordingly, it is usually removed from the final product after treatment. The process of acetylation is defined as a single-site reaction, meaning that one acetyl group interacts and is formed from one hydroxyl group; there is no polymerization process [47]. The dimensional stabilization of the wood is proportional to the weight percent gain of acetyl to the cell walls [47].

This process is complicated and patented. It also results in significant costs and is time-consuming. Additionally, there are some limitations with respect to the treatment of large wood pieces. As highlighted in the patent description, when subjecting large wood members to acetylation, only the wood's surface is subjected to acetylation with no depth of penetration. Accordingly, the middle section is often left with low to no acetylation resulting in an exterior envelope treatment only. Consequently, once the wood is cut or planned, the protection disappears as non-treated wood gets exposed.

### 2.5.2.2 Furfurylation

Furfurylation is a prominent process that relies on the chemical modification of the wood cell wall with furfuryl alcohol ($C_5H_6O_2$) [46]. Furfuryl alcohol is a liquid waste by-product from the agriculture of sugar cane and corn cobs. Furfurylation of wood is achieved by

impregnating wood with a mixture of furfuryl alcohol and a catalyst, and by applying heat to cause polymerization [48]. However, a change in the color of the wood can occur with respect to the high amount of catalyst. A higher amount of catalyst leads to an increase in red color [46].

Furthermore, the polymerization process in wood is complex and experts have different opinions on the extent of the chemical interaction with the wood cell walls [46]. The furfuryl alcohol complexes are found to predominantly deposit in the wood cavities and cell walls. Studies have found an increase in wood's hardness following the furfurylation process.

### 2.5.3 Thermal Treatment

The thermal modification of wood centers in increasing the wood temperature up to 150-240°C which leads to a molecular restructuration of the lignin, as well as a decrease in hydroxyl groups, and a degradation of amorphous carbohydrates [6]. The process is usually done in a controlled dry environment. In the end, the thermal treatment tends to increase the resistance of wood to moisture and to help enhance the dimensional stability. However, it may lead to a reduction of the mechanical properties [6].

### 2.5.4 Impregnation

The impregnation method is one of the most common and used wood treatments, it is also one of the oldest techniques applied to wood [6]. This method is still to this day among the most implemented techniques in the field of wood treatment. This technique consists of submerging wood in a pure liquid, or a solution containing active or passive ingredients, with the goal for them to penetrate and naturally diffuse through the wood's vascular system.

Usually, the impregnation solution consists of either biocidal agents, hydrophobization agents or flame-retardant compounds. Accordingly, the water-soluble chemicals then form bonds with the wood's surface, and the non-soluble and hydrophobic chemicals act as fillers clogging the pores. This technique can also be executed under vacuum pressures to enhance the process [6].

The typical conventional treated wood, which can be bought from the hardware store to withstand harsher environments, consists of pressure-treated wood of active alkaline copper quaternary (ACQ), copper azole (CA), or micronized copper azole (MCA) [49]. Pressure-treated wood helps reduce the wood's natural decay and interaction with moisture and also limits fungal and insect attacks. However, the treatment and treated wood are toxic. Such wood can't be used inside, and also the treatment can damage wood by inducing cracks and warping [49].

Research is trying to diverge from the conventional toxic chemicals and adapt to better environmentally friendly practices [6]. Over the years, various solutions for the wood impregnation process have been developed. Some of the prominent types of impregnations consist of silicate-based formulations. The silicate-based impregnations involve water glass-based formulation, alkoxysilane formulation and colloidal silica. With proper technique and curing, each of the mentioned formulations can lead to similar results with deposition of Silica particles ($SiO_2$) in the cell walls, lumens, and the pores of wood [6]. The treatments were found to prominently increase the dimensional stability of wood [6]. Having multiple advantages and versatility, researchers and industries are inclined to use this method to limit wood's water uptake [6]. The following sections will present Colloidal silica sol and the impregnation process concept.

#### 2.5.4.1 Colloidal silica Impregnation

One solution to mitigate the high water uptake capacity driven by capillary pressure in wood is to homogenously coat and impregnate the vascular system with a dense material [50]. Metal oxide ceramics are dense enough to obstruct the vascular system of wood [51]. Silicon dioxide ($SiO_2$) is a dense ceramic with a good chemical inertness [52,53], and has good compatibility with cementitious materials such as composite (e.g., Wood Wool panels).

The idea of silicate-modified wood has been around for centuries. Nevertheless, the idea took a more intensive step forward toward the end of the $20^{th}$ century with the development of nano-silica, sol-gel chemistry and wood nanotechnology. This development enabled the process of treatment with silica-based constituents [6].

Several methods have been developed to synthesize $SiO_2$, including the sol-gel technique, which involves a straightforward, effective, and economical method to produce ceramic coatings on objects with irregular geometries [54]. This method can also be used to impregnate the vascular system of natural fibers and wood [51].

The concept relies on impregnating wood with a colloidal solution of $SiO_2$ using a dip-coating technique. Due to the capillary action, wood can naturally absorb the solution. However, air entrapped within microscopic wood pores can impede the effective impregnation of the wood. To mitigate this issue and improve the effectiveness of the impregnation, the process can be conducted under vacuum. The use of a vacuum for impregnation will be discussed in the following section (see section 2.5.4.2). Another possibility to enhance the impregnation effectiveness is to repeat the impregnation process and cycle through it multiple times [6,55].

Once the wood has imbibed the solutions, the $SiO_2$ nanoparticles will agglomerate [56,57] to obstruct the vascular system of the wood.

There were some studies conducted in the past on silicate-modified wood, however, there is a need for an update of the data and further research development opportunities [6]. In general, silicate-modified wood has been found to exhibit higher mechanical properties, and to improve the biodegradation resistance and fire retardancy [6]. Generally, wood treated with silicate-based products also experiences an increase in density. Results showed that an increase of 40-60% can be obtained in the density followed by the silicate modification [6,58,59]. The research has also reported an increase in the surface hardness, mechanical strength (bending, compression, tensile, shear), and modulus of elasticity [6,60,61,62].

Colloidal silica nanoparticles' impregnation efficiency is dependent on the duration and the impregnation method condition, as well as the solid content of the colloidal solution and the type of wood [6,63]. The pH of the colloidal solution can have a key role on the effectiveness of the impregnation [6,64,65]. Neutral to mildly alkaline pH solutions of 7-9 can cause an accumulation of particles on the surface of the wood due to the neutralization of the solutions with the wood's acidic medium. Therefore, the treatment can simultaneously block the openings on the wood's surface and prevent the capillary uptake of the solutions into the lumens. Acidic colloidal solutions, on the other hand, do not significantly change pH when in contact with acidic wood's medium and thus can lead to better impregnation results. Parallelly, a higher pH of colloidal silica solution (closer to pH=11) could overcome this shortcoming and produce equally good impregnation results [6, 64]. However, a higher pH means exposure of wood to a strong alkaline solution which can cause its degradation.

### 2.5.4.2 Vacuum-aided colloidal silica Impregnation

Vacuum pressure can enhance the impregnation process and can achieve a significant improvement [6,62,63,64,65,66,67]. Applying vacuum pressure during impregnation removes the entrapped air from the wood which allows the solutions to permeate freely inside the vascular system resulting in an effective impregnation of the substrates.
Table 2.3 presents some relevant studies which show prominent results on the impregnation of wood with silicate-based solutions using vacuum pressures.

*Table 2.3: Wood vacuum $SiO_2$ impregnation studies*

| Type of wood | Impregnation substrate | Impregnation Vacuum / pressure(s) | Retention time | Tested properties | Outcomes | Ref |
|---|---|---|---|---|---|---|
| Sapwood of Pine | Levasil 200S 30%, pH 7 | -7 mbar vacuum + Atmospheric pressure | 15 min under vacuum + 2h under atmospheric | Water uptake | Significant reduction | [68] |

| | | | | | | |
|---|---|---|---|---|---|---|
| Sapwood of Pine | $SiO_2$ solution of 15% by weight | -52 kPa vacuum + Different pressures (30kPa, 60 kPa, 125 kPa) | 5 min under vacuum + 5 min under pressure | Impregnation Efficiency | Significant for all pressures | [69] |
| Sapwood of Poplar | Mixture of Nano-$SiO_2$ (particle diameter: 15 ± 5 nm; Shanghai Maikun Chemical Co. Ltd., China) and Furfuryl alcohol (chemical purity 98.0%; Sinopharm Chemical Reagent Co., Ltd., China) | -0.1 Bar vacuum | 60 min under vacuum | Surface hardness<br>Water uptake<br>Anti-swelling | All improved | [70] |
| Ganitri | Mixture of furfuryl alcohol (FA) and nano-$SiO_2$ (particle diameter 15 ± 5 nm; Anhui Elite Industrial Co., Ltd, China) | -0.5 bar vacuum + 2.5 bar pressure | 60 min under vacuum + 120 min under pressure | Weight percent gain<br>Anti-swelling efficiency<br>Water uptake<br>Density | Nano-$SiO_2$ was found throughout the lumens and pits of the impregnated wood.<br>Significant positive effect on the properties. | [71] |
| Chinese Fir | Nano silica sol, purchased from Qingdao Hengshengda Chemical Co., Ltd., Qingdao, Shandong Province, China. pH 6.97, solid content 21.24% | -0.09 MPa Vacuum + 1 MPa pressure | 10 min under vacuum + Different times (30, 60, 90 min) under pressure | Impregnation efficiency<br>Hardness<br>Bending Strength | Efficiency of impregnation increased with vacuum time. The $SiO_2$ was significantly combined with the surface of the cell lumen. Significant improvement of the properties and increase of hydrophobicity. | [72] |
| Sapwood of Rubber Wood | $SiO_2$ precursor solution made in lab | -0.08 MPa vacuum | 2h under vacuum | Heat treatment effect on mechanical and thermal properties. | Impregnation helped reduce the impact of heat treatment degradation and improved properties. | [73] |
| Simul Wood | Mixture of styrene acrylonitrile copolymer, c-methacryloyloxy trimethyl silane-modified $TiO_2$, $SiO_2$ nanoparticles and nanoclay intercalating. | Unspecified vacuum + Atmospheric pressure | Short time under vacuum + 4h under pressure | Water uptake<br>Anti-swelling | Improved | [74] |

| | | | | | | |
|---|---|---|---|---|---|---|
| Sengon Wood | Monoethylene glycol (MEG) and nano silica, MNano-Silica 0.5%, MNano-Silica 0.75%, and MNano-Silica 1% | -0.5 bar vacuum + 2.5 bar pressure | 60 min under vacuum + 120 min under pressure | Dimensional stability<br>Density | Full coverage of the pits on the vessel walls was observed.<br>Significant positive effect on the properties. | [75] |
| Sengon Wood | Monoethylene glycol (MEG) and nano silica | -0.5 bar vacuum + 2.5 bar pressure | 60 min under vacuum + 120 min under pressure | Weight percent gain<br>Density<br>Modulus of elasticity<br>Modulus of rupture<br>Hardness | Significant positive effect and increase of the properties. | [76] |
| Beech and Scots Pine Sapwood | Two substrate were used.<br>1. Pure emulsion of modified (hydrophobized) silica nanoparticles (carrier material: ethanol),<br>2. Modified (hydrophobized) silica nanoparticles in tetrahydrofuran carrier material in combination with polydimethylsiloxane (PDMS) as a bonding agent. | -100 mbar vacuum + Atmospheric pressure | 20 min under vacuum + 60 min under atmospheric | Dimensional stability<br>Water uptake | Significantly Improved | [77] |
| Poplar Wood | Colloidal silica, concentration 1.7%, average size 34 nm, pH 7 and styrene monomers | -0.8 bar vacuum + 8 bar pressure | 30 min vacuum + 1h pressure | Density<br>Modulus of elasticity<br>Modulus of Rupture<br>Hardness<br>Compression<br>Water uptake<br>Dimensional stability | Significantly Improved | [78] |

| | | | | | | |
|---|---|---|---|---|---|---|
| Sugar Maple | Sols of metal oxides (AlO(OH), $SiO_2$, and $ZrO_2$) | -81.2 MPa vacuum + Atmospheric pressure | 1h under vacuum + 2h under atmospheric | Hardness | Improved | [79] |
| Oak and Spruce | Silica including sodium metasilicate ($Na_2SiO_3$), a colloidal suspension of silica, tetraethoxysilane (TEOS), a mixture of TEOS with methyltriethoxysilane (MTEOS), and silica sol with three different particle sizes. | -100 mbar vacuum | 10 min under vacuum | Water uptake<br><br>Hardness | Significantly improved | [80] |
| Poplar | Mixture of Furfuryl alcohol (chemical purity 98.0%; Sinopharm Chemical Reagent Co., Ltd., China), nano-$SiO_2$ (particle diameter: 15 ± 5 nm; Shanghai Maikun Chemical Co., Ltd., China), maleic anhydride, and disodium tetraborate (analytically pure, Beijing Chemical Works, China) were used during these studies. 30 wt% FA solutions containing 0, 1.0 and 2.0 wt% nano-$SiO_2$, respectively. | -0.095 MPa vacuum + Atmospheric pressure | 30 min under vacuum + 2h under pressure | Dynamic mechanical properties<br><br>Thermal stability | Significantly improved | [81] |

## 2.6 Colloidal nanoparticles ($SiO_2$)

### 2.6.1 Silicon source

Silicon is rarely found free in the environment, it is usually found combined with oxygen ($SiO_2$) or other elements as silicate minerals (quartz, and feldspars). These silicate minerals are abundant within the earth's crust, they account for approximately 90% of its

weight, making Silicon readily available [82]. Silica sand, also known as quartz sand (a crystalline form of $SiO_2$), is readily available across the world and is currently the main source of raw materials for Silicon and Silicon-based products [6]. Accordingly, it is readily available and affordable.

### 2.6.2 Colloidal Silica Solutions

A colloidal silica solution consists of a mixture of dense, amorphous particles of $SiO_2$ [6]. Colloidal silica solutions exist according to different particle size ranges, solid weight % content, and pH and are readily available on the commercial market. Colloidal silicate solution particles usually vary from a few nanometers to 100nm, but can also include particle sizes up to 10µm [6]. Colloidal silica solution is compatible with wood impregnation as its particles are of adequate size for the wood's pore sizes and distributions, varying from 2nm to 58µm (58000nm) [6,17].

### 2.6.3 Stability & Non Toxicity, Environmental Friendly

Studies show that silicate compounds and colloidal silica are safe and approved to use and exploit in a multitude of different applications [6], which is a must for the development of sustainable building materials. Therefore, their exploitations are optimal and have no adverse effect on the environment, which is a significant advantage compared to the conventional harmful chemical currently used for wood treatments.

## 2.7 Gap of knowledge

One prospect solution to limit wood's water uptake and enhance its mechanical properties involves $SiO_2$ nanoparticle impregnation. This concept has been under investigation in the past and has shown promising results. This method has been proven effective in the past in reducing wood's water uptake capacity and enhance some of its mechanical properties. However, the research and studies on silicate-modified wood ($SiO_2$ impregnation) are limited and have yet to reveal the effect of vacuum pressures on the effectiveness of the impregnations. The research still has some limitations and a lack of knowledge regarding the effect of $SiO_2$ impregnation on wood's impact and viscoelastic properties and the synergistic effect with humidity. There is a need to update the results and an opportunity to further push the research for new findings [6].

## 2.8 Reference

1. Mbala, M., Aigbavboa, C., Aliu, J. (2019). Reviewing the Negative Impacts of Building Construction Activities on the Environment: The Case of Congo. In Charytonowicz, J., Falcão, C. (Eds.), *Advances in Human Factors, Sustainable Urban Planning and Infrastructure. AHFE 2018. Advances in Intelligent Systems and Computing*, vol 788 (pp. 111-117). Springer, Cham. doi: https://doi.org/10.1007/978-3-319-94199-8_11

2. Atlantic WoodWORKS!. (2017). WOOD FOR MID-RISE CONSTRUCTION. doi: https://wood-works.ca/wp-content/uploads/160601-Wood-4-Mid-Rise-Report-FINAL-2017-03-28-sm.pdf

3. Canadian Wood Council. (2022). Canadian Species. Retrieved from https://cwc.ca/en/how-to-build-with-wood/wood-products/lumber/grades/canadian-species/

4. Rowell, Roger M. (2012). *Handbook of Wood Chemistry and Wood Composites* (2nd ed.). Boca Raton: CRC Press.

5. Brunner M. (2000). On The Plastic Design Of Timber Beams With A Complex Cross-Section. Paper presented at the World Conference on Timber Engineering, British Columbia, Canada, July 31–August 3 2000.

6. Yona, A.M.C., Žigon, J., Matjaž, P. et al. (2021). Potentials of silicate-based formulations for wood protection and improvement of mechanical properties: A review. *Wood Science and Technology, 55*, 887–918. doi: https://doi.org/10.1007/s00226-021-01290-w

7. Canada Mortgage and Housing Corporation. (2013). *CANADIAN WOOD-FRAME HOUSE CONSTRUCTION* (3rd ed.). Canada: Library and Archives Canada Cataloguing in Publication.

8. Di Blasi C, Galgano A, Branca C. (2009). Influences of the chemical state of alkaline compounds and the nature of alkali metal on wood pyrolysis. *Industrial & Engineering Chemistry Research, 48*, 3359–3369. doi: 10.1021/ie801468y

9. Kretschmann, David E. (2010). Chapter 5 Mechanical properties of wood. In Centennial (Ed.), *Wood handbook: wood as an engineering material* (pp. 5.1-5.46). Madison, WI: U.S. Dept. of Agriculture, Forest Service, Forest Products Laboratory.

10. University of Cambridge. (2020). Water's effect on the mechanical behaviour of wood. In: Dissemination of IT for the Promotion of Materials Science (DoITPoMS). doi: https://www.doitpoms.ac.uk/tlplib/wood/water_effect.php.

11. David W. Green, Jerrold E. Winandy, and David E. Kretschmann. (1999). Chapter 4 - Mechanical Properties of Wood. In Forest Product Laboratory. *Wood Handbook*

- *Wood as an Engineering Material* (463). Madison, WI: U.S. Department of Agriculture, Forest Service. doi: https://www.fpl.fs.fed.us/documnts/fplgtr/fplgtr113/fplgtr113.pdf

12. Wagner et al. (2015). Effect of Water on the Mechanical Properties of Wood Cell Walls – Results of a Nanoindentation Study. *BioResources, 10*(3), 4011-4025. doi: 10.15376/biores.10.3.4011-4025

13. Reinprecht, L. (2016). *Wood deterioration, protection and maintenance*. Wiley, UK: Wiley Blackwell.

14. BUILDEROLOGY. (2018). Types of wood and their uses. Retrieved from: https://builderology.com/types-of-

15. Thomas, R.J. (1977). Chapter 1 Wood: Structure and Chemical Composition. In Irvin S. Goldstein (Ed.), *Wood Technology: Chemical Aspects* (pp. 1-23). Washington, DC: American Chemical Society. doi: 10.1021/bk-1977-0043.ch001

16. Britannica. (2022). Wood as a material. Retrieved from https://www.britannica.com/science/wood-plant-tissue/Wood-as-a-material

17. Plötze M, Niemz P. (2011). Porosity and pore size distribution of different wood types as determined by mercury intrusion porosimetry. *European Journal of Wood and Wood Product, 69*, 49–657. doi: https://doi.org/10.1007/s00107-010-0504-0

18. Bajpai, P. (2018). *Biermann's Handbook of Pulp and Paper* (3rd ed.). Elsevier. doi: https://doi.org/10.1016/C2017-0-00513-X

19. GGST DT. (2022). 4.2b Timber. Retrieved from https://www.ggspdt.com/42b-timber.html

20. Meng, Z., Zheng X., Tang K., Liu J., Qin S. (2012). Dissolution of natural polymers in ionic liquids: A review. *E-polymers, 12* (1). doi: 10.1515/epoly.2012.12.1.317

21. Alonso, D.M., Wettstein, S.G., Dumesic, J.A. (2012). Bimetallic catalysts for upgrading of biomass to fuels and chemicals. *Chemical Society Reviews*, *41*(24), 8075–8098. doi: https://doi.org/10.1039/C2CS35188A

22. G.T Kirker, A.B. Blodgett, R.A. Arango, P.K. Lebow, C.A. Clausen. (2013). The role of extractives in naturally durable wood species. *International Biodeterioration & Biodegradation, 82*, 53-58. doi: https://doi.org/10.1016/j.ibiod.2013.03.007

23. Boruvka, V., Novák, D., Šedivka, P. (2020). Comparison and Analysis of Radial and Tangential Bending of Softwood and Hardwood at Static and Dynamic Loading. *Forest*, *11*, 896. doi:10.3390/f11080896

24. Tschoegl, N.W. (1989). Energy Storage and Dissipation in a Linear Viscoelastic Material. In: The Phenomenological Theory of Linear Viscoelastic Behavior. Springer, Berlin, Heidelberg. doi: https://doi.org/10.1007/978-3-642-73602-5_9

25. Lakes, R.S. (2009). *Viscoelastic materials* (1st). New York, NY: Cambridge University Press

26. TA Instruments. (2016). Dynamic Mechanical Analysis Basic Theory & Applications Training. Retrieved from https://people.clarkson.edu/~skrishna/DMA_Basic_Theory_Applications.pdf

27. Placet, V., Passard, J. & Perré, P. (2008). Viscoelastic properties of wood across the grain measured under water-saturated conditions up to 135 °C: evidence of thermal degradation. *Journal of Materials Science, 43***,** 3210–3217. doi: https://doi.org/10.1007/s10853-008-2546-9

28. Placet, V., Passard, J., Perré, P. (2008). Viscoelastic properties of wood across the grain measured under water-saturated conditions up to 135°C: evidence of thermal degradation. *Journal of Materials Science, 43*, 3210-3217. doi: https://doi.org/10.1007/s10853-008-2546-9

29. Placet, V., Passard, J., Perré, P. (2007). Viscoelastic properties of green wood across the grain measured by harmonic tests in the range 0–95°C: Hardwood vs. softwood and normal wood vs. reaction wood. *Holzforschung, 61*(5), 548-557. doi: 10.1515/HF.2007.093

30. Fathi, H., Kazemirad, S., Nasir, V. (2020). A nondestructive guided wave propagation method for the characterization of moisture-dependent viscoelastic properties of wood materials. *Materials and Structures, 53*, 147. doi: https://doi.org/10.1617/s11527-020-01578-6

31. Li, Z., Jiang, J., Lyu, J., Cao, J. (2021). Comparative investigation on the orthotropic viscoelastic properties of wood during cooling and heating variations. Wood *Material and Science & Engineering*, 1-7. doi: https://doi-org.proxy.bib.uottawa.ca/10.1080/17480272.2021.2017478

32. Li, Z., Jiang, J., Lyu, J. (2019). The orthotropic viscoelastic properties of Chinese fir wood during the temperature ramping process. *Drying Technology, 38*(11), 1411-1420. doi: https://doi.org/10.1080/07373937.2019.1642913

33. Bučar, D. G., and Merhar, M. (2015). Impact and Dynamic Bending Strength Determination of Norway Spruce by Impact Pendulum Deceleration. *Bioresources 10*(3), 4740-4750. doi: https://bioresources.cnr.ncsu.edu/resources/impact-and-dynamic-bending-strength-determination-of-norway-spruce-by-impact-pendulum-deceleration/

34. Mindess, S., and Madsen, B. (1986). The fracture of wood under impact loading. *Material and Structures, 19*(109), 49-53. doi: 10.1007/BF02472310

35. Jansson, B. (1992). Impact loading of timber beams. Master's Thesis, Faculty of Civil Engineering, University of British Columbia, Vancouver, Canada.

36. Leijten, Ad. J. M. (2000). Literature review of impact strength of timber and joints. *Proceedings of the World Conference on Timber Engineering*, Whistler, BC.

37. Adamopoulous, S., Passialis, C. (2010). Relationship of toughness and modulus of elasticity in static bending of small clear spruce wood specimens. *European Journal of Wood and Wood Products, 68*, 109-111. doi: https://doi.org/10.1007/s00107-009-0365-6

38. Buča, D.,G., Merhar, M. (2015). Impact and Dynamic Bending Strength Determination of Norway Spruce by Impact Pendulum Deceleration. *BioResources, 10*(3), 4740-4750. doi: 10.15376/biores.10.3.4740-4750

39. Kubojima, Y., Okano., T., Ohta., M. (2000). Bending strength and toughness of heat-treated wood. *Journal of Wood Science, 46*, 8-15. doi: https://doi.org/10.1007/BF00779547

40. Gaff, M., Kačík., F., Gašparík., M. (2019). Impact of thermal modification on the chemical changes and impact bending strength of European oak and Norway spruce wood. *Composite Structures, 216*, 80-88. doi: https://doi.org/10.1016/j.compstruct.2019.02.091

41. Moreira, A., P., Silveira, E., d., Almeida, D., H., d., Almeida, T., H., Panzera, T., H., Christofo, A., L., Rocco, F., A., R. (2017). Toughness and Impact Strength in

Dynamic Bending of Wood as a Function of the Modulus of Elasticity and the Strength in Compression to the Grain. *International Journal of Materials Engineering, 7*(4), 61-67. doi:10.5923/j.ijme.20170704.01

42. Denes AR, Tshabalala MA, Rowell R, et al. (1999). Hexamethyldisiloxane-plasma coating of wood surfaces for creating water repellent characteristics. *Holzforschung*, *53(3)*, 318–326. doi: 10.1515/hf.1999.052

43. Rowell RM, Banks WB. (1985). Water repellency and dimensional stability of wood. *Forest Products Laboratory*. doi: 10.2737/fpl-gtr-50

44. Beaulieu D, Biermeier D. (2020). How to Seal a Deck With Thompson's WaterSeal. In: The Spruce. doi: https://www.thespruce.com/seal-a-deck-with-thompsons-water-seal-2131998.

45. Williams RS, Feist WC. (1999). Water repellents and water-repellent preservatives for Wood. *Forest Products Laboratory*. doi: 10.2737/fpl-gtr-109

46. Mantanis, George. I. (2017). Chemical Modification of Wood by Acetylation or Furfurylation: A Review of the Present Scaled-up Technologies. *Bioresources*, *12*(2), 4478-4489. doi 10.15376/biores.12.2.Mantanis

47. Rowell, Roger. M. (1983). *Handbook of Wood Chemistry and Wood Composite*s. Boca Raton: CRC Press.

48. Schneider, M.H. (1995). New cell wall and cell lumen wood polymer composites. *Wood Science and Technology*, *29*, 121-127. doi: https://doi.org/10.1007/BF00229341

49. The Home Depot. (2022). Types of Pressure-Treated Wood. Retrieved from https://www.homedepot.com/c/ab/types-of-pressure-treated-wood/9ba683603be9fa5395fab9052c50759

50. Choong, E. T. and F. O. Tesoro. 1989. Relationship of Capillary Pressure and Water Saturation in Wood. *Wood Science and Technology, 23*, 139–50. doi: https://doi.org/10.1007/BF00350936

51. Boulos L, Foruzanmehr MR, Tagnit-Hamou A, et al. (2017). Wetting analysis and surface characterization of flax fibers modified with zirconia by sol-gel method.

*Surface and Coatings Technology, 313*, 407–416. doi: 10.1016/j.surfcoat.2017.02.008

52. Shi X, Dalai NS, Hu XN, Vallyathan V. (1989). The chemical properties of silica particle surface in relation to silica-cell interactions. *Journal of Toxicology and Environmental Health*, *27*, 435–454. doi: 10.1080/15287398909531314

53. Meire R. da Silva, Bruno H. Fumes, Carlos E.D. Nazario, Fernando M. Lancas. (2017). Chapter Eighteen – New Materials for Green Sample Preparation: Recent Advances and Future Trends. *Comprehensive Analytical Chemistry, 76*, 575–599. doi: https://doi.org/10.1016/bs.coac.2017.03.003

54. Gao, Zhengxin, Xianglin Zhai, and Chengyu Wang. (2015). Facile Transformation of Superhydrophobicity to Hydrophilicity by Silica/Poly (ε-Caprolactone) Composite Film. *Applied Surface Science, 359*, 209–214. doi: https://doi.org/10.1016/j.apsusc.2015.09.246

55. Locs J, Berzina-Cimdina L, Zhurinsh A, Loca D. (2008). Effective impregnation of $SiO_2$ Sol-Gel solution in pine wood and following Gel localization in free cell volume. *Advances Science Technology, 58*, 72–77. doi: https://doi.org/10.4028/www.scientific.net/AST.58.72

56. Bücker, M., Jäger, C., Pfeifer, D. *et al.* (2014). Evidence of Si–O–C bonds in cellulosic materials modified by sol–gel-derived silica. *Wood Science and Technology, 48***,** 1033–1047. doi: https://doi-org.proxy.bib.uottawa.ca/10.1007/s00226-014-0657-9

57. Unger, B., Bücker, M., Reinsch, S. *et al.* (2013). Chemical aspects of wood modification by sol–gel-derived silica. *Wood Science and Technology, 47***,** 83–104 (2013). doi: https://doi-org.proxy.bib.uottawa.ca/10.1007/s00226-012-0486-7

58. Li P, Zhang Y, Zuo Y, Lu J, Yuan G, Wu Y. (2020). Preparation and characterization of sodium silicate impregnated Chinese fir wood with high strength, water resistance, flame retardant and smoke suppression. *Journal of Materials Research Technology, 9*(1), 1043–1053. doi: https://doi.org/10.1016/j.jmrt.2019.10.035

59. Zhou Y, Zhang Y, Zuo Y, Wu Y, Yuan G, Li X. (2020). Construction of a network structure in Chinese fir wood by $Na_2SiF_6$ crosslinked $Na_2SiO_3$. *Journal of Materials*

*Research and Technology, 9*(6), 14190–14199. doi: https://doi.org/10.1016/j.jmrt.2020.10.033

60. Chen H, Zhang Y, Zhong T, Wu Z, Zhan X, Ye J. (2020). Thermal insulation and hydrophobization of wood impregnated with silica aerogel powder. *Journal of Wood Science, 66*, 81. doi: https://doi.org/10.1186/s10086-020-01927-7

61. Nguyen TT, Xiao Z, Che W, Trinh HM, Xie Y. (2019). Effects of modification with a combination of styrene-acrylic copolymer dispersion and sodium silicate on the mechanical properties of wood. *Journal of Wood Science, 65*(1), 1–11. doi: https://doi.org/10.1186/s10086-019-1783-7

62. Xu E, Zhang Y, Lin L. (2020). Improvement of mechanical, hydrophobicity and thermal properties of chinese fir wood by impregnation of nano silica sol. *Polymers, 12*(8), 1632. doi: https://doi.org/10.3390/polym12081632

63. Mahltig B, Swaboda C, Roessler A, Böttcher H. (2008). Functionalising wood by nanosol application. *Journal of Materials Chemistry, 18*(27), 3180–3192. doi: 10.1039/b718903f

64. Jiang J, Cao J, Wang W. (2018). Characteristics of wood-silica composites influenced by the pH value of silica sols. *Holzforschung, 72*(4), 311–319. doi: https://doi.org/10.1515/hf-2017-0126

65. Pries M, Mai C. (2013). Treatment of wood with silica sols against attack by wood-decaying fungi and blue stain. *Holzforschung, 67*(6), 697–705. doi: 10.1515/hf-2012-0133

66. Palanti S, Vignali F, Elviri L, Lucchetti C, Mucchino C, Predieri G. (2017). Effect of amine functionalization and ageing on copper and boron leaching from wood preservatives grafted to siloxane networks. *BioResources, 12*(3), 4943–4957. doi 10.15376/biores.12.3.4943-4957

67. Pries M, Mai C. (2013). Fire resistance of wood treated with a cationic silica sol. *European Journal of Wood and Wood Products, 71*, 237–244. doi: 10.1007/s00107-013-0674-7

68. Pries, M., Mai, C. (2013). Fire resistance of wood treated with a cationic silica sol. *European Journal of Wood and Wood Products, 71*, 237–244. doi: https://doi.org/10.1007/s00107-013-0674-7

69. Locs, J., Berzina-Cimdina, L., Zhurinsh, A., Loca, D. (2009). Optimized vacuum/pressure sol impregnation processing of wood for the synthesis of porous, biomorphic SiC ceramics. *Journal of the European Ceramic Society, 29*(8), 1513-1519. doi: https://doi.org/10.1016/j.jeurceramsoc.2008.09.013

70. Dong, Y., Yan, Y., Zhang, S., Li, J. (2014). Wood/Polymer Nanocomposites Prepared by Impregnation with Furfuryl Alcohol and Nano-$SiO_2$. *BioResources, 9*(4), 6028-6040. doi: https://ojs.cnr.ncsu.edu/index.php/BioRes/article/view/5757

71. Rahayu, I., S., Wahyuningtyas, I., Zaini, L.,H., Darmawan, W., Maddu, A., Prihatini, E. (2021). Physical Properties of Impregnated Ganitri Wood by Furfuryl Alcohol and Nano-$SiO_2$. *IOP Conference Series Earth and Environmental Science, 891*(1), 01201. doi:10.1088/1755-1315/891/1/012012

72. Xu, E., Zhang, Y., Lin, L. (2020). Improvement of Mechanical, Hydrophobicity and Thermal Properties of Chinese Fir Wood by Impregnation of Nano Silica Sol. *Polymers, 12*(8), 1632. doi: https://doi.org/10.3390/polym12081632

73. Zhang, N., Cai, L. (2019). Improvement of mechanical, humidity resistance and thermal properties of heat-treated rubber wood by impregnation of $SiO_2$ precursor. *Scientific Reports, 9*, 982. doi: https://doi.org/10.1038/s41598-018-37363-3

74. Devi, R., R., Maji, T., K. (2013). Effect of nanofillers on flame retardancy, chemical resistance, antibacterial properties and biodegradation of wood/styrene acrylonitrile co-polymer composites. *Wood Science and Technology, 47*, 1135-1152. doi: https://doi.org/10.1007/s00226-013-0563-6

75. Rahayu, I., Dirna, F., C., Maddu, A., Darmawan, W., Nandika, D., Prihatini, E. (2021). Dimensional Stability of Treated Sengon Wood by Nano-Silica of Betung Bamboo Leaves. *Forest, 12*(11), 1581. doi: https://doi.org/10.3390/f12111581

76. Rahayu, I., Pratta, A., Darmawan, W., Nandika, D., Prihatini, E. (2021). Characteristics of impregnated wood by nano silica from betung bamboo leaves. *IOP Conference Series Earth and Environmental Science, 891*(1), 012019. doi:10.1088/1755-1315/891/1/012019

77. Bak, M., Molnár, F., Németh, R. (2018). Improvement of dimensional stability of wood by silica nanoparticles. *Wood Material Science & Engineering, 14*(1), 48-58. doi: https://doi.org/10.1080/17480272.2018.1528568

78. Ghorbani, M., Biparva, P., Hosseinzadeh, S. (2018). Effect of colloidal silica nanoparticles extracted from agricultural waste on physical, mechanical and antifungal properties of wood polymer composite. *European Journal of Wood and Wood Products, 76*, 749–757. doi: https://doi.org/10.1007/s00107-017-1157-z

79. Landry, V., Blanchet, P., Boivin, G. (2013). Metal Oxide Sol-Gels ($ZrO_2$, AlO(OH), and $SiO_2$) to Improve the Mechanical Performance of Wood Substrates. *Journal of Nanoparticles, 2013*, 1-8. doi: https://doi.org/10.1155/2013/273204

80. Götze,J., Möckel, R., Langhof, N., Hengst, M., Klinger, M. (2008). SILICIFICATION OF WOOD IN THE LABORATORY. Ceramics Silikaty, 52(4), 268-277. doi: https://www.researchgate.net/publication/288119119_Silicification_of_wood_in_the_laboratory

81. Dong, Y., Shen, X., Zhang, S., Li, J. (2015). Dynamic mechanical properties and thermal stability of furfuryl alcohol and nano-$SiO_2$ treated poplar wood. *IOP Conference Series Materials Science and Engineering, 87*(1), 012027. doi:10.1088/1757-899X/87/1/012027

82. Rafferty, JP. (2012). *Minerals* (1st ed.). New York, NY: Britannica Educational Publishing.

# CHAPTER 3

## The impact of vacuum pressure on the effectiveness of $SiO_2$ impregnation of spruce wood

## CHAPTER 3

## 3.0 The impact of vacuum pressure on the effectiveness of $SiO_2$ impregnation of spruce wood*

### 3.1 Abstract

Wood is a widely used construction material that has many advantageous properties. However, it suffers from weaknesses such as low dimensional stability and low durability in humid environments. These issues are associated with the porous vascular structure of wood that leads to a high water uptake capacity. This research aims to reduce the water uptake capacity of spruce wood by dip-coating samples in an aqueous colloid of silicon dioxide ($SiO_2$) nanoparticles. $SiO_2$ is a dense ceramic material with good chemical stability. It is readily available and affordable, making it an excellent candidate for this application. This study investigates the effect of $SiO_2$ impregnation on the physico-mechanical properties of spruce wood. Density measurements, water uptake tests, microscopy examination, thermogravimetric analysis (TGA), and dynamic mechanical analysis (DMA) were conducted on non-treated and $SiO_2$-treated spruce wood samples. Quantitative and qualitative analyses demonstrated that $SiO_2$ impregnation performed under higher vacuum pressure was more effective compared to the atmospheric condition and exhibited a greater presence of $SiO_2$ in the wood's vascular system. $SiO_2$ impregnation under vacuum pressure demonstrated an effective increase in the density of the wood. It also reduced the porosity, which led to a significant reduction in the water uptake of the spruce wood. The analysis of the wood's viscoelastic properties revealed that $SiO_2$ impregnation under atmospheric and vacuum conditions triggered two different reinforcing mechanisms. The results showed that a significant improvement of the spruce wood's Storage and Loss modulus could be achieved when impregnation was performed at the highest vacuum pressure of -90 kPa.

### 3.2 Keywords

Spruce Wood; $SiO_2$ Nanoparticles; Vacuum-aided Impregnation; Dynamic Mechanical Analysis; Water Uptake; Sustainability.

### 3.3 Introduction

Wood is a naturally occurring engineering material that features a high specific strength as well as excellent thermal insulating properties [1,2]. These factors, along with the environmental sustainability and short construction time of wood [2], have made it an attractive material in the construction industry [2,3]. Despite numerous advantages, wood also has some drawbacks. First, it has low durability in alkaline environments due to the presence of cellulose in its structure. Cellulose is a hydrophilic polymer with weak glycosidic bonds susceptible to hydrolysis [4]. Second, the viscoelastic behaviour of this hydrophilic polymer makes it prone to low dimensional stability [5,6]. Water molecules can act as plasticizers between the long cellulose molecular chains and introduce spaces that induce swelling. Moreover, wood possesses a porous structure with many lumens (tubular cavities inside the wood fibers). This creates a pathway for water to penetrate through

* A copy of this article was submitted to the journal of Wood Science and Technology.

capillary action [7]. Third, the mechanical properties of wood are dependent on its moisture content. Higher moisture content leads to a lower Storage modulus, higher Loss modulus, and higher ductility [8]. Finally, wood is susceptible to attacks by biological agencies such as fungi and insects [9]. The biological deterioration of wood strongly depends on the presence of moisture in its structure.

One of the best-known solutions to help prevent a high water uptake level in wood and increase its durability is to modify the wood's surface using water repellents and physico-chemical treatments. These treatments usually involve the implementation of toxic chemical mixtures, consisting of a binder and a water-repellent component such as wax [10]. However, these treatments can only create a hydrophobic surface that reduces the rate of water uptake [7]. They do not significantly decrease the water uptake capacity of wood due to the incompatibility of hydrophobic products with the hydrophilic nature of wood. They cannot entirely obstruct the vascular system of wood and leave a gap for water to penetrate [11]. Over time, treated wood will swell as much as non-treated wood [7]. Furthermore, the performance of physico-chemical treatments is dependent on the environmental conditions the wood is subjected to, and the coating product may decay or be washed away over time [12]. Consequently, such coatings need to be reapplied over the years to maintain optimal performance [12].

These shortcomings could be mitigated by homogenously coating and impregnating wood with a dense material to obstruct its vascular system [13]. Ceramic nanoparticles in an aqueous colloid state can be used to fill this porous vascular structure [14]. Silica ($SiO_2$) is an abundant inert ceramic with high fire resistance [14,15]. It also exhibits an acceptable resistance to alkaline environments [16,17]. These properties make $SiO_2$ colloids ideal candidates for an impregnation process. Through this process, the wood imbibes a colloidal solution through the vascular system. As the solvent evaporates, the nanoparticles agglomerate, fill the lumens, and obstruct the vascular structure.

Some research has already been conducted in this area. In these studies, the wood was successfully impregnated with $SiO_2$ colloids under vacuum, and the physical and mechanical properties of the wood were characterized [18,19,20,21]. However, none of these studies investigated the use of vacuum pressure to increase the effectiveness of $SiO_2$ impregnation. Accordingly, the novelty of this research is to study the effect of vacuum pressure on the effectiveness of the impregnation process for finding the optimal impregnation condition under vacuum. Moreover, research has yet to reveal the impact of vacuum-aided impregnation on the viscoelastic properties of wood.

The focus of this research is to overcome wood's weakness by reducing its water uptake capacity through an impregnation process. The primary objective is to investigate the effect of vacuum on the $SiO_2$ impregnation of wood by measuring the density and water uptake capacity of samples before and after impregnation treatment under atmospheric and three vacuum pressures to find the optimal vacuum impregnation pressure. The secondary objective of this work is to identify changes in the viscoelastic properties of wood as a result of $SiO_2$ vacuum-aided impregnation. This study could pave the way for multiple materials and applications where the simultaneous elastic behaviour of wood and its damping energy is needed. It could also pave the way for research on the synergistic effects of $SiO_2$ impregnation on the water uptake and viscoelastic behaviour of wood.

## 3.4 Methodology

### 3.4.1 Materials

The samples used in this study were prepared from spruce wood of the Picea glauca species, commonly known as Canadian spruce or White spruce. Spruce is the most frequently used type of wood in construction in eastern Canada. LUDOX HS-40 colloidal silica, a water-based colloidal suspension of nano-silica, was used as an impregnation solution. This suspension contained a 40% solution of 12 nm $SiO_2$ particles, with a pH of 9.5, and has an aqueous density of 1.3 g/cm$^3$ at 25°C. The solution was purchased from Sigma-Aldrich.

### 3.4.2 Sample Preparation

The wood specimens were cut and sanded to the required dimensions for the tests and characterization techniques. The samples' dimensions (length x width x thickness) were: (25mm x 10mm x 2mm) for dynamic mechanical analysis, (33mm x 14.5mm x 14.5mm) for pycnometry, and (3mm x 2mm x 1mm) for tensiometry. The samples were progressively sanded using sandpaper with grits of 80, 100, 120, 220, and 600 to remove any residues on the specimens and reach a consistent surface roughness. The length of the samples was cut along the longitudinal wood fibers' axis, and the base cross-section (width and thickness) was in the tangential-radial plane. The samples were placed in an oven at 103°C for 24 hours prior to the tests to dry them in order to minimize their humidity content.

### 3.4.3 Impregnation Process

The wood specimens were impregnated with the $SiO_2$ colloid using a dip-coating technique. Although the samples can naturally absorb the solution, air entrapped within the macropores will impede the effective impregnation of the sample. To mitigate this issue and improve the effectiveness of the impregnation, the process was conducted under vacuum pressure using the Buehler Cast-N-Vac 1000 vacuum chamber. The samples were impregnated under different negative pressures of -30, -60, and -90 kPa and also under atmospheric conditions for one hour. Following the impregnation process, the samples were placed in an oven at 50°C for one hour and 100°C for five minutes to accelerate the agglomeration of the $SiO_2$ nanoparticles inside the vascular system.

### 3.4.4 Sample Designations and Descriptions

Table 3.1 presents the sample designations and their respective descriptions. These designations will be used throughout the tables and figures presented in this chapter.

*Table 3.1: Sample designations and descriptions*

| Sample Designation | Description |
|---|---|
| **NT** | Non-Treated |
| **ATM** | $SiO_2$ impregnated wood at atmospheric pressure |
| **-30 kPa** | $SiO_2$ impregnated wood under a vacuum pressure of -30 kPa |
| **-60 kPa** | $SiO_2$ impregnated wood under a vacuum pressure of -60 kPa |
| **-90 kPa** | $SiO_2$ impregnated wood under a vacuum pressure of -90 kPa |

### 3.4.5 Characterizations

#### 3.4.5.1 Density Measurements

The density of samples before and after impregnation was determined using a micromeritics gas pycnometer (AccuPyc II 1340). Helium was used for the measurements. The density of each sample was measured three times to determine the mean value both before and after impregnation. Five samples were tested for each impregnation condition.

#### 3.4.5.2 Water Uptake Measurements

The water uptake of samples before and after $SiO_2$ impregnation was determined using the Washburn method for porous materials with a force balance tensiometer (DCA-100F First Ten Angstroms). In order to reach the wood saturation point quickly, small specimens of 3x2x1mm with a mass of 2–3 mg were tested. The saturation point was determined by identifying the plateau section of the water absorption graph. Five samples of each impregnation condition were tested. Each specimen was inserted into a spring-loaded immersion clip and brought into contact with distilled water. Starting from the time of immersion, the mass uptake was recorded every second for a total of 600 seconds, and the water uptake (Weight %) was calculated with Eq. (1), where $M_{wet}$ is the mass of the samples with the absorbed water and $M_{dry}$ is the mass of the samples in a dry state.

$$Weight\ \% = \frac{100 \times (M_{wet} - M_{dry})}{M_{dry}} \quad (1)$$

To quantify the water uptake reduction at saturation after impregnation, the reduction magnitude ($R_m$) was calculated with Eq. (2).

$$R_m = \text{Weight \% before impregnation} - \text{Weight \% after impregnation} \quad (2)$$

The Weight % before and after impregnation were both taken at saturation such as at $\sqrt{t}/L$ = 7, where t is the time (s), and L is the length of the sample (mm). The $\sqrt{t}/L$ represents the x-axis, and the Weight % represents the y-axis of the water uptake graph (see Appendix A). All samples reached a plateau and thus exhibited their saturation at $\sqrt{t}/L$ = 7 in the water uptake graph, hence why it was selected as the reference point for analysis and comparison.

Wood is a natural product with an irregular structure and can exhibit a high degree of variability in its properties. To offset the effects of this variability on the test results, the following experimental process was employed. First, each sample in its non-treated dry state was tested to saturation. Then the sample was dried in an oven at 103°C for 24 hours. Next, the same sample, now dry, was impregnated with $SiO_2$ and tested to saturation again. The procedure was repeated respectively for all the $SiO_2$ impregnation conditions. This procedure ensures that the differences in water uptake are induced by the impregnation conditions rather than the inherent irregularity in the sample structure.

As a result, with the above procedure, it was possible to compare the water uptake capacity of the same samples before and after impregnation and calculate the reduction magnitude using Equation 2.

#### 3.4.5.3 Scanning Electron Microscopy

The impregnated samples were analyzed using a Scanning Electron Microscope (SEM) to examine the effect of vacuum pressure on the diffusion of $SiO_2$ particles into the vascular system of wood. The samples were cold mounted and halved†. Prior to SEM analysis, all samples were polished and coated by a vapour-deposited 20 µm layer of Pd-Au. The microscopy was carried out using a JSM-7500F FESEM at 2-3 kV. Secondary electron detectors and Energy Dispersive Spectroscopy (EDS) were used for this characterization method.

#### 3.4.5.4 Transmission Electron Microscopy

Treated and non-treated samples were analyzed with a Transmission Electron Microscope (TEM) to assess the effect of vacuum pressure on the presence of $SiO_2$ nanoparticles in the lumens of the samples. The cross-sections were prepared following the method used for biological specimens [22]. The samples were sectioned at 80 nm by a microtome with a diamond blade. The sections were stained with a solution of uranyl acetate and were observed on a copper grid at 80 kV with TEM. All microscopy was carried out using a Hitachi H-7500 machine at 80 kV.

#### 3.4.5.5 Simultaneous Thermal Analysis

Thermogravimetric analysis (TGA) coupled with Differential Scanning Calorimetry (DSC) was carried out using a TA Instrument Q600 V8.3 under a nitrogen atmosphere with a heating rate of 10°C/min. The weight loss traces were recorded as a function of temperature in the range of 20-500˚C.

#### 3.4.5.6 Dynamic Mechanical Analysis

Treated and non-treated wood samples were tested in a dry state using Dynamic Mechanical Analysis (DMA). Five samples of each impregnation condition were tested. The test apparatus was equipped with a 3-point bending clamp setup. The effect of the vacuum pressure impregnation process on the viscoelastic properties of wood (i.e., Storage modulus, Loss modulus, and Tan $\delta$) was studied. The viscoelastic properties were measured before and after each impregnation. Multi-strain tests were carried out using a TA Instruments DMA Q800 testing machine set to a frequency of 1 Hz and a temperature range of 5-40°C. The temperature range was selected to analyze the effect of impregnation at ambient, below ambient, and above ambient temperature.

#### 3.4.5.7 Statistical Analysis

A two-sample t-test was applied to compare the mean values of each key property [23]. A confidence interval of 95% was considered as long as the P-value was below 0.05, indicating significant differences among the values.

† A tangential-radial cross-sectional slice from the longitudinal center of the sample was taken.

## 3.5 Results and discussion

### 3.5.1 Density Measurements

Figure 3.1 a) and b) show the results of the density tests conducted on the $SiO_2$ impregnated samples under atmospheric pressure and three vacuum pressures compared to their non-treated state. As shown in Figure 3.1 a), the impregnation process has increased the density in all samples, regardless of the impregnation vacuum pressure. Moreover, the samples impregnated using a vacuum pressure of -60 and -90 kPa exhibited higher densities compared to the samples impregnated at atmospheric pressure. Furthermore, samples impregnated at a vacuum pressure of -90 kPa experienced the highest density increase among all of the $SiO_2$ impregnated samples.

Figure 3.1 b) shows the change in the density of a given sample before and after $SiO_2$ treatment. Impregnation under vacuum increased the effectiveness of the $SiO_2$ impregnation by a factor of 2.6. The trend shown in Figure 3.1 b) indicates that a greater change in density can be expected with increasing vacuum pressure.

Table 3.2 presents the statistical analysis conducted to compare the density of the treated and non-treated samples. The P-values of the statistical analysis revealed that the change in density before and after the impregnation was significant for all samples. Moreover, the difference in density between all of the treated samples was statistically significant except for the difference between the ATM and -30 kPa samples. Subjecting wood to a vacuum during impregnation helps remove the entrapped air in the vascular system and pores, and facilitates the impregnation process. The vacuum pressure of -30 kPa did not appear to be strong enough to effectively remove the entrapped air. Therefore, the $SiO_2$ colloid could not penetrate into the core of the wood's vascular structure. The effect of vacuum pressure on the depth of penetration of the $SiO_2$ particles in the wood structure is explored more in depth in Section 3.5.3.

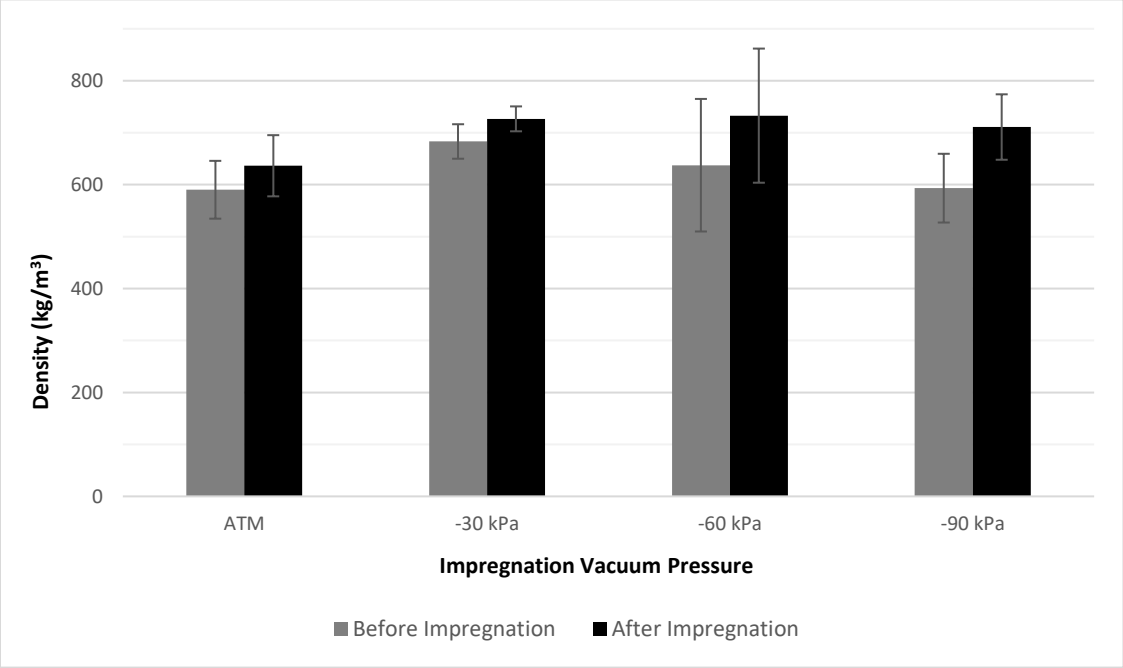


*Figure 3.1 a): Density of the samples before and after the impregnations*

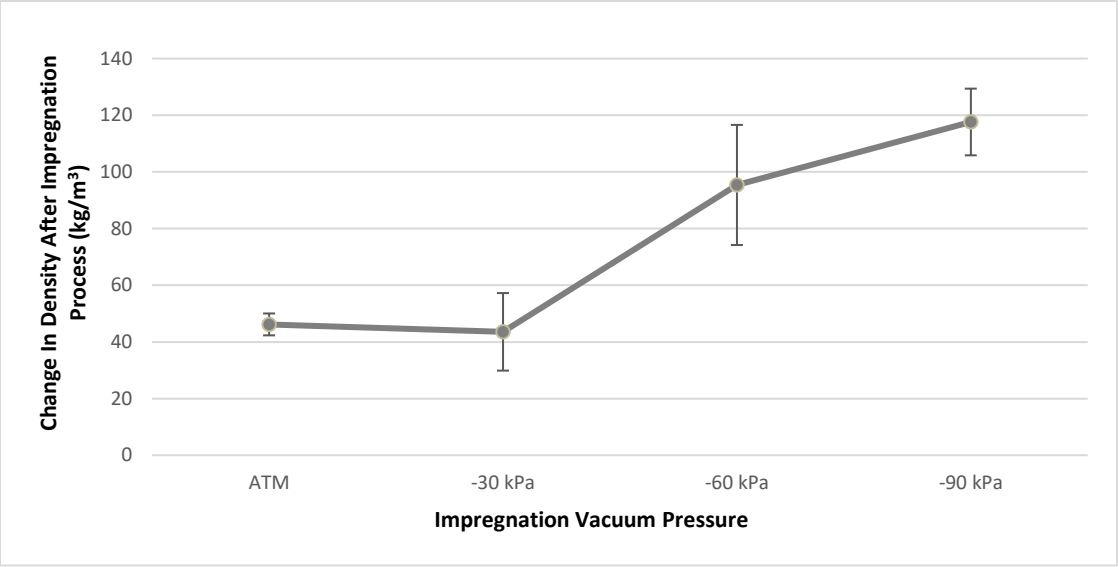


*Figure 3.1 b): Difference in density before and after the impregnations*

*Table 3.2: Statistical analysis of density tests*

| **Before** | | | **After** | | | **\|Before – After\|** | |
|---|---|---|---|---|---|---|---|
| **Type** | Average Density kg/m³ | Standard Deviation | **Type** | Average Density kg/m³ | Standard Deviation | Average Density kg/m³ | Standard Deviation |
| **Before ATM** | 590 | 6 | **After ATM** | 636 | 2 | 46 | 4 |
| **Before -30 kPa** | 683 | 18 | **After -30 kPa** | 727 | 8 | 44 | 14 |
| **Before -60 kPa** | 637 | 73 | **After -60 kPa** | 733 | 74 | 96 | 21 |
| **Before -90 kPa** | 593 | 37 | **After -90 kPa** | 711 | 34 | 118 | 12 |

| **Sample Comparison** | Z score & P-value | Statistical Significance |
|---|---|---|
| **Before ATM vs After ATM** | Z score = -9.843<br>P-value = <0.05 | Significant |
| **Before -30 kPa vs After -30 kPa** | Z score = -3.773<br>P-value = <0.05 | Significant |
| **Before -60 kPa vs After -60 kPa** | Z score = -2.603<br>P-value = <0.05 | Significant |
| **Before -90 kPa vs After -90 kPa** | Z score = -5.710<br>P-value = <0.05 | Significant |
| **ATM vs -30 kPa** | Z score = 0.314<br>P-value = 0.753 | Insignificant |
| **-30 kPa vs -60 kPa** | Z score = -4.761<br>P-value = <0.05 | Significant |
| **-60 kPa vs -90 kPa** | Z score = -2.497<br>P-value = <0.05 | Significant |

### 3.5.2 Water Uptake Measurements

Figure 3.2 a) and b) show water uptake test results before and after $SiO_2$ impregnation under atmospheric pressure and three vacuum pressures. The results show that the samples impregnated under -90 kPa exhibited the highest water weight % reduction (732 wt% [7.32x]), and hence achieved the lowest water uptake at saturation after impregnation. This water uptake reduction is significantly higher than that of the ATM samples (452 wt% [4.52x]), the -30 kPa samples (475 wt% [4.75x]), and the -60 kPa samples (478 wt% [4.78x]). This significant decrease in water uptake at saturation is caused by the reduction of void volume in the wood structure. The $SiO_2$ impregnation successfully obstructed the vascular system of the wood and effectively reduced its capacity to absorb water. The $SiO_2$ impregnated samples under a vacuum pressure of -90 kPa exhibited 7.32 and 2.80 times less water uptake than non-treated samples and impregnated samples under atmospheric pressure conditions, respectively. Impregnation under atmospheric conditions is impeded by the presence of entrapped air within the lumens which prevents the $SiO_2$ from permeating and fully obstructing the lumens. This suggests that ATM impregnation only coats the surface of the wood and is not as effective as impregnation under vacuum conditions (see also SEM analysis in Section 3.5.3). These results also confirmed the results of the density tests, where a vacuum pressure of -90 kPa provided the most effective impregnation condition to achieve the highest density increase among all of the $SiO_2$ impregnated samples.

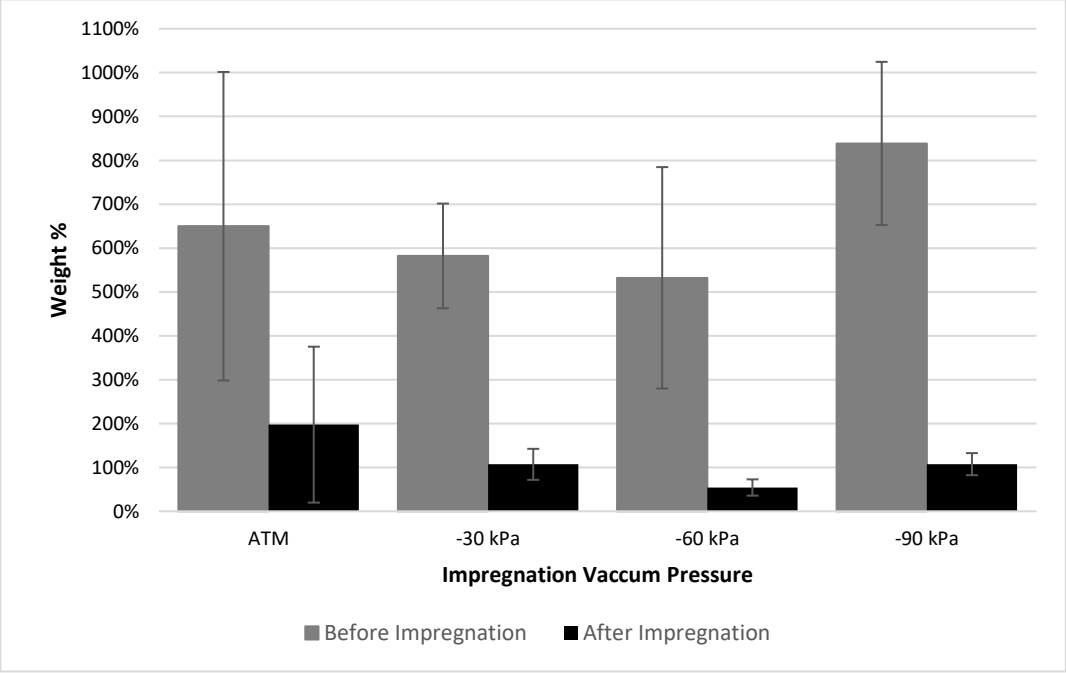


*Figure 3.2 a): Water uptake capacity at $\sqrt{t}/L$ = 7 before and after the impregnations*

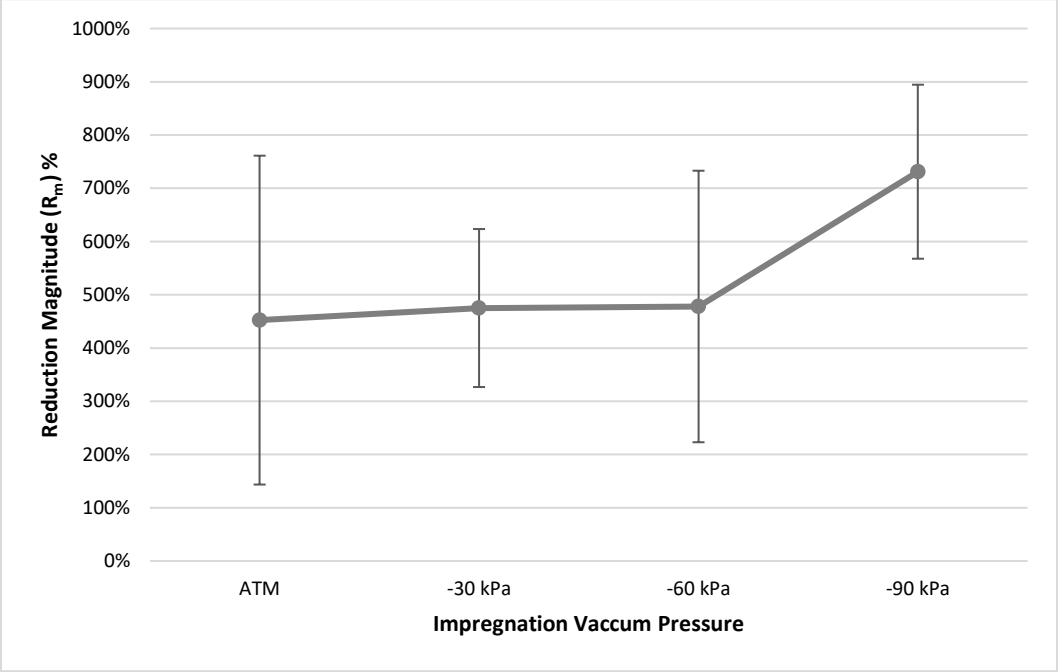


*Figure 3.2 b): Reduction magnitude in water uptake capacity at $\sqrt{t}/L$ = 7 before and after the impregnations*

Table 3.3 presents the statistical analysis conducted to compare the water uptake capacity of treated and non-treated samples. Non-treated samples showed a larger standard deviation for water uptake at saturation than treated samples. When the samples were put in contact with water, the ability of water to enter the wood pores was dependent on the size of the pores and the amount of air entrapped within them. The observed variation in water uptake is caused by the naturally occurring range of microscopic pore diameters in the non-treated samples [24]. The standard deviation of the samples after impregnation showed a significant decrease compared to the standard deviation of the same samples before impregnation. This decrease is caused by a substantial reduction in the number of microscopic pores open to the surface. The $SiO_2$ impregnation under negative pressure eliminated the microscopic pores through a two-stage mechanism. The vacuum evacuates the entrapped air and allows the $SiO_2$ colloid to permeate into the pores, inundate, and eventually clog them entirely. The standard deviation is found to be the lowest for the -90 kPa samples. The P-values of the statistical analysis demonstrated that the difference in reduction magnitude from ATM to -60 kPa is not significant, while the difference in reduction magnitude from -60 kPa to -90 kPa is significant. The results clearly show that non-treated samples absorbed significantly more water than the treated ones under all conditions. The statistical analysis (Table 3.3) revealed that the $SiO_2$ impregnation under vacuum pressure up to -60 kPa significantly decreased the water uptake at saturation of spruce wood compared to non-treated samples. However, there was not a statistically significant difference between these impregnated samples (i.e., impregnated samples from ATM to -60 kPa). Enhancing the vacuum pressure from -60 kPa to -90 kPa showed a statistically significant change in the water uptake at saturation. The results indicated that impregnation under a vacuum pressure of -90 kPa was the most effective condition to reduce the water uptake at saturation of spruce wood. This level of vacuum pressure seems to represent the optimal condition needed to evacuate air and initiate the transport of $SiO_2$ nanoparticles into the vascular structure of spruce wood.

*Table 3.3: Statistical analysis of water uptake tests*

| Before | | | | After | | | | \|Before – After\| | |
|---|---|---|---|---|---|---|---|---|---|
| **Type** | $\sqrt{t}/L$ | Average Weight% | Standard Deviation | **Type** | $\sqrt{t}/L$ | Average Weight% | Standard Deviation | $R_m$ % | Standard Deviation |
| **Before ATM** | 7 | 650 | 352 | **After ATM** | 7 | 198 | 178 | 452 | 309 |
| **Before -30 kPa** | 7 | 582 | 119 | **After -30 kPa** | 7 | 107 | 35 | 475 | 148 |
| **Before -60 kPa** | 7 | 532 | 252 | **After -60 kPa** | 7 | 54 | 19 | 478 | 255 |
| **Before -90 kPa** | 7 | 839 | 186 | **After -90 kPa** | 7 | 107 | 25 | 732 | 163 |

| Sample Comparison | Z score & P-value | Statistical Significance |
|---|---|---|
| **Before ATM vs After ATM** | Z score = 3.247<br>P-value = <0.05 | Significant |
| **Before -30 kPa vs After -30 kPa** | Z score = 8.929<br>P-value = <0.05 | Significant |
| **Before -60 kPa vs After -60 kPa** | Z score = 5.391<br>P-value = <0.05 | Significant |
| **Before -90 kPa vs After -90 kPa** | Z score = 8.709<br>P-value = <0.05 | Significant |
| **ATM vs -30 kPa** | Z score = -0.172<br>P-value = 0.863 | Insignificant |
| **-30 kPa vs -60 kPa** | Z score = -0.03<br>P-value = 0.980 | Insignificant |
| **-60 kPa vs -90 kPa** | Z score = -2.181<br>P-value = <0.05 | Significant |

### 3.5.3 Scanning Electron Microscopy

Figure 3.3 presents micrographs of the Scanning Electron Microscopy (SEM) and Energy Dispersive Spectroscopy (EDS) analyses performed on the cross-section of halved samples. Because the middle of a sample is at the maximum distance from the sample extremities, the presence of $SiO_2$ particles in the micrographs represents the maximum depth of diffusion in the vascular system of the wood. The EDS analyses were performed to survey the dispersion of silica particles in the wood's structure. Figure 3.3 a) and b) show that under atmospheric pressure, only a few lumens are filled with $SiO_2$. Most lumens remain empty due to an abundance of entrapped air present in the open pores, preventing the $SiO_2$ colloid from permeating into the pores. EDS analysis revealed that under atmospheric pressure, the $SiO_2$ remains primarily on the surface of the specimen. In this case, the colloidal solution permeates into the wood cavities through capillary action. However, the capillary pressure was not high enough to displace the entrapped air and allow the $SiO_2$ colloid to permeate into the core of the wood's structure, resulting in a low depth of $SiO_2$ particle diffusion. In addition, the colloid (weakly alkaline solution with pH 9.2-9.9) precipitated on the surface, allowing the particles to aggregate and form a solid film on the surface of the wood. This phenomenon occurs because wood is generally acidic in nature [9] and neutralizes the alkaline colloid [25], causing the $SiO_2$ particles to precipitate.

*a) SEM ATM*

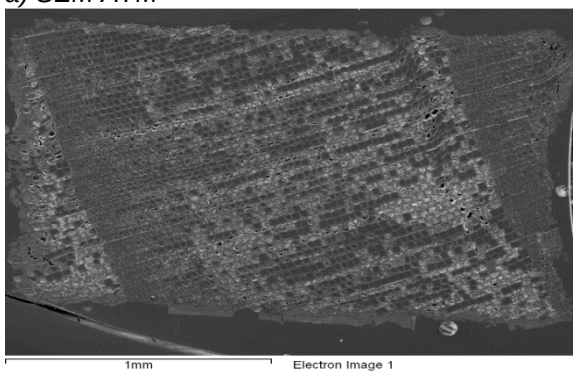


*b) EDS ATM*

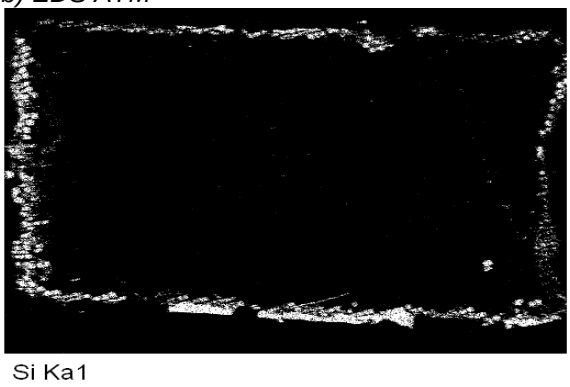


*c) SEM -30 kPa*

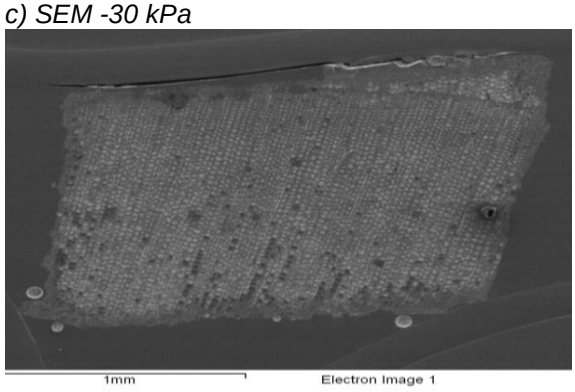


*d) EDS -30 kPa*

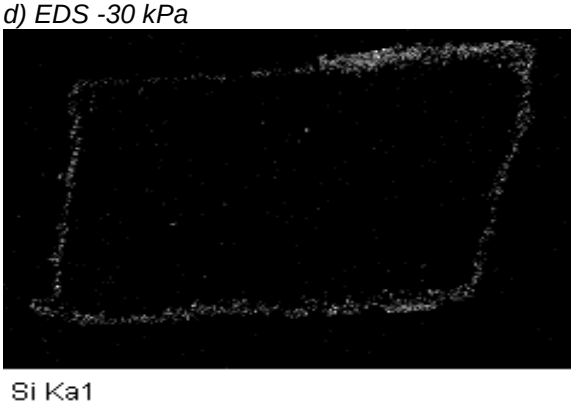


*e) SEM -60 kPa*

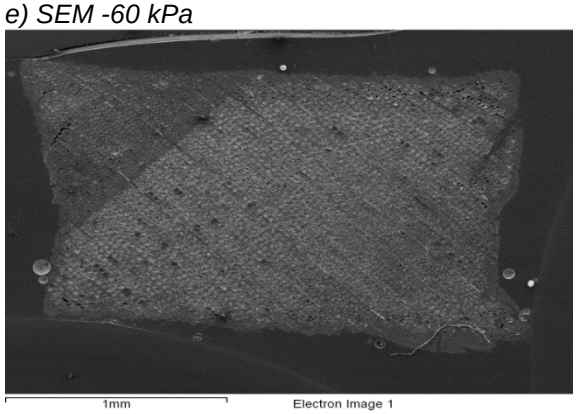


*f) EDS -60 kPa*

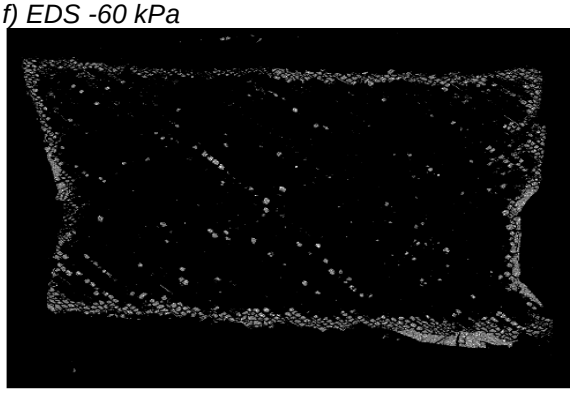


*g) SEM -90 kPa*

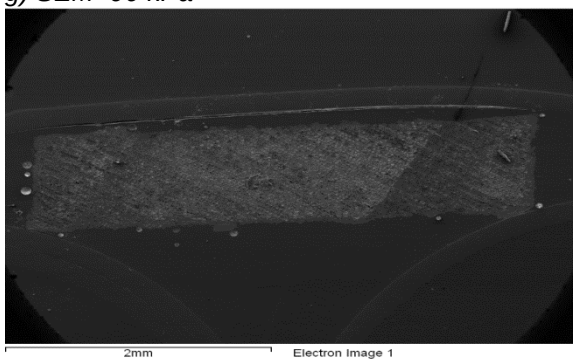


*h) EDS -90 kPa*

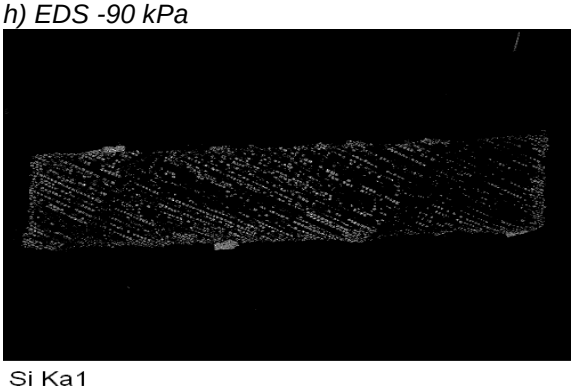


*Figure 3.3: SEM, EDS micrographs of a,b) ATM c,d) -30 kPa e,f) -60 kPa g,h) -90 kPa*

The SEM micrograph of the ATM sample also reveals the lack of diffusion of $SiO_2$ particles in the longitudinal direction and a shallow diffusion of particles at the surface in the radial direction. Figure 3.3 c) and d) show that when a vacuum pressure of -30 kPa was used, there was a slight increase in the depth of diffusion of the particles into the wood's vascular structure. Figure 3.3 e) and f) show that changing the vacuum pressure to -60 kPa improved the impregnation process. A vacuum pressure of -60 kPa helped the $SiO_2$ colloid permeate further into the wood's vascular structure, but it was not effective enough to eliminate the entrapped air and fill the open pores. Figure 3.3 g) and h) show that under a vacuum pressure of -90 kPa, the majority of the lumens are clogged with $SiO_2$ particles. These micrographs qualitatively confirmed that using a vacuum pressure of -90 kPa helped remove the entrapped air. This effectively enhanced the impregnation process and reduced the porosity by obstructing the vascular system of the wood with the agglomerated $SiO_2$ particles.

### 3.5.4 Transmission Electron Microscopy

Figure 3.4 shows TEM micrographs (longitudinal sections) of non-treated and -90 kPa treated samples. The -90 kPa vacuum was selected to represent the most effective impregnation condition versus the reference (non-treated) sample. Non-treated and -90 kPa samples were analyzed under microscopy to reveal the presence of nanoparticles in the vascular system of the wood. The presence of $SiO_2$ can be observed as well as the vascular system of the spruce wood. Figure 3.4 a) and c) do not show the existence of $SiO_2$ nanoparticles in the lumens, but the presence of dense particles is noticeable in Figure 3.4 b) and d). These images support the results obtained in the SEM analysis and previous measurements (density and water uptake capacity). The originally empty lumens are now obstructed with $SiO_2$ nanoparticles, which helps reduce the water uptake.

*a) NT low magnification*

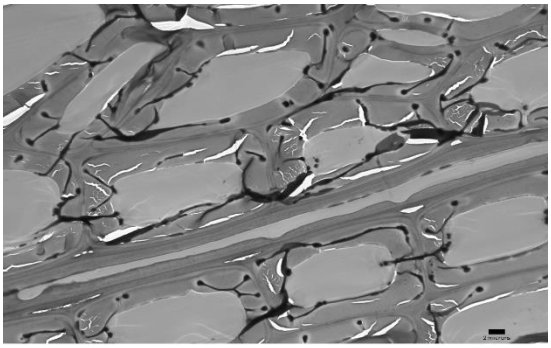

*b) -90 kPa low magnification*

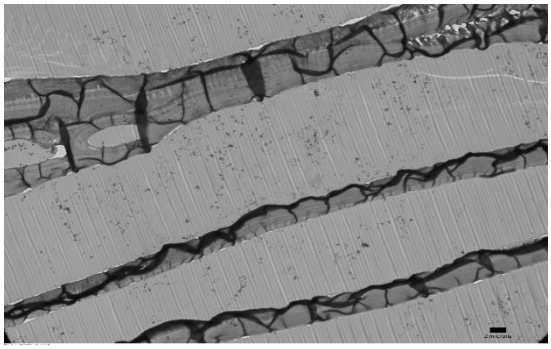

*c) NT High magnification*

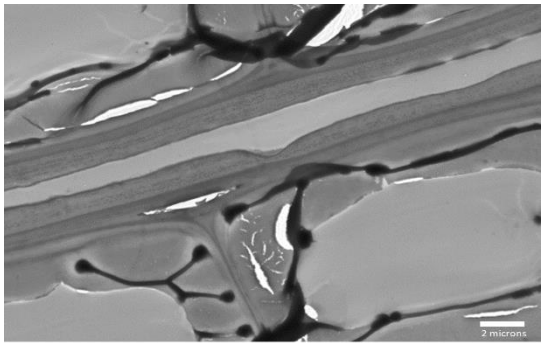


*d) -90 kPa High magnification*

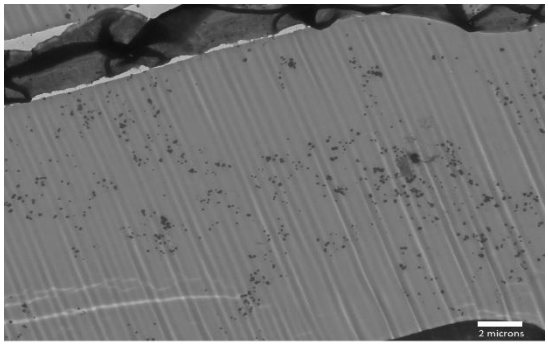


*Figure 3.4: TEM micrographs of NT and -90 kPa treated wood samples*

### 3.5.5 Simultaneous Thermal Analysis

Figure 3.5 depicts the Derivative Thermo-Gravimetry (DTG) and Differential Scanning Calorimetry (DSC) thermograms of the $SiO_2$ impregnated samples within the temperature region where cellulose degrades thermally (330-350˚C), as shown by the endothermic peak in Figure 3.5 a). The ATM sample had the highest peak temperature and enthalpy for the degradation of cellulose of all impregnated samples. Additionally, the endothermic peak decreases as the vacuum pressure intensifies (see Table 3.4). As discussed in Section 3.5.3, at atmospheric conditions, the colloid was unable to permeate deeply into the wood pores and cavities due to the presence of entrapped air in the wood. Therefore, the cellulose was not exposed to the alkaline solution and was able to remain intact. By contrast, under vacuum pressure, the entrapped air was evacuated and allowed the alkaline colloid to diffuse into the vascular system of the wood. Consequently, the vacuum facilitated the infiltration of the liquid phase of the colloid (containing $OH^-$ ions) through the vascular structure of the wood. This colloid can attack the glycosidic cellulose bonds and cause degradation-solubilization and the loss of properties [26]. As a result of this chemically induced degradation, the enthalpy of the thermal degradation of cellulose decreased by 77% for the impregnated sample at -30 kPa vacuum pressure. The sample showed a drop of 11˚C in the peak temperature of cellulose thermal degradation compared to the ATM sample. This side effect was exacerbated as the vacuum increased. However, the magnitude of the degradation of cellulose due to chemical attack reached a plateau for vacuum pressures beyond -60 kPa. The temperature at which the samples exhibit a maximum mass loss is also used as a criterion to examine the degradation of lignocellulosic materials [27]. These temperatures confirm that the negative effect of the vacuum impregnation of wood with the $SiO_2$ colloid was less pronounced at a vacuum pressure of -90 kPa.

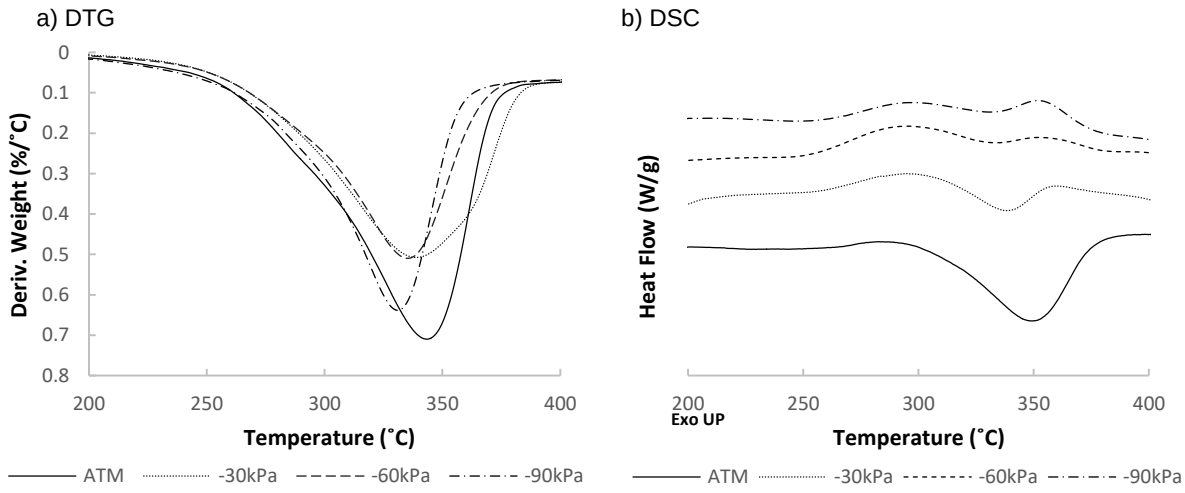


*Figure 3.5: DTG and DSC thermograms of $SiO_2$ impregnated samples*

*Table 3.4: Thermal degradation properties of the $SiO_2$ impregnated samples*

| Device | Measured Parameter | ATM | -30 kPa | -60 kPa | -90 kPa |
|---|---|---|---|---|---|
| **TGA** | Maximum Mass Loss Temperature (˚C) | 344 | 339 | 335 | 333 |
| **DSC** | Cellulose Degradation Temperature (˚C) | 349 | 338 | 332 | 330 |
| | Cellulose Degradation Enthalpy (J/g) | 48.8 | 11 | 3.4 | 3.1 |

### 3.5.6 Dynamic Mechanical Analysis

Figure 3.6 shows the Storage modulus, Loss modulus, and Tan δ before and after the impregnation of the wood samples. Three temperatures (ambient, below ambient, and above ambient) were selected to compare the viscoelastic properties of the samples. Table 3.5 and 3.6 present the quantitative data along with the statistical analysis of the DMA results before and after the impregnation process respective to these three temperatures. The results showed that the $SiO_2$ impregnation under the atmospheric and -90 kPa vacuum conditions caused significant alterations in the Storage and Loss moduli of spruce wood. Although the -30 kPa and -60 kPa samples exhibited noticeable changes in their viscoelastic properties, for the majority of the temperature ranges, these changes were not statistically significant compared to the samples before impregnation.

Table 3.5 and Table 3.6 indicate a significant increase in the Storage and Loss moduli of the ATM samples at temperatures between 5˚C and 35˚C. The general performance of solid viscoelastic material indicates that an increase in Storage modulus is accompanied by a decrease in Loss modulus [28]. In other words, in solid viscoelastic materials, the elastic and viscous properties measured from the Storage and Loss moduli, respectively, are negatively correlated. However, $SiO_2$ impregnation of samples at atmospheric conditions simultaneously enhanced both the elastic and viscous properties of the treated samples, likely due to the precipitation-aggregation of $SiO_2$ particles, as discussed in Section 3.5.3. The resulting formation of a rigid layer on the surface of the samples may have reinforced the wood and caused the Storage modulus to increase. Additionally, the increase in Loss modulus indicates that the ability of the ATM samples to dissipate energy increased. The ATM samples formed a solid film that could dissipate energy at the interface between the film and the wood fibers through friction, as described by the stick-slip oscillation model [29].

Detailed investigations revealed that impregnation under vacuum could enhance the Storage modulus of wood, but only at high vacuum pressures, since there are two competing mechanisms at work. The impregnation under vacuum is a double-edged sword. On the one hand, the vacuum helps the $SiO_2$ particles (the solid phase of the colloid) diffuse and disperse into the vascular system of the wood. On the other hand, this process exposes the inner structure of the wood to an alkaline solution. This can cause the structure to degrade and result in a deterioration of the properties. However, this loss of rigidity (i.e., degradation) can be partially or completely compensated by the addition of $SiO_2$ nanoparticles depending on the strength of the vacuum to uniformly disperse the particles into the wood's structure.

For example, a vacuum pressure of -30 kPa was able to partially remove the entrapped air but was not strong enough to allow the particles to diffuse deeply into the wood's vascular structure. As a result, the $SiO_2$ particles primarily aggregated on the surface and, similar to the ATM samples, formed a solid layer on the surface as shown in Figure 3.3 d). However, the infiltration of hydroxyl ions into the wood's structure may have undermined the solid film reinforcing effect and made the increase in the Storage modulus become insignificant. Furthermore, the results showed that the Loss modulus of -30 kPa samples increased similar to the ATM samples. This correlation could also be related to the formation of a $SiO_2$ film on the surface of the -30 kPa samples. However, the change in Loss modulus before and after impregnation was statistically insignificant at 5˚C, as shown in Table 3.6. One hypothesis to explain this phenomenon is the positive effect of

the mild vacuum (-30 kPa) on the diffusion of $SiO_2$ particles into the surface cavities of the wood. This penetration of the $SiO_2$ film into the surface openings created an integrated texture at the surface that could reduce the interfacial friction at low temperatures. The results also revealed that in the -60 kPa samples, the effect of degradation was dominant compared to the reinforcing effect of $SiO_2$ impregnation, as they exhibited the minimum increase in Storage modulus among all the impregnated samples.

Finally, the results showed that at -90 kPa, the vacuum pressure was high enough to successfully remove the entrapped air in the wood's structure, allowing the colloid to infiltrate through capillary action and transport the $SiO_2$ nanoparticles to the core of the samples. Consequently, the $SiO_2$ particles were uniformly dispersed in the vascular system of the spruce wood samples, leading to a significant increase in Storage modulus as the voids filled with rigid $SiO_2$ nanoparticles. This increase in rigidity reflects the rule of mixtures in composites [30]. In this case, the dominant modifying mechanism was the reinforcing effect of the impregnation and not the degradation side effect. However, the mechanism by which the Loss modulus improved was different from the one shown in the ATM samples. In samples treated under -90 kPa vacuum, the uniform dispersion of $SiO_2$ particles in the lumens caused the dissipation of energy through particle-particle and particle-lumen wall frictions when the samples underwent deformations. Another key observation in the viscoelastic behaviour of the -90 kPa samples shown in Table 3.7 is the decrease in Tan δ. Although the decrease was only significant at a temperature of 5˚C, this is the only impregnation condition that caused a statistically significant decrease in Tan δ at low temperatures. This effect could be beneficial for applications requiring greater creep-resistant wood. Recent research has shown a direct relationship between the suppression of viscous properties and the increase in creep resistance [31]. In contrast, the ATM and -30 kPa samples showed a significant increase in Tan δ, which can be useful for applications where vibration or sound damping properties are needed [32].

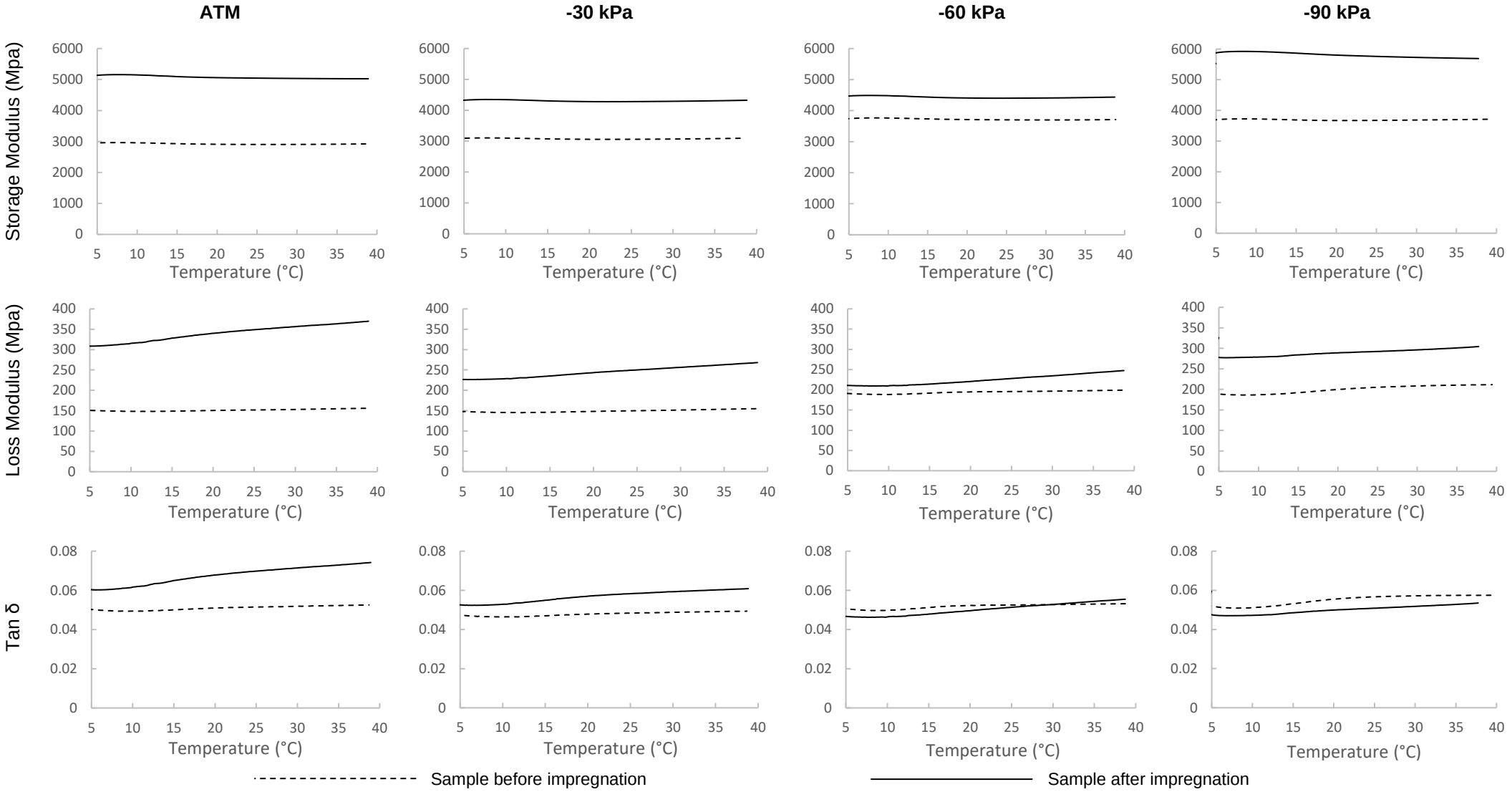


*Figure 3.6: DMA test results of the Storage modulus, Loss modulus, and Tan δ before and after the impregnations*

*Table 3.5: DMA test results of the Storage modulus before and after the impregnations*

| Impregnation Condition | Average Storage Modulus (MPa) at 5°C | | | Average Storage Modulus (MPa) at 25°C | | | Average Storage Modulus (MPa) at 35°C | | |
|---|---|---|---|---|---|---|---|---|---|
| | Before | After | %Difference | Before | After | %Difference | Before | After | %Difference |
| **ATM** | 2954 | 5136 | 74 | 2903 | 5044 | 74 | 2912 | 5026 | 73 |
| **-30 kPa** | 3094 | 4327 | 40 | 3060 | 4281 | 40 | 3083 | 4308 | 40 |
| **-60 kPa** | 3741 | 4469 | 19 | 3702 | 4400 | 19 | 3702 | 4421 | 19 |
| **-90 kPa** | 3692 | 5876 | 59 | 3676 | 5760 | 57 | 3702 | 5702 | 54 |
| **Sample Comparison** | Z score & P-value | | Statistical Significance | Z score & P-value | | Statistical Significance | Z score & P-value | | Statistical Significance |
| **ATM Before vs ATM After** | Z score = -3.496<br>P-value = <0.05 | | Significant | Z score = -3.541<br>P-value = <0.05 | | Significant | Z score = -3.502<br>P-value = <0.05 | | Significant |
| **-30 kPa Before vs -30 kPa After** | Z score = -1.644<br>P-value = 0.100 | | Insignificant | Z score = -1.631<br>P-value = 0.103 | | Insignificant | Z score = -1.658<br>P-value = 0.097 | | Insignificant |
| **-60 kPa Before vs -60 kPa After** | Z score = -1.221<br>P-value = 0.222 | | Insignificant | Z score = -1.201<br>P-value = 0.23 | | Insignificant | Z score = -1.237<br>P-value = 0.216 | | Insignificant |
| **-90 kPa Before vs -90 kPa After** | Z score = -4.093<br>P-value = <0.05 | | Significant | Z score = -4.013<br>P-value = <0.05 | | Significant | Z score = -3.832<br>P-value = <0.05 | | Significant |

*%Difference = ((After – Before) / Before) x 100

*Table 3.6: DMA test results of the Loss modulus before and after the impregnations*

| Impregnation Condition | Average Loss Modulus (MPa) at 5°C | | | Average Loss Modulus (MPa) at 25°C | | | Average Loss Modulus (MPa) at 35°C | | |
|---|---|---|---|---|---|---|---|---|---|
| | Before | After | %Difference | Before | After | %Difference | Before | After | %Difference |
| **ATM** | 151 | 308 | 104 | 152 | 349 | 130 | 155 | 363 | 135 |
| **-30 kPa** | 148 | 227 | 53 | 150 | 250 | 67 | 153 | 263 | 72 |
| **-60 kPa** | 191 | 211 | 10 | 196 | 228 | 16 | 198 | 242 | 22 |
| **-90 kPa** | 189 | 278 | 47 | 205 | 292 | 42 | 210 | 301 | 43 |
| **Sample Comparison** | Z score & P-value | | Statistical Significance | Z score & P-value | | Statistical Significance | Z score & P-value | | Statistical Significance |
| **ATM Before vs ATM After** | Z score = -4.370<br>P-value = <0.05 | | Significant | Z score = -5.432<br>P-value = <0.05 | | Significant | Z score = -5.492<br>P-value = <0.05 | | Significant |
| **-30 kPa Before vs -30 kPa After** | Z score = -1.945<br>P-value = 0.0518 | | Insignificant | Z score = -2.240<br>P-value = <0.05 | | Significant | Z score = -2.289<br>P-value = <0.05 | | Significant |
| **-60 kPa Before vs -60 kPa After** | Z score = -0.546<br>P-value = 0.585 | | Insignificant | Z score = -0.877<br>P-value = 0.380 | | Insignificant | Z score = -1.179<br>P-value = 0.238 | | Insignificant |
| **-90 kPa Before vs -90 kPa After** | Z score = -3.735<br>P-value = <0.05 | | Significant | Z score = -3.228<br>P-value = <0.05 | | Significant | Z score = -3.145<br>P-value = <0.05 | | Significant |

*%Difference = ((After – Before) / Before) x 100

*Table 3.7: DMA test results of the Tan δ before and after the impregnations*

| Impregnation Condition | Average Tan Delta at 5°C | | | Average Tan Delta at 25°C | | | Average Tan Delta at 35°C | | |
|---|---|---|---|---|---|---|---|---|---|
| | Before | After | %Difference | Before | After | %Difference | Before | After | %Difference |
| **ATM** | 0.0502 | 0.0603 | 20 | 0.0515 | 0.0699 | 36 | 0.0523 | 0.0729 | 40 |
| **-30 kPa** | 0.0473 | 0.0526 | 11 | 0.0484 | 0.0583 | 21 | 0.0491 | 0.0602 | 23 |
| **-60 kPa** | 0.0507 | 0.0467 | -8 | 0.0525 | 0.0513 | -2 | 0.0530 | 0.0544 | 3 |
| **-90 kPa** | 0.0519 | 0.0475 | -9 | 0.0567 | 0.0509 | -10 | 0.0574 | 0.0528 | -8 |
| **Sample Comparison** | Z score & P-value | | Statistical Significance | Z score & P-value | | Statistical Significance | Z score & P-value | | Statistical Significance |
| **ATM Before vs ATM After** | Z score = -4.223<br>P-value = <0.05 | | Significant | Z score = -6.457<br>P-value = <0.05 | | Significant | Z score = -7.019<br>P-value = <0.05 | | Significant |
| **-30 kPa Before vs -30 kPa After** | Z score = -2.201<br>P-value = <0.05 | | Significant | Z score = -4.760<br>P-value = <0.05 | | Significant | Z score = -4.703<br>P-value = <0.05 | | Significant |
| **-60 kPa Before vs -60 kPa After** | Z score = 1.669<br>P-value = 0.0951 | | Insignificant | Z score = 0.506<br>P-value = 0.613 | | Insignificant | Z score = -0.662<br>P-value = 0.508 | | Insignificant |
| **-90 kPa Before vs -90 kPa After** | Z score = 1.994<br>P-value = 0.0462 | | Significant | Z score = 1.752<br>P-value = 0.0798 | | Insignificant | Z score = 1.591<br>P-value = 0.112 | | Insignificant |

*%Difference = ((After – Before) / Before) x 100

## 3.6 Conclusion

This research has demonstrated that $SiO_2$ impregnation can simultaneously reduce water uptake capacity and improve the mechanical properties of spruce wood if it is performed under vacuum pressure. However, the impregnation needs to be conducted at elevated vacuum pressure so that the change of the properties will become statistically significant. Various characterization methods such as pycnometry, tensiometry, SEM, TEM, TGA, DMA, and statistical analyses were used to determine the optimal vacuum pressure condition.

The results showed that all impregnation conditions were able to significantly decrease the water uptake capacity of the wood in comparison with the non-treated samples. However, the impregnated samples did not exhibit a significant change in $R_m$, except for the $SiO_2$ samples impregnated under a vacuum pressure of -90 kPa.

The density of the samples impregnated under vacuum was higher than those treated under atmospheric conditions, which was congruous with the water uptake results that indicated the reduction in void of the wood samples that led to a considerable decrease in water uptake capacity. However, the results revealed that the effectiveness of the impregnation is significant when performed at -90 kPa pressures. This outcome was confirmed by performing electron microscopy on the samples. The micrographs showed that a vacuum pressure of -90 kPa was required to homogeneously disperse $SiO_2$ nanoparticles in the vascular system of the wood.

DMA tests along with TGA and microscopic analyses revealed that $SiO_2$ impregnation under vacuum pressure is subject to two competing mechanisms. On the one hand, the vacuum helps the $SiO_2$ particles (the solid phase of the colloid) diffuse and disperse into the vascular system of the wood. On the other hand, this process exposes the inner structure of the wood to an alkaline solution. Accordingly, vacuum impregnation can cause a degradation-solubilization phenomenon due to the alkaline nature of the colloid. However, the extent of this side effect is dependent on the strength of the vacuum, and thus on the dispersion of $SiO_2$ particles in the structure of the wood. The side effect can be partially or completely compensated by the addition of $SiO_2$ nanoparticles depending on the strength of the vacuum to uniformly disperse the particles into the wood's structure, as shown in the -90 kPa samples. A detailed investigation of the viscoelastic properties showed that a vacuum pressure of -90 kPa could induce the full recovery and improve the Storage and Loss modulus of wood. The -90 kPa samples were effectively impregnated and had a uniform dispersion of $SiO_2$ particles in the lumens, which reinforced wood and caused the dissipation of energy through particle-particle and particle-lumen wall frictions when the samples underwent deformations. On the other hand, at vacuum pressures of -60 kPa and -30 kPa, the impregnation was unable to have a statistically significant effect on the viscoelastic properties. Moreover, the impregnation under atmospheric conditions did not allow the colloid to permeate inside the wood's structure and thus resulted in the formation of a solid film. The film reinforced the sample and increased the dissipation of energy through stick-slip oscillation. $SiO_2$ impregnation under atmospheric conditions could be useful in the development of materials that require vibration reduction or sound damping properties, whereas vacuum impregnation under -90 kPa could be advantageous for improving the creep resistance of spruce wood.

## 3.7 References


1. Brunner M. (2000). On The Plastic Design Of Timber Beams With A Complex Cross-Section. Paper presented at the World Conference on Timber Engineering, British Columbia, Canada, July 31–August 3 2000.

2. Canada Mortgage and Housing Corporation. (2013). *CANADIAN WOOD-FRAME HOUSE CONSTRUCTION* (3rd ed.). Canada: Library and Archives Canada Cataloguing in Publication.

3. Atlantic WoodWORKS!. (2017). WOOD FOR MID-RISE CONSTRUCTION*.* Doi : https ://wood-works.ca/wp-content/uploads/160601-Wood-4-Mid-Rise-Report-FINAL-2017-03-28-sm.pdf

4. Di Blasi C, Galgano A, Branca C. (2009). Influences of the chemical state of alkaline compounds and the nature of alkali metal on wood pyrolysis*. Industrial & Engineering Chemistry Research, 48*, 3359–3369. Doi: 10.1021/ie801468y

5. Olsson A-M, Salmén L. (1997). The effect of lignin composition on the viscoelastic properties of wood. *Nordic Pulp & Paper Research Journal, 12*, 140–144. Doi: 10.3183/npprj-1997-12-03-p140-144

6. Thoemen H, Irle M, Sernek M. (2010). *Wood-Based Panels – An Introduction for Specialists.* London, England: Brunel University Press

7. Rowell RM, Banks WB. (1985). Water repellency and dimensional stability of wood. *Forest Products Laboratory*. Doi: 10.2737/fpl-gtr-50

8. University of Cambridge. (2020). Water's effect on the mechanical behaviour of wood. In: Dissemination of IT for the Promotion of Materials Science (DoITPoMS). doi: https://www.doitpoms.ac.uk/tlplib/wood/water_effect.php.

9. Illston J.M, Domone P. (2001). *Construction Materials – Their Nature and Behavior* (3rd ed.). London, England: CRC Press.

10. Williams RS, Feist WC. (1999). Water repellents and water-repellent preservatives for Wood. *Forest Products Laboratory*. Doi: 10.2737/fpl-gtr-109

11. Denes AR, Tshabalala MA, Rowell R, et al. (1999). Hexamethyldisiloxane-plasma coating of wood surfaces for creating water repellent characteristics. *Holzforschung*, *53(3)*, 318–326. Doi: 10.1515/hf.1999.052

12. Beaulieu D, Biermeier D. (2020). How to Seal a Deck With Thompson's WaterSeal. In: The Spruce. doi: https://www.thespruce.com/seal-a-deck-with-thompsons-water-seal-2131998.

13. Grosse C, Noël M, Thévenom M.F, Rautkari L, Gérardin P. (2018). Influence of Water and Humidity on Wood Modification with Lactic Acid. *Journal of Renewable Materials, 6*(3), 259-269. doi:10.7569/JRM.2017.634176

14. Boulos L, Foruzanmehr MR, Tagnit-Hamou A, et al. (2017). Wetting analysis and surface characterization of flax fibers modified with zirconia by sol-gel method. *Surface and Coatings Technology, 313*, 407–416. doi: 10.1016/j.surfcoat.2017.02.008

15. Miklós Bak, Ferenc Molnár & Róbert Németh. (2018). Improvement of dimensional stability of wood by silica nanoparticles. *Wood Material Science & Engineering, 14*(11), 1-11. Doi: 10.1080/17480272.2018.1528568

16. Shi X, Dalai NS, Hu XN, Vallyathan V. (1989). The chemical properties of silica particle surface in relation to silica-cell interactions. *Journal of Toxicology and Environmental Health*, *27*, 435–454. Doi: 10.1080/15287398909531314

17. Meire R. da Silva, Bruno H. Fumes, Carlos E.D. Nazario, Fernando M. Lancas. (2017). Chapter Eighteen – New Materials for Green Sample Preparation: Recent Advances and Future Trends. *Comprehensive Analytical Chemistry, 76*, 575–599. Doi: https://doi.org/10.1016/bs.coac.2017.03.003

18. Enguang Xu, Yanjuan Zhang, Lanying Lin. (2020). Improvement of Mechanical, Hydrophobicity and Thermal Properties of Chinese Fir Wood by Impregnation of Nano Silica Sol. *Polymers 2020, 12*(8), 1632. doi : https://doi.org/10.3390/polym12081632

19. Zhang, N., Xu, M. & Cai, L. (2019). Improvement of mechanical, humidity resistance and thermal properties of heat-treated rubber wood by impregnation of $SiO_2$ precursor. *Scientific Reports, 9*, 982. doi: https://doi.org/10.1038/s41598-018-37363-3

20. Przystupa K, Pieniak D, Samociuk W, Walczak A, Bartnik G, Kamocka-Bronisz R, Sutuła M. (2020). Mechanical Properties and Strength Reliability of Impregnated Wood after High Temperature Conditions. *Materials, 13*(23), 5521. Doi: https://doi.org/10.3390/ma13235521

21. Lin, Lan Ying, and Feng Fu. (2012). The Composite Wood Impregnated with Silicon Sol Solution. *Advanced Materials Research*, 466–467, 121–126. doi: https://doi.org/10.4028/www.scientific.net/amr.466-467.121

22. Luft JH. (1961). Improvements in epoxy resin embedding methods. *The Journal of Biophysical and Biochemical Cytology, 9*, 409–414. Doi: 10.1083/jcb.9.2.409

23. Livingston EH. (2004). Who was student and why do we care so much about his T-test? *Journal of Surgical Research, 118*, 58–65. doi: 10.1016/j.jss.2004.02.003

24. Prošek Z, Králík V, Topič J, et al. (2015). A description of the microstructure and the micromechanical properties of spruce wood. *Acta Polytechnica, 55*, 39–49. Doi : 10.14311/ap.2015.55.0039

25. Jiang J, Cao J, Wang W. (2018). Characteristics of wood-silica composites 64nfluenced by the pH value of silica sols. *Holzforschung, 72*(4), 311–319. doi: https://doi.org/10.1515/hf-2017-0126

26. Borůvka V, Ziedler A, Doubek S. (2016). Impact of silicon-based chemicals on selected physical and mechanical properties of wood. *Wood Research, 61*(4), 513–524. Doi: http://www.woodresearch.sk/cms/impact-of-silicon-based-chemicals-on-selected-physical-and-mechanical-properties-of-wood/

27. Foruzanmehr, M., Boulos, L., Vuillaume, P.Y. et al. (2017). The Effect of cellulose oxidation on interfacial bonding of nano-TiO2 coating to flax fibers. *Cellulose 24*, 1529–1542. Doi: https://doi.org/10.1007/s10570-016-1185-6

28. Ferry, John D. (1980). *Viscoelastic Properties of Polymers* (3rd ed.). New York: Wiley.

29. J.A.C. Martins, J.T. Oden, F.M.F. Simões. (1990). A study of static and kinetic friction. *International Journal of Engineering Science*, *28*(1), 29-92. doi: https://doi.org/10.1016/0020-7225(90)90014-A.

30. William D. Callister Jr., David G. Rethwisch. (2018). *Materials Science and Engineering: An Introduction* (10th ed.). Hoboken, NJ: Wiley.

31. Gray, A, Orecchia, D, Beake, Ben D. (2009). Nanoindentation of Advanced Polymers Under Non-Ambient Conditions: Creep Modelling and Tan Delta. *Journal of Nanoscience and Nanotechnology*, *9*(7), 4514-4519(6). doi: https://doi.org/10.1166/jnn.2009.M86

32. Brémaud, I., Minato, K., Langbour, P. et al. (2010). Physico-chemical indicators of inter-specific variability in vibration damping of wood. *Annals of Forest Science*, *67*(707). Doi: https://doi.org/10.1051/forest/2010032

# CHAPTER 4

## The study of physico-mechanical properties of $SiO_2$ impregnated wood in dry and saturated conditions

## CHAPTER 4

## 4.0 The study of physico-mechanical properties of $SiO_2$ impregnated wood in dry and saturated conditions

### 4.1 Abstract

This research has demonstrated that $SiO_2$ impregnation under high vacuum pressure of -90 kPa can significantly reduce porosity by almost 10%, and improve mechanical and viscoelastic properties of spruce wood under dry and saturated states. Characterization methods, such as Impact test, DMA, SEM, EDS, Porosity and SAXS tests were conducted on non-treated and -90 kPa treated spruce wood samples under dry, saturated and submerged states to analyze the synergistic effect of high vacuum $SiO_2$ impregnation pressure on wood's properties. The results showed that high vacuum impregnation pressure had a significant positive reinforcing effect on wood's properties. It increased the impact resistance of wood under dry and saturated conditions. Additionally, a high vacuum impregnation was able to overcome the softening effect from water and caused a significant increase in the Storage modulus by strengthening the wood's vascular structure, which accordingly increased the wood's capacity to absorb energy. High vacuum impregnation was also able to counteract the lubricating effect of water and significantly increased the Loss modulus by increasing the internal friction of the wood with the addition of the nanoparticles to the vascular system, which increased the wood's capacity to absorb and diffuse the energy. Quantitatively and qualitatively, impregnation under a vacuum pressure of -90 kPa was shown to effectively obstruct the vascular structure of spruce wood with $SiO_2$ particles. In all conditions and states, high vacuum impregnated samples showed significant benefits over non-treated samples. High vacuum $SiO_2$ impregnation was a good addition to wood and had a significant positive effect on wood's properties. Multiple materials and applications could benefit from this research wherein example instantaneous loading and deformation are expected to occur or when simultaneous elastic behavior of wood and its damping energy is needed. This study could also pave the way for research on the synergistic effect of $SiO_2$ impregnation and water absorption on the viscoelastic behavior of wood.

### 4.2 Keywords

Wood Fibers; $SiO_2$; Impregnation; Synergistic Effect; Submerged Viscoelastic Properties; Sustainability; Impact Properties; SEM.

### 4.3 Introduction

Wood exhibits good mechanical properties and a high strength-to-weight ratio. It also offers shorter construction times [1]. Additionally, wood is renewable and a good sustainable material when harvested and exploited appropriately. For many reasons, wood is an attractive material to the construction industry [2]. However, wood's physico-mechanical properties are dependent on its water content [3,4,5].

Most mechanical properties of wood are influenced and altered when its moisture content changes below the fiber saturation point (FSP) [3,4,5]. This phenomenon is related to the plasticizing and softening effects of water molecules in wood [3,4,5]. Water molecules introduce free space between long cellulose molecular chains and

facilitate their movement [5], which causes a significant change in physico-mechanical properties. Moreover, the high water uptake capacity of wood makes it susceptible to degradation and lowers its durability [4,6].
Researchers and industries have developed many treatments to decrease the water absorption capacity of wood [7]. However, one of the most commonly known and implemented solutions to mitigate wood's water uptake and enhance durability consist of externally applied coatings which are not highly effective as they do not prevent water uptake capacity in wood [7]. Over time, coated wood, just like non-coated wood, will swell due to the incompatibility of the products with the wood. Additionally, over time, the coatings will decay and wash away. Therefore, products need to be reapplied for optimal performance, which requires more maintenance [7]. A prospect method to decrease the water absorption capacity of wood consists of obstructing the wood's vascular system with dense materials like ceramics. Ceramic nanoparticles, in an aqueous colloid state, can be used to fill this porous vascular structure [8]. Through this process, the wood imbibes a colloidal solution through the vascular system. As the liquid phase evaporates, the nanoparticles agglomerate, fill the lumens and obstruct the vascular structure.

Unlike the properties of wood that are negatively affected by moisture content (e.g., stiffness, hardness, and durability), impact strength is enhanced under high relative humidity and saturated conditions [9]. However, this opposite behavior limits the use of wood in applications in which energy absorption is required (e.g., guard rails post and off-set block, fence post, decking boards, etc.). In other words, although an increase in water content improves impact strength, it causes wood to lose its stiffness and become more susceptible to degradation.

The impact strength of a solid material depends on its ability to absorb and dissipate energy under instantaneous load and deformation [9]. However, the intricate nature of wood and the effect of moisture content make the impact behavior of wood multifaceted [9]. The impact resistance of wood is dependent on fiber orientation [9]. For coniferous trees, such as spruce, the impact resistance is higher in the radial rather than in the tangential direction. The impact strength of wood is also related to its density. A higher density leads to higher impact strength [9]. A few studies have investigated the effect of moisture content on the impact strength of wood. However, the accuracy of the data is debatable. For example, Kollmann *et al*. showed in their study that impact strength increased with an increase in moisture content when the moisture content was above 20%, but the relationship was incongruous when the moisture content was below 20% [10].

The effect of water content on impact strength of wood can be better revealed if the viscoelastic behavior of wood is characterized in parallel. Viscoelastic properties (Storage Modulus, Loss Modulus, and Tan δ) are a measure and indication of the capacity of a material to absorb and dissipate energy [11]. Ultimately, all together, they identify the viscous and elastic responses of materials when they undergo oscillating loads or deformations [11]. When wood undergoes such loads, some energy is dissipated as heat [4]. Energy dissipation occurs through internal friction and is reflected in the viscoelastic properties, and the dissipation mechanism depends on the temperature and moisture content of the wood. There is an optimal moisture content that varies with temperature below the Fiber Saturation Point (FSP) at which internal friction is minimal [4]. When moisture content drops below the optimal point, static friction increases, which improves energy absorption (i.e., Storage modulus). On the

other hand, when moisture content increases toward the FSP, kinetic friction increases, which improves energy dissipation (i.e., Loss modulus). An increase in moisture content beyond the FSP reduces internal friction and thus both Storage and Loss modulus due to the wood softening and plasticizing effects of water molecules [4].

In addition, there is an optimal temperature at which the internal friction is minimal; this temperature depends on moisture content [4]. The temperature at which minimal internal friction is achieved is negatively correlated with moisture content [4]. A decrease in moisture content increases the temperature threshold. For wood that has a temperature above 0°C and moisture content above 10%, the internal kinetic friction strongly increases with temperature rise. However, for dry wood, internal kinetic friction usually decreases as the temperature rises [4].

The previous part of this research, as presented in chapter 3, studied the effect of vacuum pressures on the $SiO_2$ impregnation of wood in a dry state. The study revealed that $SiO_2$ impregnation performed at a high vacuum pressure of -90 kPa was the optimal impregnation condition that showed the best results. The results revealed that -90 kPa $SiO_2$ impregnation could significantly increase wood's density and reduce water absorption and also simultaneously increase the Storage modulus and Loss modulus of spruce wood in an oven-dried condition. However, the synergistic effect of moisture content and $SiO_2$ impregnation on spruce wood's impact and viscoelastic properties are still unknown.

Accordingly, this chapter will pursue the previous study by focusing on the -90 kPa $SiO_2$ impregnation conditions, considering that it is the optimal impregnation condition, and further characterize the aforementioned properties of spruce wood under dry and saturated conditions. Therefore, impact strength and the alteration of viscoelastic properties of samples before and after vacuum impregnation respective to dry and saturated conditions will be analyzed. It is worth mentioning that there are currently few studies on the effect of $SiO_2$ impregnation on the mechanical properties of wood, as well as little information on their impact and viscoelastic behavior. Therefore, this article is taking a step forward to fill the gap of knowledge accordingly. Additionally, this article will make use of scanning electron microscopy and small angle X-ray scattering to further analyze and validate the results and hypotheses.

## 4.4 Methodology

### 4.4.1 Materials

The samples used in this study were prepared from spruce wood of the Picea glauca species, commonly known as Canadian spruce or White spruce. Spruce is the most frequently used type of wood in construction in eastern Canada. LUDOX HS-40 colloidal silica, a water-based colloidal suspension of nano-silica, was used as an impregnation solution. This suspension contained a 40% solution of 12 nm $SiO_2$ particles, with a pH of 9.5, and has an aqueous density of 1.3 g/cm$^3$ at 25°C. The solution was purchased from Sigma-Aldrich.

### 4.4.2 Sample Preparation

The wood specimens were cut and sanded to the required dimensions for the tests and characterization techniques. The samples' dimensions (length x width x thickness) were: (25mm x 10mm x 2mm) dynamic mechanical analysis, (127mm x 12.7mm x

7mm) for Impact test, and (33mm x 14.5mm x 14.5mm) for porosity analysis. The samples were progressively sanded using sandpaper with grits of 80, 100, 120, 220, and 600 to remove any residues on the specimens and reach a consistent surface roughness. The length of the samples was cut along the longitudinal wood fibers' axis, and the base cross-section (width and thickness) was in the tangential-radial plane. The samples were dried in an oven at 103°C for 24 hours to minimize humidity content. To test the samples under saturated conditions, when required, samples were kept in distilled water at room temperature and weighed periodically until the difference between two consequent measurements became less than 1%. To test the samples in the submerged condition when required, the samples were first saturated with the same procedure explained previously, and then further kept and tested under distilled water.

### 4.4.3 Impregnation Process

The wood specimens were impregnated with the $SiO_2$ colloid using a dip-coating technique. Although the samples can naturally absorb the solution, air entrapped within the macropores will impede the effective impregnation of the sample. To mitigate this issue and improve the effectiveness of the impregnation, the process was conducted under vacuum pressure using the Buehler Cast-N-Vac 1000 vacuum chamber. The most effective vacuum impregnation pressure was previously determined in chapter 3 to be -90 kPa. Accordingly, for this chapter, the samples were impregnated under pressures of -90 kPa for one hour. Following the impregnation process, the samples were placed in an oven at 50°C for one hour and 100°C for five minutes to accelerate the agglomeration of the $SiO_2$ nanoparticles inside the vascular system.

### 4.4.4 Sample Designations and Descriptions

Table 4.1 presents the sample designations with their respective descriptions. These designations will be used throughout the tables and figures presented in this chapter.

*Table 4.1: Sample designations and descriptions*

| Sample Designation | Description |
|---|---|
| **NT** | Non-Treated |
| **-90 kPa** | $SiO_2$ impregnated wood under a vacuum pressure of -90 kPa |

*Suffix: Sub = Under Submerged State, Sat = Under Saturated State

**No suffix = Dry State

### 4.4.5 Characterizations

#### 4.4.5.1 Impact Test Analysis

The mechanical behavior of treated and non-treated samples were assessed through impact testing under dry and saturated states. Twenty samples of each condition were tested. The tests were performed using a Zwick Roell HIT5.5P Pendulum Impact Tester with a charpy setup with a 5.4J hammer, and by following the standard ASTM D6110.

#### 4.4.5.2 Dynamic Mechanical Analysis under Dry and Submerged Conditions

The treated and non-treated wood samples were tested by Dynamic Mechanical Analysis (DMA) equipped with a submerged 3-point bending clamp setup. Ten samples of each condition were tested. The synergistic effects of the vacuum pressure impregnation process on the viscoelastic properties of wood (i.e., Storage modulus, Loss modulus, and Tan δ) under submerged conditions were studied. Accordingly, the

viscoelastic properties were measured before and after each impregnation under dry and submerged conditions. Multi-strain tests were carried out using a TA Instruments DMA Q800 testing machine set to a frequency of 1 Hz and a temperature range of 5-40°C. The temperature range was selected to analyze the effect of impregnation at ambient, below ambient, and above ambient temperature. The temperature range for testing in submerged conditions is restrained above 0°C to prevent freezing, and below 80°C to prevent high water evaporation. In conjunction, considering there was no significant change in properties over 40°C, the upper limit of 40°C was selected to save time.

#### 4.4.5.3 Scanning Electron Microscopy

The treated and non-treated wood samples were analyzed with a Scanning Electron Microscope (SEM) to observe morphology and fracture mechanics at failure following impact tests. The fractures occur in the middle of the samples, which is the maximum distance from each extremity. Accordingly, after impact, the samples were cut in half at the middle location to reveal the inner section of the vascular system of the wood. Prior to SEM analyses, all samples were polished and coated with a vapour-deposited 20 µm layer of Pd-Au. Microscopy was carried out using a JSM-7500F FESEM SEM at 2-3 kV.

#### 4.4.5.4 Porosity analysis

The porosity of samples before and after impregnation was determined by identifying the true and apparent densities of the samples. First, the true density of the samples was obtained using a micromeritics gas pycnometer (AccuPyc II 1340). Helium was used for the measurements. The density of each sample was measured three times to determine the mean value both before and after impregnation. Second, the apparent density of the samples was measured with respect to ASTM D2395 Test Method A. These two measurements were performed on each sample before and after impregnation. Accordingly, porosity of the samples before and after the impregnation was calculated using Eq. (1), where *Apparent Density* is the density of the samples obtained using ASTM D2395 Test Method A, and *True Density* is the density of the samples obtained using the pycnometer.

$$Porosity = 1 - \left(\frac{Apparent\ Density}{True\ Density}\right) \quad (1)$$

#### 4.4.5.5 Small Angle X-ray Scattering

Treated and non-treated wood samples were tested with Small Angle X-ray Scattering (SAXS) to complement the results obtained through microscopy. The results help to indicate the impregnation efficacy and confirm the presence of $SiO_2$ within the samples. These tests were conducted with a Bruker AXS Nanostar system.

#### 4.4.5.6 Statistical Analysis

A two-sample t-test was applied to compare the mean values of each key property [12]. A confidence interval of 95% was considered as long as the P-value was below 0.05, indicating significant differences among the values.

## 4.5 Results and discussion

### 4.5.1 Porosity Analysis

Figure 4.1 shows the results of the porosity analysis conducted on -90 kPa before and after impregnation. The results showed that -90 kPa impregnation caused a reduction in porosity of almost 10%. Table 4.2 presents the statistical analysis conducted to compare the porosity of the samples before and after impregnation. The P-values of the statistical analyses revealed that the change in porosity before and after impregnation was significant. Accordingly, $SiO_2$ impregnation conducted under -90 kPa of vacuum pressure was confirmed effective and capable of significantly reducing porosity.

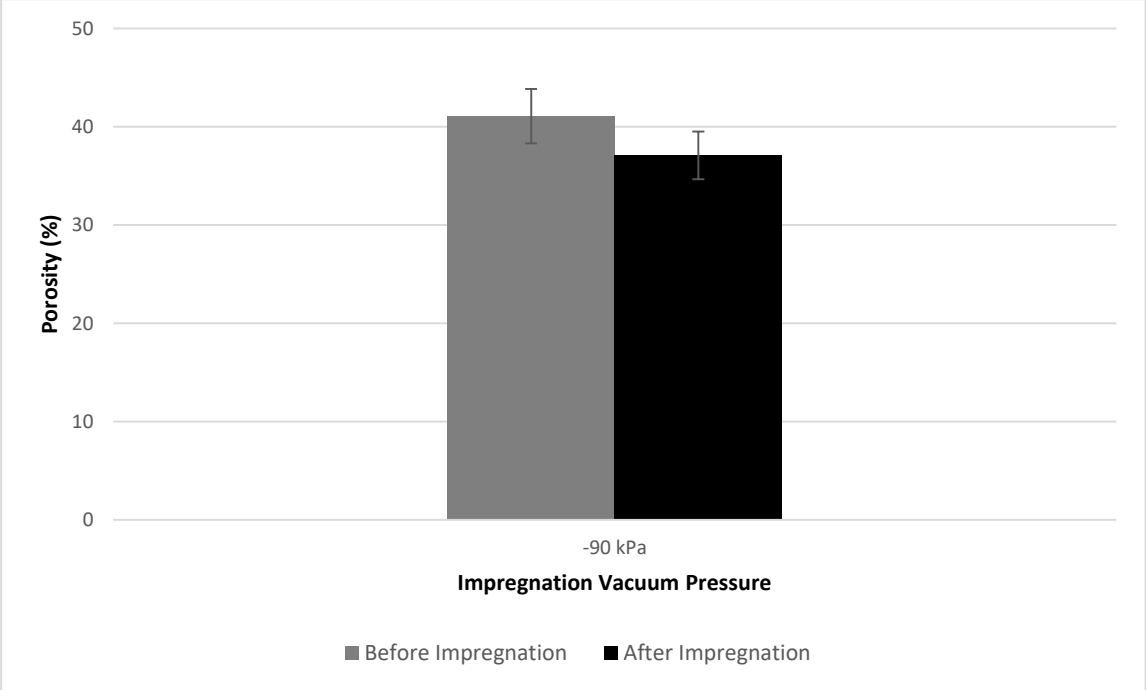


*Figure 4.1: Porosity analysis of the -90 kPa samples before and after impregnation*

*Table 4.2: Statistical analysis of the porosity measurements*

| **Before** | | | **After** | | | **\|Before – After / Before\|** | |
|---|---|---|---|---|---|---|---|
| **Type** | Average Porosity % | Standard Deviation | **Type** | Average Porosity % | Standard Deviation | Average Porosity %Difference | Standard Deviation |
| **Before -90 kPa** | 41.1 | 2.8 | **After -90 kPa** | 37.1 | 2.4 | 9.7 | 5.3 |
| **Sample Comparison** | | | Z score & P-value | | | Statistical Significance | |
| **Before -90 kPa vs After -90 kPa** | | | Z score = 2.651<br>P value = <0.05 | | | Significant | |

### 4.5.2 Small Angle X-ray Scattering

Figure 4.2 and Figure 4.3 present the results of the SAXS tests conducted on non-treated and -90 kPa $SiO_2$ treated samples. The SAXS intensity distribution was greater for the $SiO_2$ treated wood compared to the non-treated wood. The -90 kPa sample exhibited a significant increase in particle count scattering intensity after impregnation. The number of counts for the -90 kPa sample (73,586 counts) was two times higher than that obtained for non-treated wood (36,191 counts). These results confirmed the presence of $SiO_2$ within the wood's vascular system after impregnation.

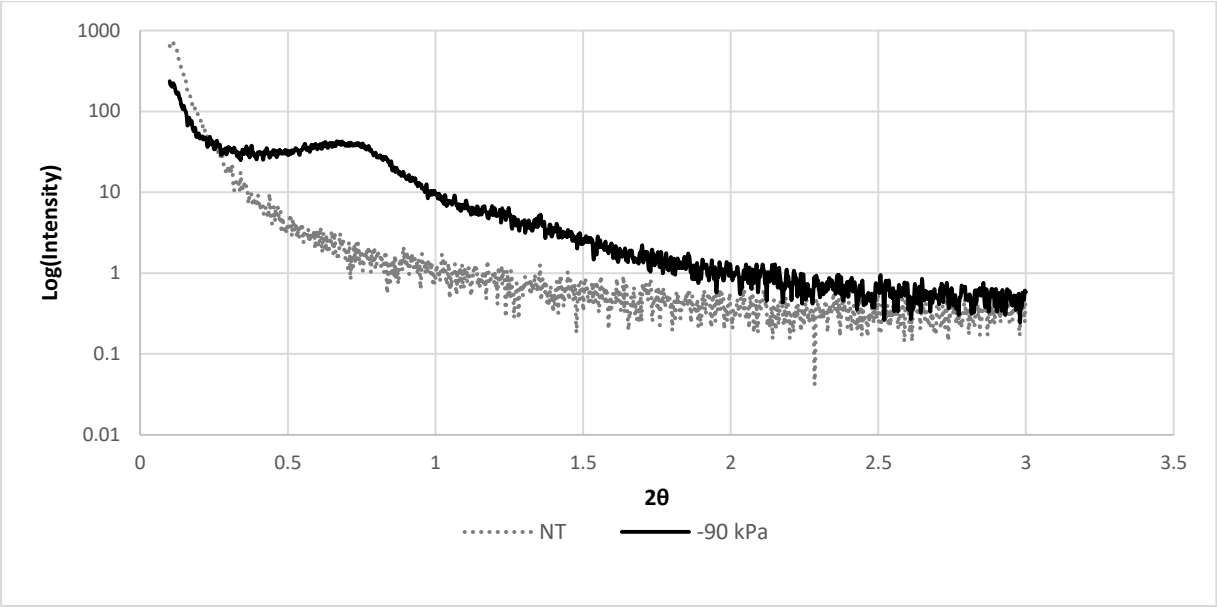


*Figure 4.2: SAXS test results for non-treated and -90 kPa treated samples*

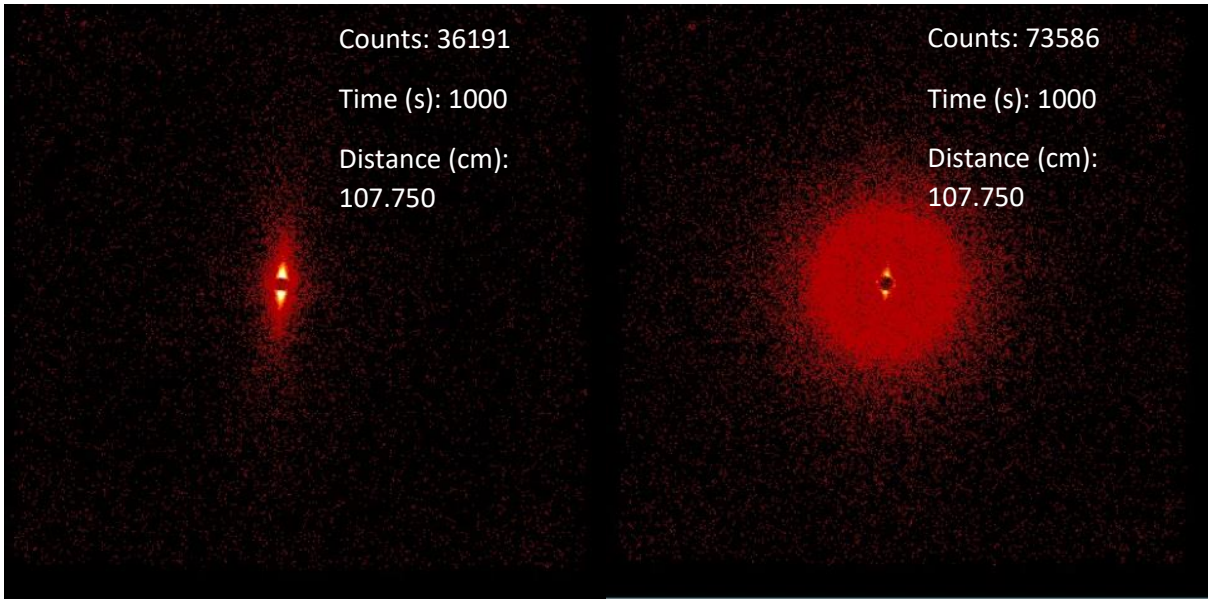


a) NT b) -90 kPa

*Figure 4.3: 2D-SAXS patterns from Non-Treated and -90 kPa treated samples with the X-ray beam directed perpendicular to the sample axis*

### 4.5.3 Impact Test Analysis

Impact tests are destructive; accordingly, it was not possible to directly assess the effect of the $SiO_2$ impregnation by testing the same samples before and after impregnation. Instead, the different conditions were tested separately and averages were compared. To minimize the effect of the substrate, a greater population of tests were performed on the different conditions.

Figure 4.4 shows the results of the impact tests of the -90 kPa treated and non-treated oven-dried wood samples. The -90 kPa samples exhibited the highest impact resistance of 372.52 J/m, while the lowest impact resistance of 270.63 J/m was recorded for the non-treated samples. Accordingly, the results showed that -90 kPa vacuum impregnation enhanced the impact resistance of wood under dry conditions. Table 4.3 presents the conducted statistical analysis to compare the impact resistance

of the -90 kPa and NT samples under dry conditions. The P-values of the statistical analyses revealed that the difference/increase in impact resistance was significant. According to the results, -90 kPa $SiO_2$ treated wood was 1.38 times more resistant to impact under dry conditions compared to the non-treated wood. In general, the higher the density of wood, the higher the impact strength. Impregnated samples had a lower porosity (i.e., higher density) and thus possessed a higher impact resistance. One hypothesis to justify this phenomenon is that the $SiO_2$ nanoparticles totally or partially filled in the lumens where the crack had to cross. Therefore the crack required a higher amount of energy to propagate through the $SiO_2$ particles. Another possible hypothesis is that high vacuum $SiO_2$ impregnation increased the dispersion of $SiO_2$ particles in the vascular system of wood. This enhanced dispersion increased internal friction in the wood's vascular system where fiber pull-out occurred to complete the impact fracture process. As a result, the impregnated samples exhibited higher impact resistance due to a higher energy dissipation capacity. The accuracy of these hypotheses has been verified and discussed in sections 4.5.4 and 4.5.5.

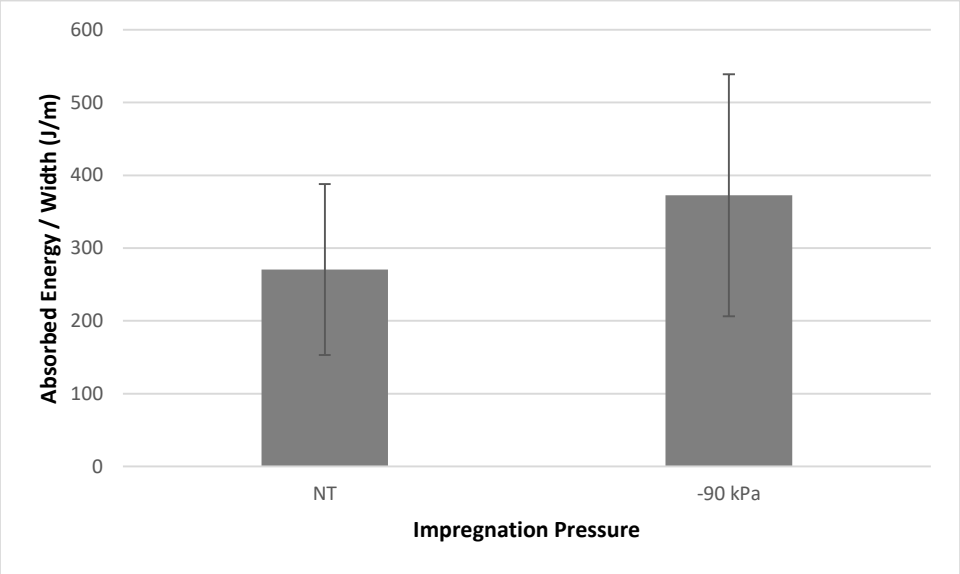


*Figure 4.4: Impact strength of the treated and non-treated oven dry wood samples*

*Table 4.3: Statistical analysis of the impact strength of the treated and non-treated oven dry wood samples*

| Impregnation Condition | Average Impact Strength (J/m) | Standard Deviation |
|---|---|---|
| **NT** | 270.63 | 117.42 |
| **-90 kPa** | 372.52 | 166.31 |
| **%Difference** | 37.6% | |
| **Sample Comparison** | Z score & P-value | Statistical Significance |
| **NT vs -90 kPa** | Z score = -2.328<br>P value = < 0.05 | Significant |

Figure 4.5 shows the results of the impact tests of the -90 kPa and NT samples under saturated conditions. The -90 kPa samples demonstrated an average impact energy of 570.80 J/m in contrast to the NT samples with 281.61 J/m. Table 4.4 presents the statistical analysis comparing the impact resistance of -90 kPa treated and non-treated

samples under saturated conditions. The statistical analysis revealed that the difference/increase in impact resistance was significant. According to the results, -90 kPa $SiO_2$ treated wood was 2 times more resistant to impact under saturated conditions compared to the non-treated wood. Interestingly, -90 kPa samples under saturated conditions significantly increased in resistance compared to the -90 kPa samples under dry conditions. The results showed that -90 kPa saturated samples had the highest impact strength among all the tested samples. The difference in the impact resistance revealed by the tests in the dry and saturated conditions could be because of two combined factors. The presence of water in the vascular system of wood enhanced the damping effect by introducing a viscous barrier against the propagation of the crack. Moreover, as hypothesized, the dispersion of $SiO_2$ particles in the wood's vascular system enhanced the internal kinetic friction and thus the wood's capacity for energy dissipation. These factors could synergistically boost the impact strength of spruce wood under saturated conditions. The results demonstrated that the increase in impact strength of the saturated -90 kPa samples was 1.5 times higher compared to the dry -90 kPa samples. This outcome revealed a synergy between the effect of $SiO_2$ impregnation and water content at saturation on the impact resistance of spruce wood.

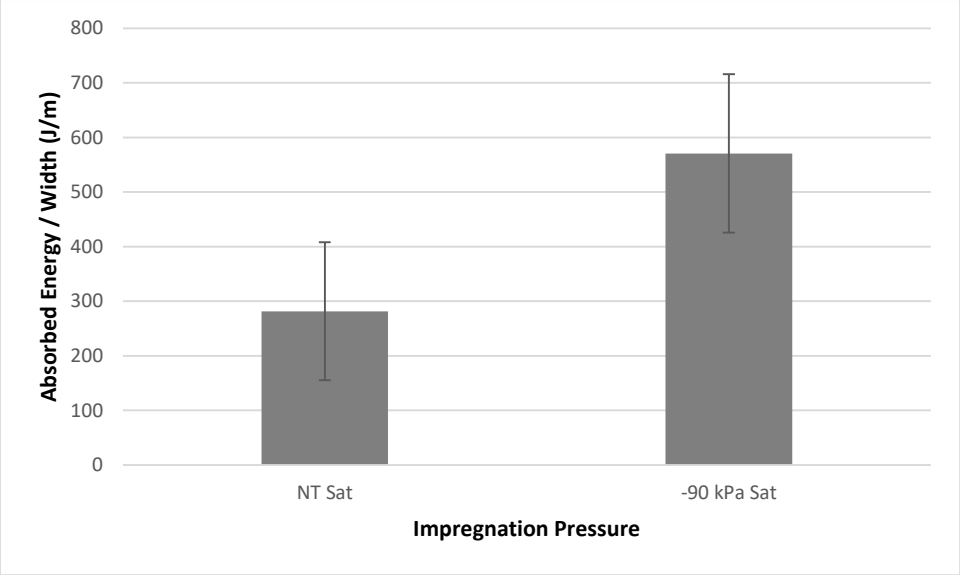


*Figure 4.5: Impact strength of the treated and non-treated saturated wood samples*

*Table 4.4: Statistical analysis of the impact strength of the treated and non-treated saturated wood samples*

| Impregnation Condition | Average Impact Strength (J/m) | Standard Deviation |
|---|---|---|
| **NT Sat** | 281.61 | 126.45 |
| **-90 kPa Sat** | 570.80 | 145.12 |
| **%Difference** | 102.7% | |
| **Sample Comparison** | Z score & P-value | Statistical Significance |
| **NT Sat vs -90 kPa Sat** | Z score = -4.751<br>P value = <0.05 | Significant |

Ultimately, -90 kPa treated samples show a greater impact resistance in all moisture states and significantly improve the impact resistance of wood and thus is a valuable addition.

### 4.5.4 Dynamic Mechanical Analysis in Dry and Submerged Conditions

Figure 4.6 shows the Storage modulus results of the dynamic mechanical analysis that was conducted on the -90 kPa and NT samples in dry and submerged conditions. The dry -90 kPa exhibited the highest Storage modulus of 5923 MPa, followed by the dry NT, the submerged -90 kPa, and the submerged NT with the Storage moduli of 3725 MPa, 1720 MPa, and 1000 MPa, respectively. The results showed that in the dry condition, the -90 kPa samples had 1.6 times more rigidity than non-treated wood. The tests in submerged conditions showed a similar increase in magnitude in the Storage moduli (1.72 times) of the -90 kPa and NT samples.

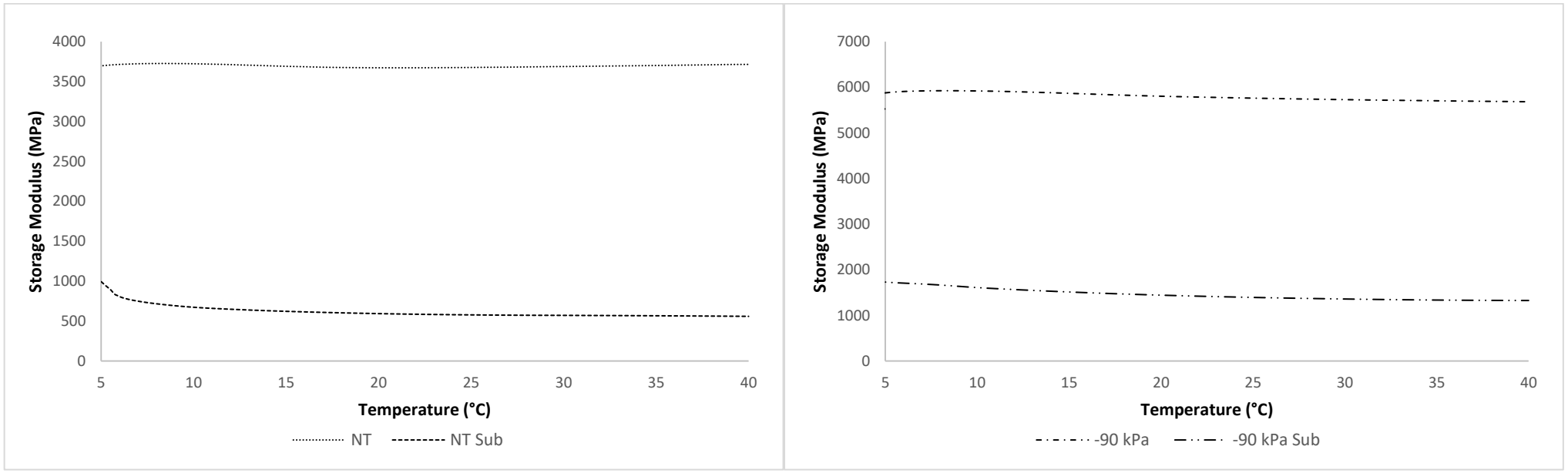


*a) Non-treated dry and submerged* *b) -90 kPa dry and submerged*

*Figure 4.6: Dynamic mechanical analysis results of the Storage modulus*

Table 4.5 presents the statistical analysis conducted to compare the Storage modulus of the treated and non-treated samples in dry and submerged states. The P-values of the statistical analyses revealed that the change in Storage modulus before and after the impregnation in dry and submerged conditions was significant for all the samples. Amongst all the conditions, the -90 kPa samples exhibited a significant increase in the Storage modulus. This increase is most likely attributed to the reduction of porosity and increase in density as a result of the obstruction of the wood's vascular system by $SiO_2$ nanoparticles. The addition of the nanoparticles with higher Storage modulus (compared to the wood) reinforced the wood's structure based on the rule of mixture [13]. The results showed that under submerged conditions, -90 kPa samples have 2 times more rigidity than the NT samples under the same conditions. Results show that impregnation counteracted the effect of water molecules that softened the wood's structure; and thus, helped strengthen the wood. Accordingly, in both dry and submerged cases, the impregnated sample effectively increased and better maintained rigidity.

*Table 4.5: DMA test results of the -90 kPa dry and submerged Storage modulus before and after the $SiO_2$ impregnations*

| **Test Condition** | **Average Storage Modulus (MPa) at 5°C** | | | **Average Storage Modulus (MPa) at 25°C** | | | **Average Storage Modulus (MPa) at 35°C** | | |
|---|---|---|---|---|---|---|---|---|---|
| | Impregnation Status | | %Difference | Impregnation Status | | %Difference | Impregnation Status | | %Difference |
| | Before | After | | Before | After | | Before | After | |
| **Dry** | 3690 | 5876 | 65 | 3676 | 5760 | 62 | 3701 | 5702 | 59 |
| **Submerged** | 857 | 1720 | 152 | 576 | 1391 | 197 | 573 | 1340 | 185 |
| **%Difference** | -75 | -71 | | -84 | -76 | | -84 | -77 | |
| **Sample Comparison** | Z score & P-value | | Statistical Significance | Z score & P-value | | Statistical Significance | Z score & P-value | | Statistical Significance |
| **Before Dry vs Before Sub** | Z score = 8.401<br>P value = <0.05 | | Significant | Z score = 9.925<br>P value = <0.05 | | Significant | Z score = 10.134<br>P value = <0.05 | | Significant |
| **Before Dry vs After Dry** | Z score = -4.099<br>P value = <0.05 | | Significant | Z score = -4.014<br>P value = <0.05 | | Significant | Z score = -3.835<br>P value = <0.05 | | Significant |
| **Before Sub vs After Sub** | Z score = -3.405<br>P value = <0.05 | | Significant | Z score = -3.647<br>P value = <0.05 | | Significant | Z score = -3.478<br>P value = <0.05 | | Significant |
| **After Dry vs After Sub** | Z score = 8.575<br>P value = <0.05 | | Significant | Z score = 9.274<br>P value = <0.05 | | Significant | Z score = 9.186<br>P value = <0.05 | | Significant |

*%Difference = ((After – Before) / Before) x 100

Figure 4.7 shows the Loss modulus results of the dynamic mechanical analysis that was conducted on the -90 kPa and NT samples under dry and submerged conditions. Accordingly, dry -90 kPa achieved the highest Loss modulus of 304.5 MPa, followed by the submerged -90 kPa, the dry NT, and the submerged NT with Loss moduli of 227 MPa, 211.5 MPa, and 116.5 MPa, respectively. The results showed that under dry conditions, -90 kPa impregnated wood exhibited a Loss modulus of 1.44 times higher than the NT. It also showed that under the submerged condition, the Loss modulus of the -90 kPa samples was even higher, being 1.95 times larger than that of the NT samples.

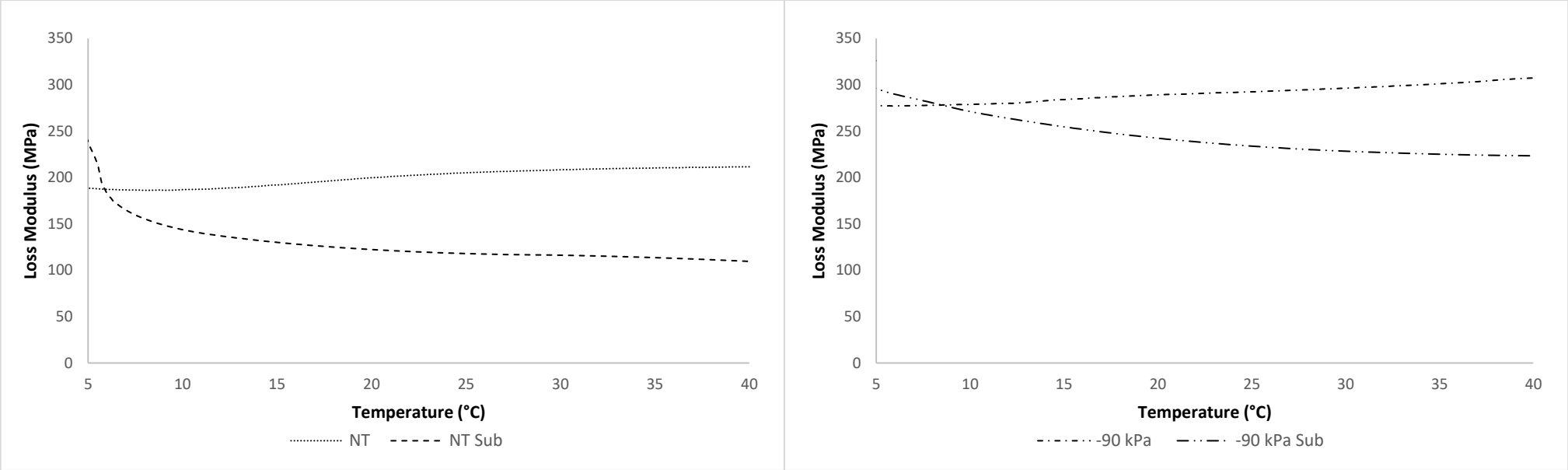


*a) Non-treated dry and submerged* *b) -90 kPa dry and submerged*

*Figure 4.7: Dynamic mechanical analysis results of the Loss modulus*

Table 4.6 presents the statistical analysis conducted to compare the Loss modulus of the -90 kPa and NT samples under dry and submerged conditions. The statistical analyses revealed that the change in Loss modulus before and after impregnation under dry and submerged conditions was significant for all the samples. All the DMA tests under dry and submerged conditions showed a significant increase in Loss modulus after the $SiO_2$ impregnation. The only samples that underwent a reduction in Loss modulus were the NT samples under the submerged condition. Interestingly, the results also showed a stabilization of the Loss modulus between -90 kPa dry and -90 kPa submerged, as their difference was insignificant at all the tested temperatures. The increase in Loss modulus due to impregnation of the nanoparticles is attributed to the increase in the internal friction in the wood's vascular structure. In other words, the capacity of wood to dissipate energy increased because of a higher amount of kinetic friction between fibers and particles. High vacuum impregnation was able to efficiently disperse the $SiO_2$ nanoparticles in the wood's structure and transform mechanical energy into heat through internal kinetic friction even in the presence of the plasticizing effect of water molecules. Accordingly, under both dry and submerged conditions, high vacuum $SiO_2$ impregnation had an enhancing effect on the Loss modulus, and thus could be a valuable wood treatment for applications when high energy damping is required. The impregnation of $SiO_2$ nanoparticles under -90 kPa of vacuum pressure could also improve the degradation resistance of spruce wood by decreasing water uptake capacity, which can make infrastructures like guard rails and off-set blocks more effective and durable.

*Table 4.6: DMA test results of the -90 kPa dry and submerged Loss modulus before and after the $SiO_2$ impregnations*

| **Test Condition** | **Average Loss Modulus (MPa) at 5°C** | | | **Average Loss Modulus (MPa) at 25°C** | | | **Average Loss Modulus (MPa) at 35°C** | | |
|---|---|---|---|---|---|---|---|---|---|
| | Impregnation Status | | %Difference | Impregnation Status | | %Difference | Impregnation Status | | %Difference |
| | Before | After | | Before | After | | Before | After | |
| **Dry** | 189 | 278 | 52 | 205 | 292 | 50 | 210 | 301 | 51 |
| **Submerged** | 202 | 293 | 90 | 118 | 233 | 143 | 117 | 226 | 135 |
| **%Difference** | 11 | 7 | | -41 | -19 | | -43 | -23 | |
| **Sample Comparison** | Z score & P-value | | Statistical Significance | Z score & P-value | | Statistical Significance | Z score & P-value | | Statistical Significance |
| **Before Dry vs Before Sub** | Z score = -0.439<br>P value = 0.661 | | Insignificant | Z score = 3.998<br>P value = <0.05 | | Significant | Z score = 4.155<br>P value = <0.05 | | Significant |
| **Before Dry vs After Dry** | Z score = -3.731<br>P value = <0.05 | | Significant | Z score = -3.221<br>P value = <0.05 | | Significant | Z score = -3.147<br>P value = <0.05 | | Significant |
| **Before Sub vs After Sub** | Z score = -2.060<br>P value = <0.05 | | Significant | Z score = -3.308<br>P value = <0.05 | | Significant | Z score = -3.130<br>P value = <0.05 | | Significant |
| **After Dry vs After Sub** | Z score = -0.387<br>P value = 0.699 | | Insignificant | Z score = 1.542<br>P value = 0.123 | | Insignificant | Z score = 1.914<br>P value = 0.0556 | | Insignificant |

*%Difference = ((After – Before) / Before) x 100

Figure 4.8 shows the Tan δ results of the -90 kPa and NT samples under dry and submerged conditions. The results revealed that testing the samples under submerged conditions increased Tan δ for both NT and -90 kPa samples. This increase is because of the plasticizing effect of water molecules when moisture content is beyond FSP. Among the samples, the submerged NT exhibited the highest Tan δ of 0.23, followed by the submerged -90 kPa with 0.17. Ultimately, -90 kPa impregnation led to a reduction of Tan δ of the wood.

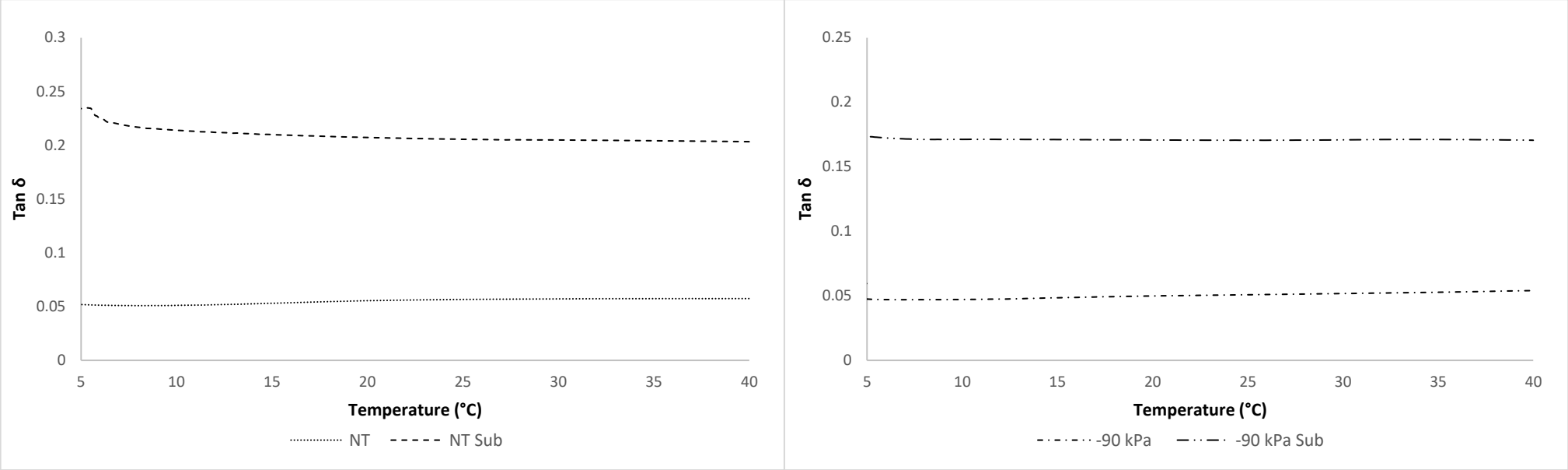


*a) Non-treated dry and submerged* *b) -90 kPa dry and submerged*

*Figure 4.8: Dynamic mechanical analysis results of the Tan δ*

Table 4.7 summarizes the statistical analysis conducted to compare the Tan δ of the -90 kPa and NT samples under dry and submerged conditions. The results revealed that the change in Tan δ before and after impregnation under dry and submerged conditions was significant for all the samples and conditions except for -90 kPa dry compared to non-treated dry over 25°C. A decrease in Tan δ means a reduction of viscous behavior and an increase in elastic response. These results confirmed that impregnation had a positive effect on the stabilization and enhancement of spruce wood's properties under dry and submerged conditions.

*Table 4.7: DMA test results of the -90 kPa dry and submerged Tan δ before and after the $SiO_2$ impregnations*

| **Test Condition** | **Average Tan δ at 5°C** | | | **Average Tan δ at 25°C** | | | **Average Tan δ at 35°C** | | |
|---|---|---|---|---|---|---|---|---|---|
| | Impregnation Status | | %Difference | Impregnation Status | | %Difference | Impregnation Status | | %Difference |
| | Before | After | | Before | After | | Before | After | |
| **Dry** | 0.052 | 0.047 | -8 | 0.057 | 0.051 | -9 | 0.057 | 0.053 | -7 |
| **Submerged** | 0.231 | 0.173 | -25 | 0.205 | 0.170 | -17 | 0.205 | 0.172 | -17 |
| **%Difference** | 347 | 267 | | 270 | 238 | | 263 | 228 | |
| **Sample Comparison** | Z score & P-value | | Statistical Significance | Z score & P-value | | Statistical Significance | Z score & P-value | | Statistical Significance |
| **Before Dry vs Before Sub** | Z score = -23.982<br>P value = <0.05 | | Significant | Z score = -44.287<br>P value = <0.05 | | Significant | Z score = -53.608<br>P value = <0.05 | | Significant |
| **Before Dry vs After Dry** | Z score = 2.010<br>P value = <0.05 | | Significant | Z score = 1.752<br>P value = 0.080 | | Insignificant | Z score = 1.587<br>P value = 0.113 | | Insignificant |
| **Before Sub vs After Sub** | Z score = 6.301<br>P value = <0.05 | | Significant | Z score = 6.196<br>P value = <0.05 | | Significant | Z score = 6.229<br>P value = <0.05 | | Significant |
| **After Dry vs After Sub** | Z score = -21.549<br>P value = <0.05 | | Significant | Z score = -21.219<br>P value = <0.05 | | Significant | Z score = -21.621<br>P value = <0.05 | | Significant |

*%Difference = ((After – Before) / Before) x 100

### 4.5.5 Scanning Electron Microscopy

Figure 4.9 & 4.10 present SEM micrographs performed on the NT and -90 kPa impact test samples after failure in dry and saturated states, respectively. The SEM analysis was performed in conjunction with Energy Dispersive Spectroscopy (EDS) to survey the presence and dispersion of silica nanoparticles in the wood's structure. The EDS micrographs with the element spectrum that highlight the sample's composition are presented in Appendix B. Accordingly, in conjunction with SEM and EDS, it is possible to assess the dispersion of $SiO_2$ particles within the vascular system of the wood before and after the impregnation.

Figure 4.9 & 4.10 (a, c, e) show the cross-sectional view (longitudinal-tangential plane) of the lumens for the NT sample after the impact tests in the dry and saturated conditions, respectively. In both cases, no particles were detected in the lumens. That absence of $SiO_2$ particles was also confirmed by EDS (see Appendix B).

Figure 4.9 & 4.10 (b, d, f) show the cross-sectional view (longitudinal-tangential plane) of the lumens for the -90 kPa sample after the impact tests in the dry and saturated conditions, respectively. The SEM micrographs and EDS analysis (Appendix B) confirmed the presence of $SiO_2$ in the lumens for the -90 kPa samples tested in both conditions.

In the dry state, SEM micrographs revealed the presence of $SiO_2$ particles in the form of microscopic agglomerates attached to the inner walls of the lumens. However, in the saturated state, the inner wall morphology of the lumens appeared to be different from the one in the dry condition. The SEM analysis revealed that the $SiO_2$ particles were uniformly precipitated on the inner wall of the lumen in the form of a dense film. This could be because of the mediating effects of water molecules to anchor the $SiO_2$ particles on the inner walls of the lumens through the formation of hydrogen bonds between the oxygen of silicon dioxide and the hydroxyl groups of cellulose during the water submersion period.

The SEM analysis confirmed a decrease in porosity (Figure 4.1), followed by the impregnation, rooted in the obstruction of the wood's lumen. This finding also supported the reasoning behind the DMA test results that showed that -90 kPa significantly increased the Storage and Loss moduli compared to the NT samples. The high dispersion of $SiO_2$ particles in the lumens simultaneously increased the Storage modulus with the reinforcing effect of $SiO_2$ nanoparticles, and Loss modulus by enhancing the internal friction in the wood's structure. Also, as discussed in section 4.5.3, and hereby confirmed by the micrographs, the -90 kPa samples exhibited a higher impact strength because the dispersion of $SiO_2$ particles in the vascular system of wood could increase the required energy to propagate a fracture.

Ultimately, the micrographs show and confirm positive impregnation efficiency and the effect of the -90 kPa vacuum pressure. The micrographs highlight a high diffusion and agglomeration, and a dense solid film of $SiO_2$ nanoparticles in the vascular system of wood under dry, and saturated conditions, respectively. As discussed in section 4.5.3, the -90 kPa saturated samples achieved the highest impact resistance of all the samples. As discussed in section 4.5.4, the -90 kPa submerged samples achieved an increase in the Storage and Loss moduli compared to the NT submerged samples. These increases are hereby confirmed and justified to be due to the agglomeration and dense solid film of $SiO_2$ in the vascular system and to the positive reinforcement effect of the wood-$SiO_2$ interaction. The wood-$SiO_2$ interaction following high vacuum impregnation pressure was able to mitigate the effect of water on wood and enhanced the mechanical and viscoelastic properties.

*a) NT Low Magnification*

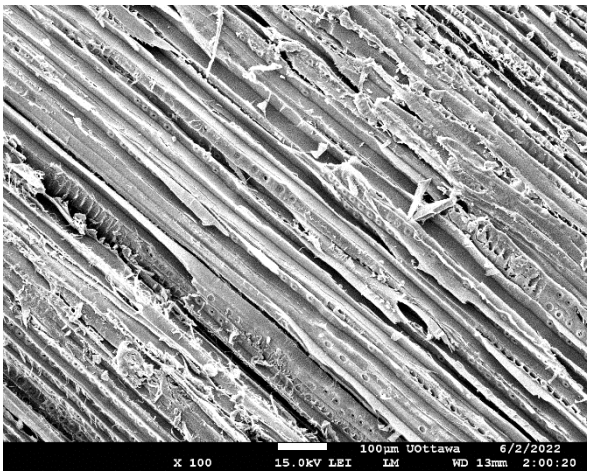


*b) -90 kPa Low Magnification*

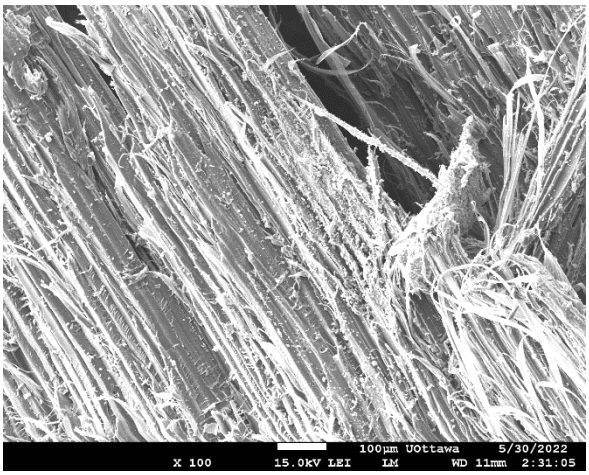


*c) NT Medium Magnification*

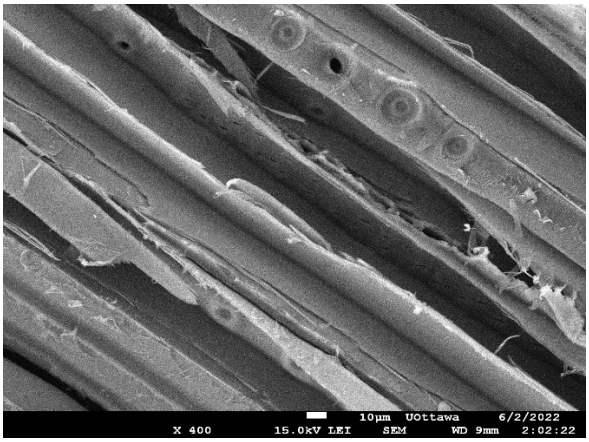


*d) -90 kPa Medium Magnification*

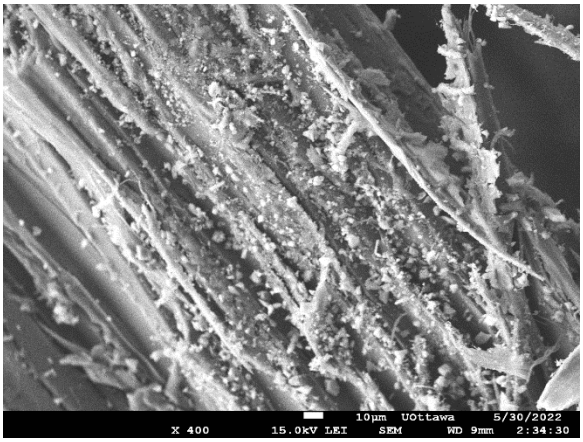


*e) NT High Magnification*

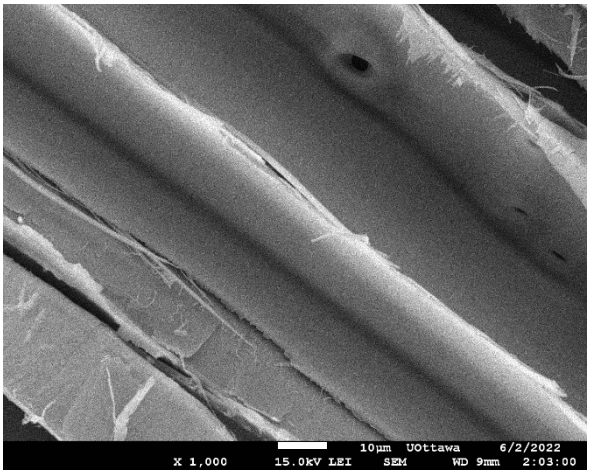


*f) -90 kPa High Magnification*

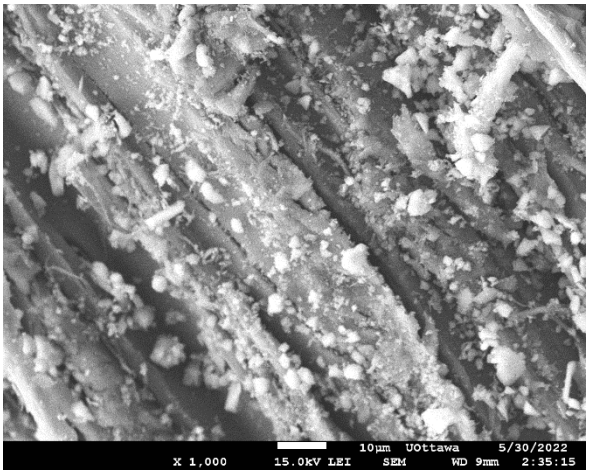


*Figure 4.9: SEM micrographs of a,c,e) non-treated and b,d,f) -90 kPa treated samples dry*

*a) NT Sat Low Magnification*

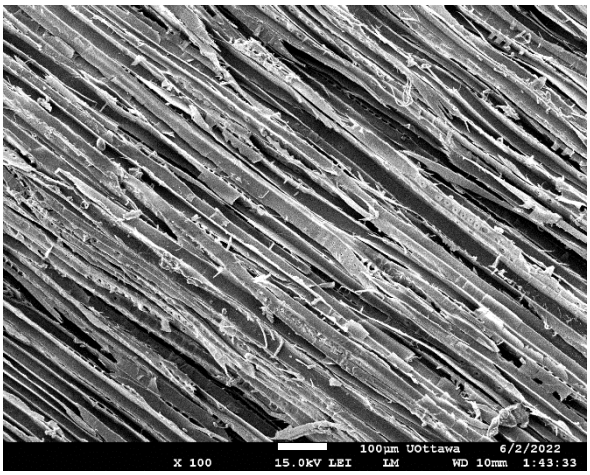


*b) -90 kPa Sat Low Magnification*

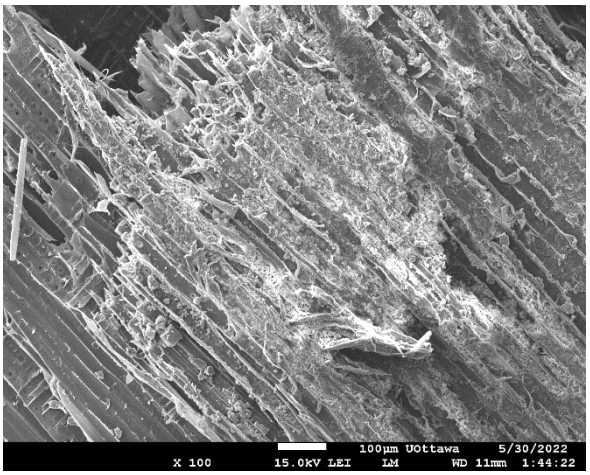


*c) NT Sat Medium Magnification*

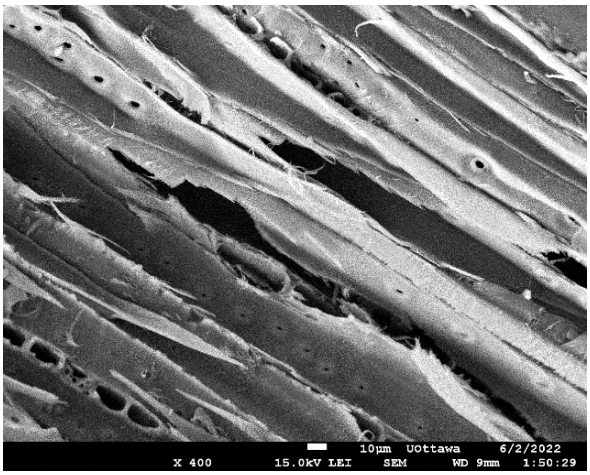


*d) -90 kPa Sat Medium Magnification*

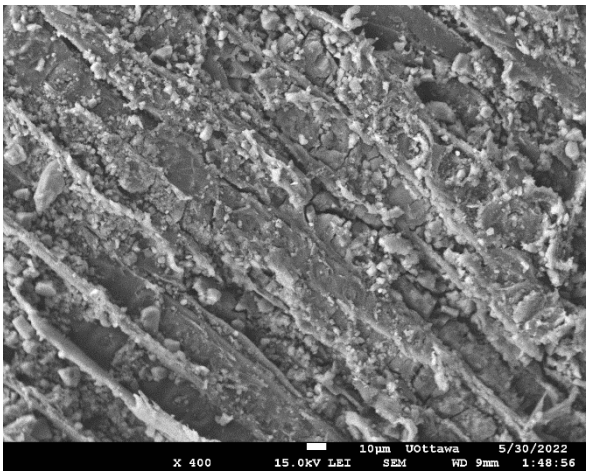


*e) NT Sat High Magnification*

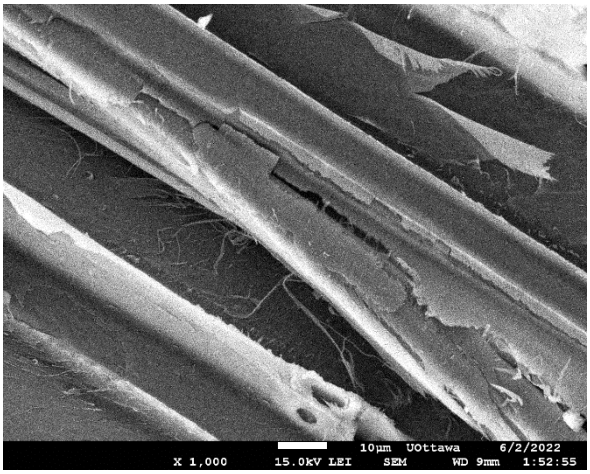


*f) -90 kPa Sat High Magnification*

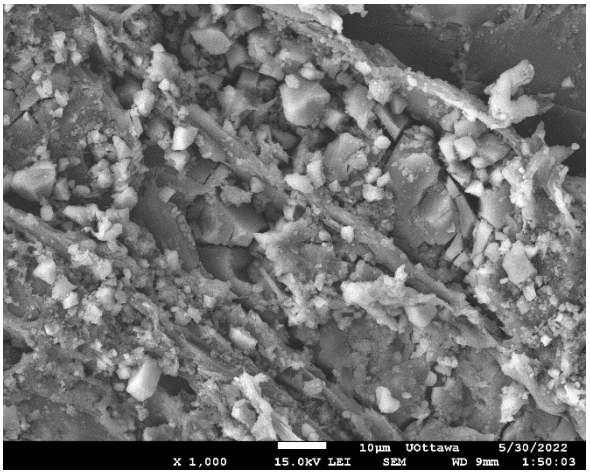


*Figure 4.10: SEM micrographs of a,c,e) non-treated and b,d,f) -90 kPa treated samples saturated*

## 4.6 Conclusion

This research has demonstrated that $SiO_2$ impregnation done under high vacuum pressure of -90 kPa can significantly reduce porosity by almost 10%, and improve mechanical and viscoelastic properties of spruce wood under dry and saturated states. Characterization methods such as Impact test, DMA, SEM, EDS, Porosity and SAXS test were conducted on non-treated and -90 kPa treated spruce wood samples under dry, saturated and submerged states to analyze the synergistic effect of high vacuum $SiO_2$ impregnation pressure on wood's properties.

The results showed that high vacuum impregnation pressures have significant positive reinforcing effects on wood's properties. It increased impact resistance of wood by 1.38 times in dry state and 2 times in saturated conditions. It also led to an increase in Storage modulus in dry and submerged states by 1.6 times and 1.72 times, respectively. It also demonstrated an increase in Loss modulus in dry and submerged states by 1.44 times and 1.95 times, respectively, contrastingly to non-treated samples, which were subjected to a reduction in Loss modulus following submersion. It also led to a reduction in Tan δ in both dry and submerged conditions, contrastingly to non-treated samples that underwent an increase in Tan δ after submersion. Accordingly, high vacuum impregnation was able to overcome the softening effect from water and caused a significant increase in the Storage modulus by strengthening the wood's vascular structure, which accordingly increased wood's capacity to absorb energy. High vacuum impregnation was also able to counteract the lubricating effect of water and significantly increased the Loss modulus by increasing the internal friction of the wood with the addition of the nanoparticles to the vascular system, which increased the wood's capacity to absorb and diffuse the energy.

Ultimately, high vacuum impregnation was efficient to counteract the softening and lubrication effect of water by strengthening the wood's vascular system and increasing the internal friction with the addition of the nanoparticles. Furthermore, it caused an increase in the wood's capacity to absorb and diffuse the energy and at the same time showed an increase of elastic behavior.

SEM and EDS analysis revealed the positive effect of high vacuum pressure on $SiO_2$ impregnation. The micrographs revealed the vascular system of the wood to be efficiently obstructed with a high diffusion of $SiO_2$ agglomeration all the way up to the core of the wood samples.

SAXS tests also demonstrated that $SiO_2$ impregnation performed under higher vacuum pressure was efficient and exhibited a significant presence of $SiO_2$ in the lumens quantitatively and qualitatively. Impregnation under a vacuum pressure of -90 kPa was shown to effectively obstruct the vascular structure of spruce wood with $SiO_2$ particles.

Under all conditions and states, high vacuum impregnated samples showed significant benefits over non-treated samples. This research shows great potential for permanent reinforcement of the lumens. It goes to say that high vacuum $SiO_2$ impregnation is a good addition to wood and has a significant positive effect on wood's properties.

Multiple materials and applications could benefit from this research wherein, for example, instantaneous loading and deformation are expected to occur, or where simultaneous elastic behavior of wood and its damping energy is needed. This study could also pave the way for research on the synergistic effect of $SiO_2$ impregnation and water absorption on the viscoelastic behavior of wood.

## 4.7 References


1. Brunner M. (2000). On The Plastic Design Of Timber Beams With A Complex Cross-Section. Paper presented at the World Conference on Timber Engineering, British Columbia, Canada, July 31–August 3 2000.

2. Atlantic WoodWORKS!. (2017). WOOD FOR MID-RISE CONSTRUCTION. doi: https://wood-works.ca/wp-content/uploads/160601-Wood-4-Mid-Rise-Report-FINAL-2017-03-28-sm.pdf

3. University of Cambridge. (2020). Water's effect on the mechanical behaviour of wood. In: Dissemination of IT for the Promotion of Materials Science (DoITPoMS). doi: https://www.doitpoms.ac.uk/tlplib/wood/water_effect.php.

4. David W. Green, Jerrold E. Winandy, and David E. Kretschmann. (1999). Chapter 4 - Mechanical Properties of Wood. In Forest Product Laboratory. *Wood Handbook - Wood as an Engineering Material* (463). Madison, WI: U.S. Department of Agriculture, Forest Service. doi: https://www.fpl.fs.fed.us/documnts/fplgtr/fplgtr113/fplgtr113.pdf

5. Wagner et al. (2015). Effect of Water on the Mechanical Properties of Wood Cell Walls – Results of a Nanoindentation Study. *BioResources, 10*(3), 4011-4025. doi: 10.15376/biores.10.3.4011-4025

6. Illston J.M, Domone P. (2001). *Construction Materials – Their Nature and Behavior* (3rd ed.). London, England: CRC Press.

7. Rowell RM, Banks WB. (1985). Water repellency and dimensional stability of wood. *Forest Products Laboratory*. doi: 10.2737/fpl-gtr-50

8. Boulos L, Foruzanmehr MR, Tagnit-Hamou A, et al. (2017). Wetting analysis and surface characterization of flax fibers modified with zirconia by sol-gel method. *Surface and Coatings Technology, 313*, 407–416. doi: 10.1016/j.surfcoat.2017.02.008

9. Bučar, D. G., and Merhar, M. (2015). Impact and Dynamic Bending Strength Determination of Norway Spruce by Impact Pendulum Deceleration. *Bioresources 10*(3), 4740-4750. doi: https://bioresources.cnr.ncsu.edu/resources/impact-and-dynamic-bending-strength-determination-of-norway-spruce-by-impact-pendulum-deceleration/

10. Kollmann, F. F. P., and Cote, W. A. (1984). *Principles of Wood Science and Technology: I Solid Wood (1)*. Berlin: Springer-Verlag.

11. Tschoegl, N.W. (1989). Energy Storage and Dissipation in a Linear Viscoelastic Material. In: The Phenomenological Theory of Linear Viscoelastic Behavior. Springer, Berlin, Heidelberg. https://doi.org/10.1007/978-3-642-73602-5_9

12. Livingston EH. (2004). Who was student and why do we care so much about his T-test? *Journal of Surgical Research, 118*,58–65. doi: 10.1016/j.jss.2004.02.003

13. William D. Callister Jr., David G. Rethwisch. (2018). *Materials Science and Engineering: An Introduction* (10th ed.). Hoboken, NJ: Wiley.

# CHAPTER 5

**Conclusion**

# CHAPTER 5

## 5.0 Conclusion

This study investigated the efficiency of $SiO_2$ impregnation under vacuum pressures to overcome wood's weakness by reducing its water uptake capacity and analyzed the effect on the mechanical and viscoelastic properties under dry, saturated and submerged conditions. The research was conducted in a two-stage process. The first stage consisted of evaluating the effect and efficiency of vacuum pressure on the $SiO_2$ impregnation and finding the optimal impregnation pressure. The second one explored the synergistic effect of the optimal impregnation pressure in conjunction with humidity on the wood's properties. In both stages, to truly assess the vacuum impregnation effect on wood's properties, non-destructive tests were performed on the same sample before and after the treatments where applicable. This procedure ensured that the differences in properties were induced by the impregnation conditions rather than the inherent irregularity in the sample structure.

The first part of this research has demonstrated that $SiO_2$ impregnation can simultaneously reduce water uptake capacity and improve the mechanical properties of spruce wood if it is performed under vacuum pressure. However, the impregnation needs to be conducted at an elevated vacuum pressure so that the change of the properties will become statistically significant. Various characterization methods such as pycnometry, tensiometry, SEM, TEM, TGA, DMA, and statistical analyses were used to determine the optimal vacuum pressure condition.

After the analyses, the optimal impregnation vacuum pressure was found to be -90 kPa. A vacuum pressure of -90 kPa was proven optimal and most effective to significantly reduce wood's water uptake capacity and offered the highest Reduction magnitude. It showed the highest increase in density and resulted in the lowest porosity. SEM micrographs revealed that the vacuum pressure of -90 kPa was required to homogeneously disperse $SiO_2$ nanoparticles in the vascular system of the wood and make them diffuse into the cell walls.

DMA tests along with TGA and microscopic analyses revealed that $SiO_2$ impregnation under vacuum pressure was subjected to two competing mechanisms. On the one hand, the vacuum helped the $SiO_2$ particles (the solid phase of the colloid) diffuse and disperse into the vascular system of the wood and strengthen it. On the other hand, this process exposed the inner structure of the wood to an alkaline solution which could cause a degradation-solubilization phenomenon. The extent of this side effect is dependent on the strength of the vacuum, and thus on the dispersion of $SiO_2$ particles in the structure of the wood. The vacuum pressure of -30 kPa and -60 kPa was not strong enough to allow the nanoparticles to infiltrate and strengthen the wood and as a result underwent predominant degradation with minimum reinforcement. A detailed investigation of the viscoelastic properties showed that a vacuum pressure of -90 kPa was the only vacuum pressure (among the tested pressures) that could induce the full recovery and significantly improve the Storage and Loss modulus of wood. The -90 kPa samples were effectively impregnated and had a uniform dispersion of $SiO_2$ particles in the lumens, which reinforced wood and caused the dissipation of energy through particle-particle and particle-lumen wall frictions when the samples underwent deformations. Moreover, the impregnation under atmospheric conditions did not allow

the colloid to permeate inside the wood's structure and thus resulted in the formation of a solid film. The film reinforced the sample and increased the dissipation of energy through stick-slip oscillation.

The second part of this research has demonstrated that $SiO_2$ impregnation done under high vacuum pressure of -90 kPa can significantly reduce the porosity by almost 10% and improve the mechanical and viscoelastic properties of spruce wood under dry and saturated states. Characterization methods such as Impact test, DMA, SEM, EDS, porosity measurements, and the SAXS test were conducted on non-treated and -90 kPa treated spruce wood samples in dry, saturated, and submerged states to analyze the synergistic effect of high vacuum $SiO_2$ impregnation and water content on wood's properties.

The results showed that high vacuum impregnation pressure of -90 kPa had a significant positive reinforcing effect on the wood's properties under dry and saturated conditions. High vacuum impregnation led to a significant increase in the impact strength, the Storage modulus, and the Loss modulus in both dry and saturated states. It also caused a reduction in the Tan δ.

Ultimately, high vacuum impregnation was effective in counteracting the softening and plasticizing effect of water by strengthening the wood's wall structure and vascular system and increasing the internal friction with the addition of the nanoparticles. Furthermore, it caused an increase in the wood's capacity to absorb and diffuse the energy and, at the same time, showed an increase in the elastic behavior.

SEM and EDS analysis confirmed the high diffusion and agglomeration of $SiO_2$ after high vacuum impregnation pressure of -90 kPa. A pressure of -90 kPa was shown to be effective to impregnate and obstruct the wood's lumens all the way to the core of the vascular system of the wood samples. In conjunction, the SAXS test also revealed a significant presence of $SiO_2$ within the -90 kPa samples.

This research showed a great potential for permanent reinforcement of the lumens and enhancement and stabilization of the wood's properties. In all conditions and states, high vacuum impregnated samples of -90 kPa showed significant benefits over non-treated samples. In other words, high vacuum $SiO_2$ impregnation is an effective wood treatment and has a significant positive effect on the wood's properties.

### 5.1 Application & Recommendation

$SiO_2$ impregnation under atmospheric conditions could be useful in the development of materials that require vibration reduction or sound damping properties, whereas vacuum impregnation under -90 kPa could be advantageous for improving the creep resistance of spruce wood.

Multiple materials and applications could benefit from this research wherein, for example, instantaneous loading and deformation are expected to occur, or where simultaneous elastic behavior of wood and its damping energy is needed.

### 5.2 Future Work:

The next step to push this study forward would be to analyze the durability of $SiO_2$ impregnation by conducting durability tests such as hydrolytic degradation, UV degradation, freeze-thaw and dimensional stability.

# CHAPTER 6

**Appendices**

# CHAPTER 6

## 6.0 Appendices

## 6.1 Appendix A

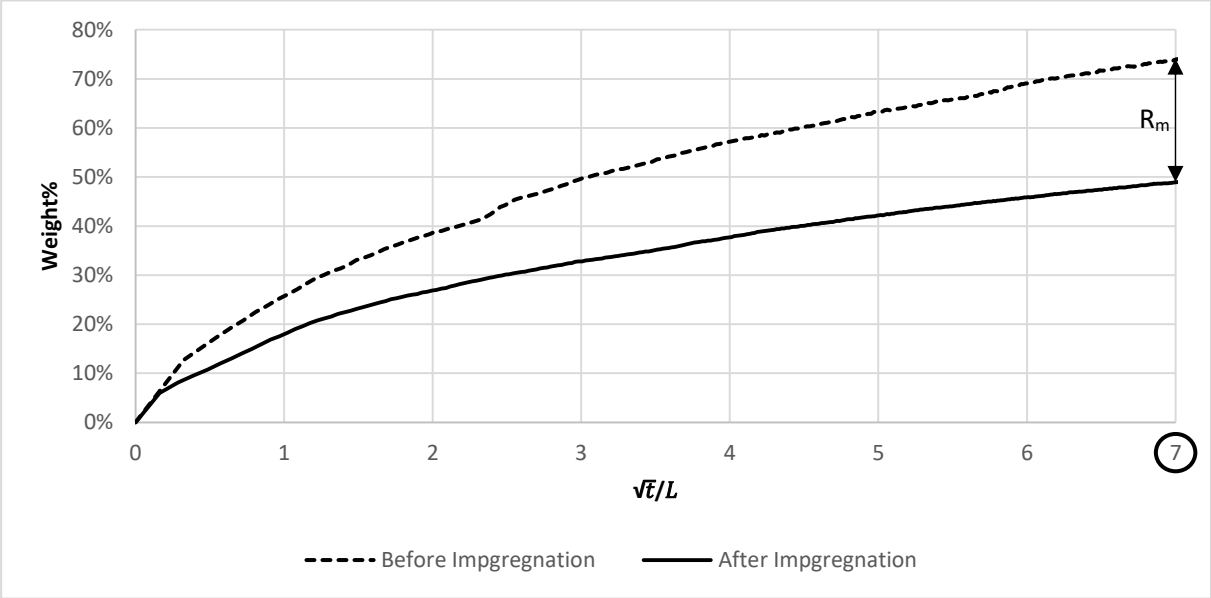


*Figure A1: Water uptake graph, reduction magnitude example Weight% vs* $\sqrt{t}/L$ *=7*

## 6.2 Appendix B

*a) SEM Non-Treated*

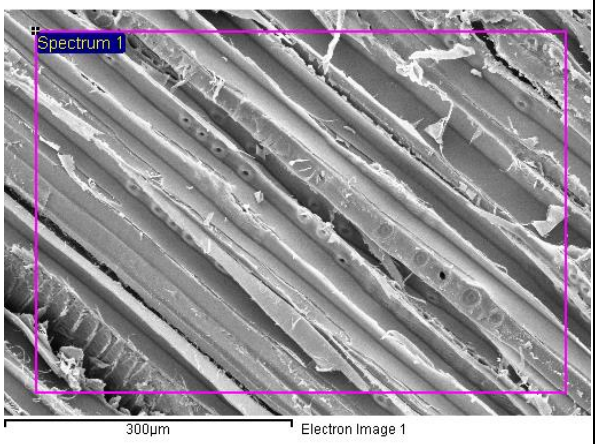


*b) SEM -90 kPa*

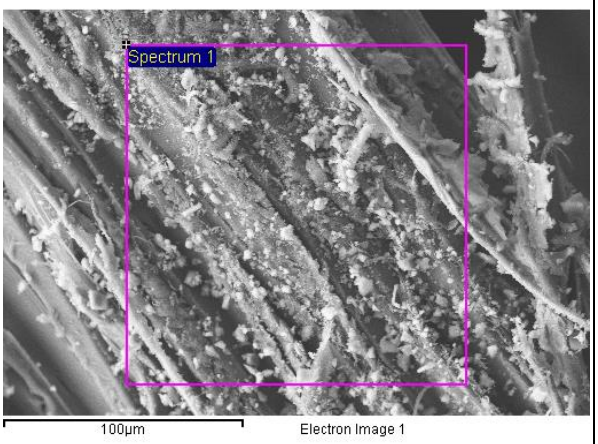


*c) EDS Non-Treated*

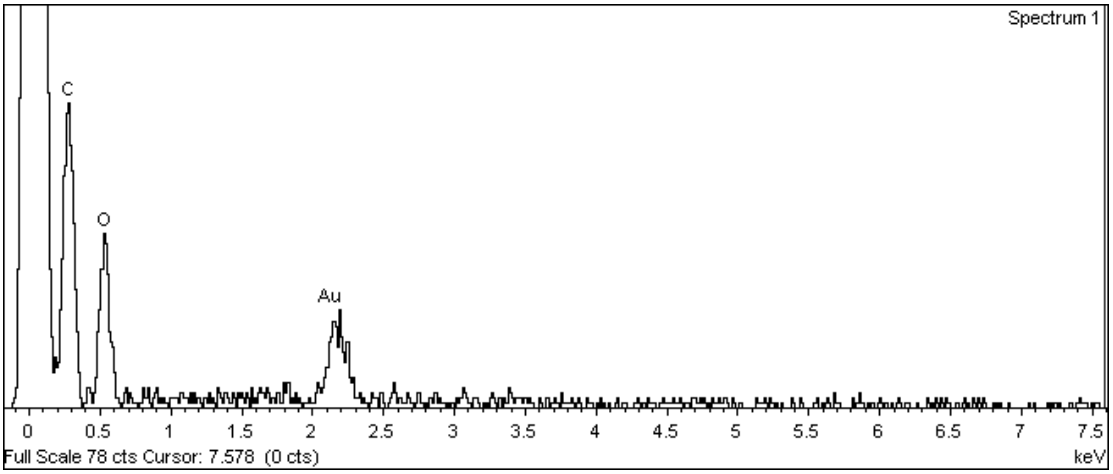


*d) EDS -90 kPa*

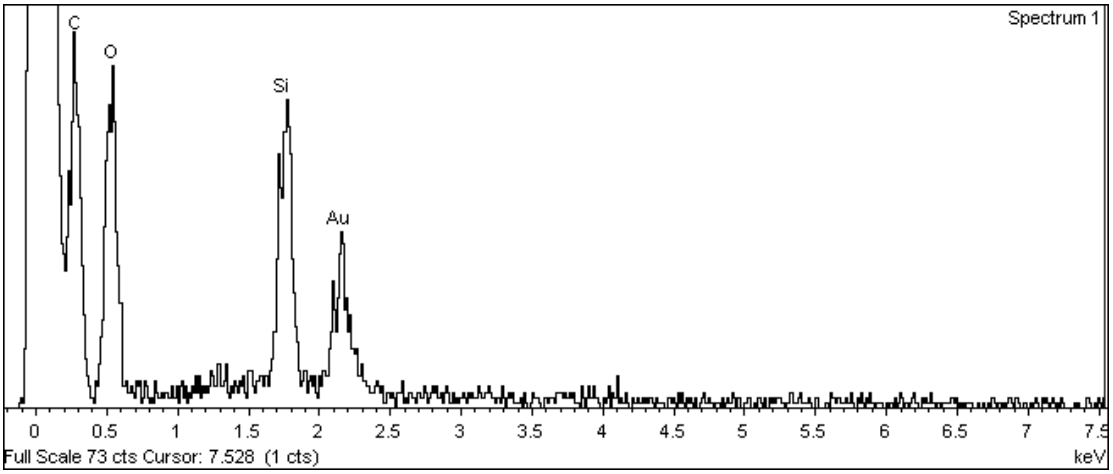


*Figure B1: SEM, EDS micrographs of a,c) non-treated and b,d) -90 kPa treated samples dry*

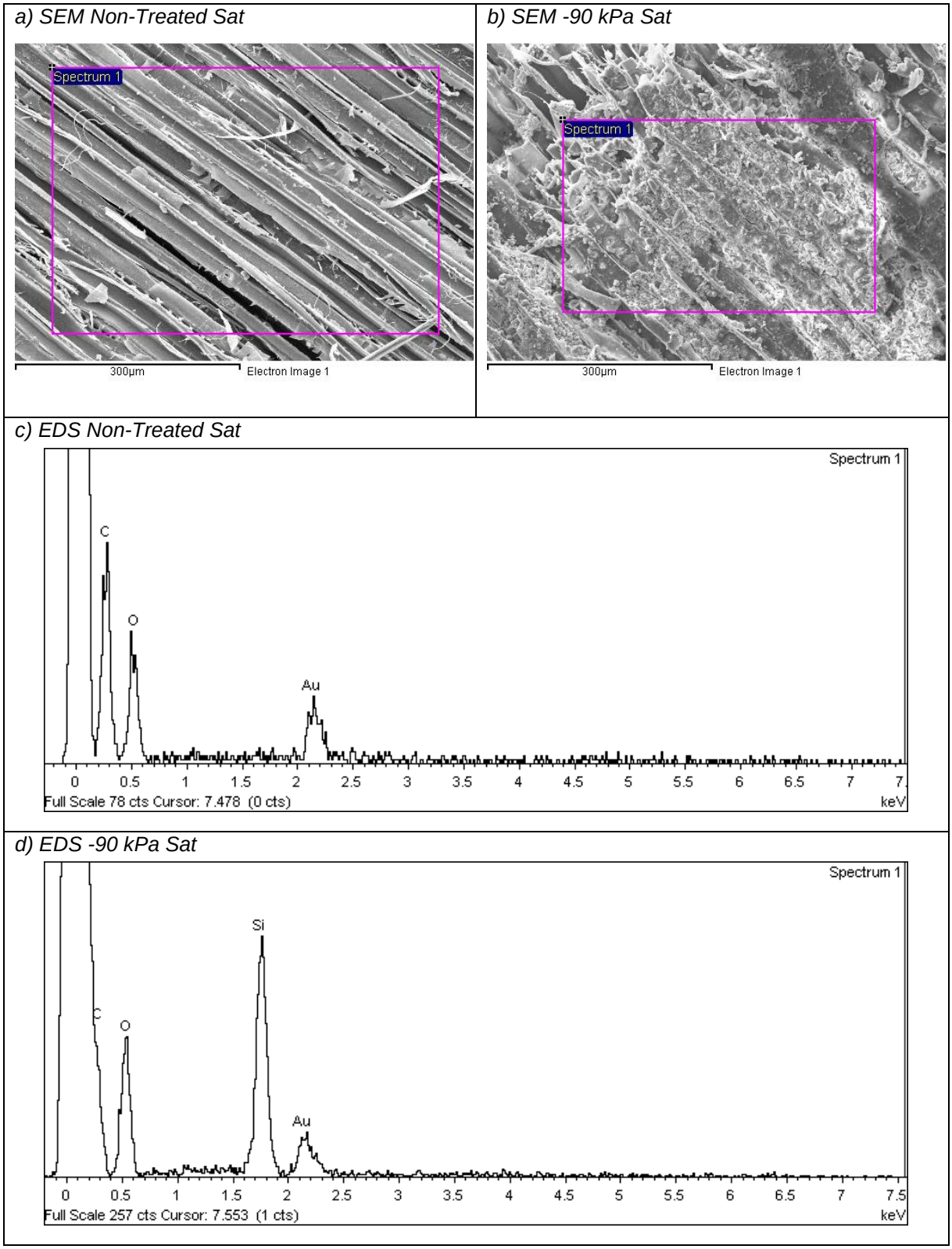


*Figure B2: SEM, EDS micrographs of a,c) non-treated and b,d) -90 kPa treated samples saturated*